Aus dem Institut für Physiologie und Pathophysiologie (Geschäftsführender Direktor: Prof. Dr. Dr. Jürgen Daut) des Fachbereichs Medizin der Philipps-Universität Marburg

Philipps Universität Marburg

ON THE MECHANISM OF TASK CHANNEL INHIBITION BY G-PROTEIN COUPLED RECEPTORS

Inaugural-Dissertation zur Erlangung des Doktorgrades der gesamten Humanmedizin, dem Fachbereich Medizin der Philipps-Universität Marburg vorgelegt von

Moritz Lindner aus Witten

Marburg, 2012

Angenommen vom Fachbereich Medizin der Philipps-Universität Marburg

am: 13. Dezember 2012

Gedruckt mit Genehmigung des Fachbereichs.

Dekan: Prof. Dr. Matthias Rothmund

Referent: Prof. Dr. Dominik Oliver

1. Korreferent: Prof. Dr. Timothy David Plant

To my dear parents

Abbreviations

AMP-PCP	β,γ-Methyleneadenosine-5′-triphosphate
ATP	Adenosine-tri-phosphate
BAPTA	2,2′-(Ethylenedioxy)dianiline-N,N,N′,N′-tetraacetic acid
CF-Inp54	Fusion construct of a CFP with the FKBP domain from the FK506 binding protein and the yeast Inp54p Phosphatase
CFP	Cyan fluorescent protein
CHO	Chinese Hamster Ovary
Ci-VSP	Ciona intestinalis voltage-sensitive phosphatase
DAG	Diacylglycerol
DNA	Deoxyribonucleic acid
EGTA	Ethylenglycol-bis(aminoethylether)-N,N,N′N′-tetraacetic acid
Et-1	Endothelin-1
Ex-0	Standard extracellular solution
GFP	Green-fluorescent protein
GPCR	G-protein coupled receptor
G_qPCR	G_q-protein coupled receptor
$G_q\alpha$	Q-type alpha-subunit of the G-protein
GTP	Guanosine-tri-phosphate
HEPES	4-(2-Hydroxyethyl)piperazine-1-ethanesulfonic acid
ICS	Intracellular solution
Ins(1,4,5)P_3	Inositol-1,4,5-tris-phosphate
K_{2P}	Two-pore-domain potassium
K_{ATP}	ATP-sensitive inward rectifying potassium channel
K_{ir}	Inward rectifying Potassium channel
K_v7	Family of voltage-gated potassium channels, subfamily 7
Lyn11-FRB	Fusion construct of lyn11 and the FRB domain from the “mammalian target of rapamycin”-protein
m1R	Muscarinic acetylcholine receptor 1
Me_2SO	Dimethyl-sulfoxide
NMDG	N-methyl-D-glucamine
Osh2p-PH	Fusion protein of two PH domains from oxysterol binding protein homologue in tandem
OxoM	Oxotremorine-Methiodide
PH	Pleckstrin homology
PKC	Protein kinase C
PLC-β	Phospholipase C isoform β
PLC-δ1-PH	PH-domain of Phospholipase C isoform δ1
PSF	Point spread function
PtdIns	Phosphoinositide
PtdIns(3,4,5)P_3	Phosphatidyl-inositol-3,4,5-tris-phosphate
PtdIns(4)P	Phosphatidyl-inositol-4-mono-phosphate
PtdIns(4,5)P_2	Phosphatidyl-inositol-4,5-bis-phosphate
RFP	Red fluorescent protein
ROI	Region of interest
TASK	TWIK-related-acid-sensitive-potassium
TIRF	Total internal reflection fluorescence microscopy
TREK	TWIK-related potassium channel
TWIK	Two-pore-weakly-inward rectifying
XE991	(10,10-bis[4-pyridinylmethyl]-9[10H]-anthracenone-dihydrochloride)
Not listed	Abbreviations as defined in the *Système international d’unités (SI)* and *in the Periodic table* by the *International Union of Pure and Applied Chemistry (IUPAC)*

Abstract

Background K^+ conductance TASK channels belong to the family of two pore domain potassium channels. They are involved in regulation of neuronal excitability, cardiovascular homeostasis and endocrine activity. TASK channel activity is down-regulated by activation G_q-protein coupled receptors (G_qPCR). In various tissues this regulatory mechanism is crucial for proper organ function. Well studied examples of G_qPCR mediated TASK channel inhibition are the cholinergic inhibition of $I_{K,SO}$ in cerebellar granule neurons, angiotensin II stimulated aldosterone secretion in adrenal zona-glomerulosa cells and vasoconstriction of the pulmonary artery by endothelin-1.

Despite intense research, the mechanism underlying this inhibition remains elusive. Strong evidence exists for two competing hypotheses: TASK channels could be either blocked directly by the Gq-alpha subunit released on G_qPCR activation, or their closure could be a direct consequence of Phospholipase C (PLC)-mediated phosphatidyl-inositol(4,5)-bis-phosphate (PtdIns(4,5)P_2) depletion.

In the present study I investigated the role of PLC mediated phosphoinositide cleavage in the process of TASK channel regulation by G_qPCR in the intact cell. Recently developed genetically encoded switchable phosphoinositide-phosphatases were used to specifically deplete PtdIns(4,5)P_2. Additionally, I interfered with PtdIns(4,5)P_2 resynthesis and PLC activity. I found that blockage of PLC results in abolishment of G_qPCR induced TASK inhibition. However depletion of the PLC substrate PtdIns(4,5)P_2 alone was not sufficient to inhibit TASK.

These results show that PLC activation is an indispensable step in TASK channel inhibition. They further demonstrate that the depletion of PtdIns(4,5)P_2 does not directly inhibit TASK and therefore suggest that a regulatory mechanism downstream of PtdIns(4,5)P_2-hydrolysis mediates TASK channel inhibition.

Zusammenfassung

Die Hintergrund-K^+-Strom leitenden TASK Kanäle gehören zur Familie der Zwei-Poren-Domänen-Kalium-Kanäle. Sie sind an der Regulation der neuronalen Erregbarkeit, der kardiovaskulären Homöostase und der endokrinen Aktivität beteiligt. Die TASK Kanal Aktivität wird durch G_q-Protein gekoppelte Rezeptoren (G_qPCR) herunterreguliert. In verschiedenen Geweben ist dieser regulatorische Mechanismus entscheidend für die korrekte Organfunktion. Gut untersuchte Beispiele der G_qPCR vermittelten TASK Inhibition sind die cholinerge Inhibition von $I_{K,SO}$ in zerebellären Körnerzellen, die Aldosteron-Sekretion durch Angiotensin II in Zona-glomerulosa-Zellen der Nebenniere und die Depolarisation von glatten Gefäßmuskelzellen durch Endothelin-1.

Trotz intensiver Forschung ist der Mechanismus, der dieser Inhibition zugrunde liegt kaum verstanden. Es gibt starke experimentelle Hinweise für zwei konkurrierende Hypothesen: TASK Kanäle könnten entweder direkt durch die $G_q\alpha$-Untereinheit blockiert werden, die durch G_qPCR-Aktivierung freigesetzt wird. Alternativ könnte ihr Schließen direkte Konsequenz des Phospholipase C (PLC) vermittelten Phosphatidyl-inositol(4,5)-bis-phosphate (PtdIns(4,5)P_2) Abbaus sein.

In der vorliegenden Studie habe ich die Rolle des PLC-vermittelten PtdIns(4,5)P_2-Abbaus im Prozess der TASK Kanal Regulation durch G_qPCR in der intakten Zelle untersucht. Es wurden neu entwickelte genetisch kodierte schaltbare Phosphatasen genutzt, um PtdIns(4,5)P_2 spezifisch abzubauen. Zudem habe ich in die PtdIns(4,5)P_2-Resynthese und die PLC-Aktivität eingegriffen. Ich konnte zeigen, dass die Blockierung der PLC die TASK Kanal Inhibition durch G_qPCR verhindert. Jedoch bewirkt der Abbau des PLC-Substrats PtdIns(4,5)P_2 selbst nicht die TASK Inhibition.

Diese Ergebnisse zeigen dass PLC Aktivierung ein notwendiger Schritt für die TASK Kanal Inhibition ist. Zudem zeigen sie, dass der Abbau von PtdIns(4,5)P_2 TASK nicht direkt inhibiert und legen daher einen der PtdIns(4,5)P_2-Hydrolyse nachgeschalteten regulatorischen Mechanismus für die Inhibition der TASK Kanäle nahe.

Table of Contents

1 Introduction 1

1.1 The Two pore domain potassium channel family 1

1.1.1 Structural characteristics of K_{2P} Channels 1

1.1.2 Electrophysiological characteristics of K_{2P} Channels 2

1.1.3 Physiological importance of K_{2P} channels 3

1.2 The TASK channel subfamily 4

1.2.1 Structure and functional characteristics 4

1.2.2 Physiological relevance and G_qPCR mediated inhibition 5

1.3 The G_qPCR signaling pathway 6

1.4 Phosphoinositides and the role of Phospholipase C 9

1.4.1 Chemical structures of phosphoinositides and their distribution at the plasma membrane 9

1.4.2 Phospholipase C mediates G_qPCR induced PtdIns signaling 10

1.4.3 Various ion channels are modulated by Phosphoinositides 12

1.4.4 Phosphoinositides do not only regulate ion channels 13

1.5 Recent insight into the regulation of TASK channels by G_q-protein coupled receptors 14

1.5.1 $G_q\alpha$ is essential for receptor inhibition TASK channels 14

1.5.2 Activated $G_q\alpha$ may directly inhibit TASK channels 14

1.5.3 The role Phospholipase C is unclear 15

1.5.4 TASK inhibition may result from PtdIns(4,5)P_2 depletion 15

1.5.5 Downstream messengers have been tested 16

1.6 Tools for monitoring and manipulating PtdIns levels 17

1.6.1 Live cell imaging of PtdIns dynamics 17

1.6.2 Manipulation of PtdIns(4,5)P_2 levels in intact cells 18

1.7 Aim of this study 20

2 Materials and methods 22

2.1 Molecular biology 22

2.2 Cell culture and transfection 22

2.3 Chemicals 23

2.4 Solutions 24

2.5 Patch-clamp experiments 25

2.6 Microscopy 26

2.6.1 Total internal reflection fluorescence microscopy (TIRF) 26

2.6.2 Confocal microscopy 27

2.7 Bath chamber and application of chemicals 29

2.8 Data analysis 30

3 Results 31

3.1 Reconstitution of G_qPCR induced TASK channel inhibition in an experimentally suitable model system 31

3.2 Specific depletion of PtdIns(4,5)P_2 does not inhibit TASK channels 35

3.3 Depletion of overall PtdIns leaves TASK channels unaffected 38

3.4 Recovery of TASK channels from G_qPCR mediated inhibition occurs independently of PtdIns(4,5)P_2 resynthesis. 42

3.5 Inhibition of PLC-β abolishes G_qPCR mediated TASK inhibition 43

3.5.1 Interfering with PLC-β activity by removal of intracellular calcium 44

3.5.2 Effect of the PLC-β blocker U-73122 on m1R inhibition of TASK 45

3.5.3 U-73122 also abolishes endothelin-1 induced TASK channel inhibition 49

3.6 G_qPCR mediated TASK inhibition is slower when PtdIns(4,5)P_2 levels are reduced 52

3.7 In absence of PtdIns(4,5)P_2 available to PLC-β G_qPCR activation fails to inhibit TASK 56

4 Discussion 58

4.1 Does PtdIns(4,5)P_2 directly influence TASK channel activity? 58

4.2 Are other PtdIns involved in TASK channel regulation? 60

4.3 May specific PtdIns(4,5)P_2 pools be involved in the regulation of TASK channels? ... 61
4.4 Can a direct inhibitory mechanism by $G_q\alpha$ be excluded? ... 62
4.5 What is the role of PLC-β activity in the inhibition process? ... 64
4.6 The mechanism of G_qPCR mediated TASK inhibition ... 64
4.6.1 PKC ... 65
4.6.2 Calcium ... 65
4.6.3 Ins(1,4,5)P_3 and DAG ... 66
4.6.4 Protons ... 67
4.6.5 Non-canonical inhibitory mechanisms ... 67
4.7 Concluding remarks ... 68
5 Appendix ... I
5.1 Reference ... I
5.2 Academic teachers ... XIII
5.3 Acknowledgements ... XIV

1 Introduction

1.1 The Two pore domain potassium channel family

Two pore domain acid sensitive potassium (TASK) channels belong to the superfamily of "two pore domains in tandem" potassium channels (K_{2P}). It is named after their two pore domains in a tandem structure that is unique among potassium channels. K_{2P} channels give raise to the "leak" potassium conductance, which has already been observed in the early days of electrophysiology when the high resting permeability of the cell membrane for potassium ions became apparent (Hodgkin & Huxley, 1947, 1952). However its molecular entities remained unknown until the late 90ies when an ion channel was cloned from saccaromyces cervisiae with biophysical properties similar to that of the "leak" conductances (Fink *et al.*, 1996). Soon the first mammalian channel was cloned and the unique structure of two pore domains in tandem was revealed (Lesage *et al.*, 1996). The name "leak" conductance arose from the early idea that this conductance was essentially unregulated. However this is not the case, they are in contrast subject to modulation by diverse physiological and pharmacological stimuli (Enyedi & Czirjak, 2010).

1.1.1 Structural characteristics of K_{2P} Channels

The K_{2P} family is diverse in both, functional and structural aspects. Structural key features conserved throughout the family are the two pore domains and four transmembrane domains architecture. Each pore domain consists of two transmembrane domains which are linked by a pore loop. Both pore domains follow one on another, i.e. they are in "tandem" (Fig. 1) (Lesage et al., 1996; Brohawn, 2012; Miller, 2012). As four pore domains are necessary to form a functional channel, K_{2P} channels are the only mammalian potassium channels where a functional channel is assembled by only a dimer (Hille, 2001; Brohawn, 2012; Miller, 2012).

These structural characteristics were initially identified in TWIK (two pore weakly inward rectifying K^+) channels, the first mammalian K_{2P} channel to be cloned (Lesage *et al.*, 1996). Subsequent research led to the identification of 18 K_{2P} channels. They were named numerically as $K_{2P}1.1$ to $K_{2P}18.1$ according to their gene names (KCNK1 to KCNK18, see Fig. 2) (Goldstein et al., 2005). The overall sequence homology of K_{2P} channels is low compared to other potassium channels. This low sequence homology goes along with high functional diversity. It was therefore reasonable to categorize K_{2P}

channels into six subfamilies (TWIK, TREK, TASK, TALK, THIK, and TRESK, see Tab. 1 and Fig. 2) by functional considerations (Enyedi & Czirjak, 2010).

Tab. 1: The K_{2P} Channel Subfamilies

Abbreviation	In words
TWIK	Two pore weakly inward rectifying K^+
TREK	TWIK-related K^+
TASK	TWIK-related acid sensitive K^+
TALK	TWIK-related alkaline pH activated K^+
THIK	Tandem pore domain halothane inhibited K^+
TRESK	TWIK-related spinal cord K^+

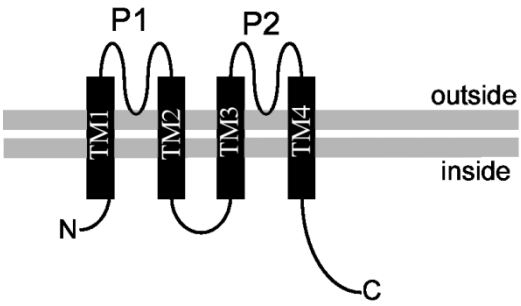

Fig. 1: Topology of K_{2P} channels. P1, P2: First and second pore domain. TM1-4: transmembrane regions. The plasma membrane is indicated in grey.

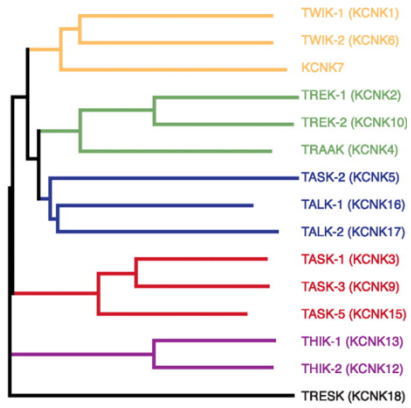

Fig. 2: Human K_{2P} dendrogram. Abbreviations used as given in Tab. 1. Figure taken from Enyedi & Czirjak, 2010.

1.1.2 Electrophysiological characteristics of K_{2P} Channels

The biophysical properties of K_{2P} channels closely resemble the ideal potassium leak conductance as observed by Hodgkin and Huxley (Hodgkin & Huxley, 1947). To fit the observations, a potassium leak channel has to exhibit three key properties: First of all it is open at resting potential and its conductance is insensitive to voltage changes. Furthermore both activation and deactivation kinetics are instantaneous and no inactivation is present. Finally it does not show any rectification: when electrolytes are distributed symmetrically over the membrane its conductance shows a linear and symmetric current-voltage dependency. According to these properties its current can be well described by the Goldman-Hodgkin-Katz equation (Goldman, 1943; Hodgkin & Katz, 1949). All these criteria are almost perfectly met by the current carried by K_{2P}

channels. They are therefore often referred to as open- or outward-rectifying (Fig. 3) (Goldstein *et al.*, 2001; Hille, 2001) The term “outward-rectifying” reflects the fact that a potassium leak current shows larger outward currents due to the asymmetrical distribution of electrolytes (in particular potassium) over the cell membrane. K_{2P} channels thereby provide a continuous potassium flux that shifts the membrane potential towards the equilibrium potential of potassium resulting in stabilization of the resting membrane potential and facilitation of repolarisation (Goldstein *et al.*, 2005; Enyedi & Czirjak, 2010).

Noteworthy K_{2P} channels do not totally resemble an ideal potassium leak conductance. In fact they slightly deviate from an ideal leak channel. For instance TWIK channels show a weak inward rectification (Lesage *et al.*, 1996), while TASK channels exhibit slight outward rectification also at symmetrical potassium concentrations. In addition their activation is time dependent (although with very fast kinetics) (Duprat *et al.*, 1997).

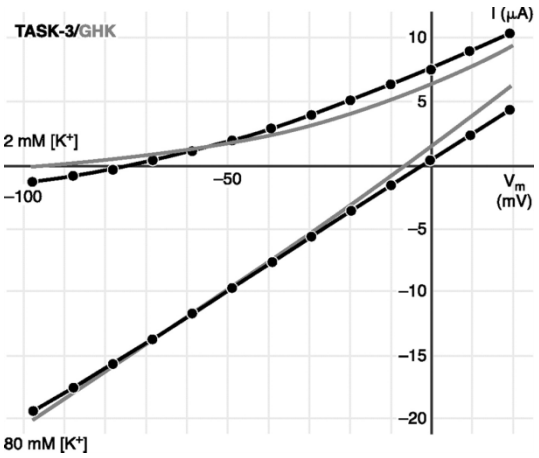

Fig. 3: Comparison of TASK currents and Goldman-Hodgkin-Katz current equation. Current-voltage relationship of TASK-3 as measured in xenopus oocytes (black traces) and as estimated by the Goldman-Hodgkin-Katz current equation (grey traces). Experiments and calculations were performed for 80 mM and 2 mM extracellular K+. Figure obtained from Enyedi & Czirjak, 2010.

1.1.3 Physiological importance of K_{2P} channels

Despite early expectations suggesting a unregulated leak, K_{2P} channels are subject to regulation by a diverse number of physiological and pharmacological stimuli. K_{2P} channels serve as essential sensors for the metabolic state of the body. TASK, TALK and TREK are sensitive to changes in pH (Duprat *et al.*, 1997; Reyes *et al.*, 1998; Lesage *et al.*, 2000). By this mechanism TASK channels (inhibited by protons) are involved in chemoreception in the carotid body while TALK channels (activated by protons) contribute to the re-absorption of bicarbonate in kidney’s tubules (Duprat *et*

al., 2007; Bayliss & Barrett, 2008). By a not yet fully understood mechanism TASK are also involved in oxygen sensing in carotid body glomus-cells (Duprat *et al.*, 2007). Another key feature of K_{2P} is their sensitivity to volatile anesthetics. Application of e.g. halothane activates various channels of this group, thereby stabilizing the resting membrane potential of a cell (Patel *et al.*, 1999; Talley *et al.*, 2001; Liu *et al.*, 2004). As K_{2P} channels are involved in arousal, pain sensation, generation of motor impulses and setting of vascular tone, the direct action of volatile anesthetics on K_{2P} channels explains the bulk of the clinical effects of these drugs (i.e. immobilization, sedation and analgesia) (Bayliss & Barrett, 2008).

Physiologically K_{2P} are involved in diverse signaling cascades by coupling to G-protein coupled receptors (GPCR). TREK channels are inhibited by stimulation of G_s- and G_qPCR, e.g. in dorsal raphe nuclei, where attenuation of these inhibition pathways may cause depression (Bayliss & Barrett, 2008). Inhibition of TREK channels via protein-kinase C (PKC) mediates NO release in vascular endothelium cells and thereby provokes vasodilatation (Enyedi & Czirjak, 2010). Also TASK are subject to inhibition by G_qPCR. In contrast to TREK channel inhibition, the mechanism underlying TASK channel inhibition remains elusive. As the aim of this study is to resolve this mechanism, its physiological relevance and suggested signaling pathways will be detailed in the next chapters.

1.2 The TASK channel subfamily

1.2.1 Structure and functional characteristics

The TASK channel subfamily consists of three members: TASK-1, TASK-3 and TASK-5 (Goldstein *et al.*, 2005). TASK-1 and TASK-3 are the closest known relatives within the K_{2P} family (Kim *et al.*, 2000) and also share the main electrophysiological features (Enyedi & Czirjak, 2010). In contrast TASK-5 is apparently non-functional (Enyedi & Czirjak, 2010). TASK-1 and TASK-3 exhibit currents that are strongly inhibited by extracellular acidification, although the range of pH sensitivity differs between both channels (Rajan *et al.*, 2000; Morton *et al.*, 2003). While TASK-3 is maximally activated at a physiological pH of 7.4 TASK-1 is about half active at the same value (Duprat *et al.*, 1997; Kim *et al.*, 2000). Another key feature of TASK channels is their activation by halothane. Clinically relevant concentrations of halothane increase TASK-1 currents by 50% and TASK-3 by 130% (Talley & Bayliss, 2002). Also

G_qPCR mediated inhibition is present in both channels. Robust receptor activation results in almost complete inhibition of both channels (Talley & Bayliss, 2002; Mathie, 2007). Noteworthy activation by halothane and inhibition by G_qPCR share a common site of action: they both require a six-amino acid motif (VLRFXT) which is conserved among the TASK channel family (Talley & Bayliss, 2002).

1.2.2 Physiological relevance and G_qPCR mediated inhibition

TASK channels are widely expressed throughout the whole body. In many organs their regulation is essential to carry out basic organ functions. For instance they are involved in the integration of motor impulses, sensation of chemical stimuli, the regulation of vascular tone and respiratory frequency (Duprat *et al.*, 2007; Bayliss & Barrett, 2008; Gurney & Manoury, 2009). Furthermore TASK channels mediate non-organ specific processes as being involved in oncogenesis and apoptosis (Patel & Lazdunski, 2004; Bayliss & Barrett, 2008). In many of these processes their inhibition by G_qα-protein coupled receptor (G_qPCR) activation is a crucial modulatory mechanism. As TASK channel functions are diverse, this chapter will exemplify only some key functions where modulation by G_qPCR is of outstanding importance.

Generation and modulation of motor impulses is influenced by TASK channels in the brain and in peripheral neurons. In giant motorneurons of the caudal pontine reticular formation TASK-3 channels are under the regulation of 5-hydroxytryptamin-2 receptors, also belonging to the family of G_qPCR. Serotoninergic input from the raphe-nuclei leads to receptor activation and subsequent depolarization of the giant neurons, presumably influencing the startle motor response (Weber *et al.*, 2008). Similar findings were made for the TASK-like conductance in dorsal vagal neurons (Hopwood & Trapp, 2005). Additionally a current mainly carried by TASK-1/TASK-3 heterodimers, called $I_{K,SO}$ (SO for standing outward), in cerebellar granule neurons is subject to inhibition by stimulation of various G_qPCR, like the muscarinic acetylcholine receptor 1 (m1R) (Millar *et al.*, 2000; Talley *et al.*, 2001; Chemin *et al.*, 2003; Kang *et al.*, 2004). In these cells, knock-out of TASK-1 leads to marked changes of their electrophysiological properties. As cerebellar granule neurons are involved in processing motor impulses, TASK-1 knock-out mice show altered motor behavior (Aller *et al.*, 2005). Moreover TASK-1 is responsible for a remarkable “leak” current in motorneurons of the hypoglossal nerve. This current is under inhibitory regulation of various G_qPCR, such as 5-hydroxytryptamin-2 receptors, adrenoreceptors, type I metabotropic glutamate receptors and thyreotropin releasing hormone receptors (Talley *et al.*, 2000). As

G_qPCR inhibition of TASK is such a prominent mechanism in motor system it is believed to strongly influence the generation of motor impulses (Bayliss & Barrett, 2008).

G_qPCR inhibition of TASK furthermore strongly affects the cardiovascular system. A well studied example in this context is the inhibition of heteromeric TASK-1/TASK-3 channels by angiotensin II in zona glomerulosa adrenal cells. Stimulation of AT_1-type G_qPCR leads to an inhibition of a TASK-like conductance, resulting in a pronounced depolarization of these cells (Czirjak *et al.*, 2000). This triggers the release of aldosterone and thereby influences glomerular filtration rate and systemic blood pressure (Bayliss & Barrett, 2008). Consequently the phenotype of TASK-1 or TASK-1/TASK-3 double knock-out mice reconstitutes the clinical features of a primary hyperaldosteronism (Bayliss & Barrett, 2008; Davies *et al.*, 2008; Heitzmann *et al.*, 2008).

A TASK-like conductance was also found in rat cardiomyocytes. This conductance, mediated by TASK-1 has been shown to be modulated by stimulation of α_1-type adrenoreceptors and platelet-activating factor receptor, both G_qPCR (Besana *et al.*, 2004; Putzke *et al.*, 2007). Adrenergic stimulation results in an increased action potential frequency and membrane depolarization (Putzke *et al.*, 2007). Accordingly TASK-1 knock-out mice showed a decreased variability in the heart rate (Donner *et al.*, 2010).

Motor function, aldosterone secretion and heart rate modulation are just three examples for the relevance of G_qPCR mediated TASK channel inhibition. They demonstrate that this mechanism is of crucial physiological relevance and understanding of this mechanism can possibly help to understand and treat various related diseases.

1.3 The G_qPCR signaling pathway

G_qPCR belong to the heterogeneous family of G-protein coupled receptors (GPCR) (Foord *et al.*, 2005). They initiate diverse intracellular signaling cascades. The signaling pathway is mainly routed by the type of the coupling G-protein. In the context of the current work, only the group of G_q-protein coupled receptors (G_qPCR) is of further interest. Muscarinic acetylcholine receptors type 1 and 3, 5-hydroxytryptamin-2 receptors, α1-adrenoreceptors, metabotropic glutamate receptors type I, thyreotropin

releasing hormone receptors, endothelin A and B receptors are common representatives of this group (Foord *et al.*, 2005). The general principle of G_qPCR signaling is well established. In brief G-proteins are heterotrimers assembled of a GTP/GDP binding α- and a βγ subunit complex. The α-subunit determines the species of G-protein (e.g. G_q) (Foord *et al.*, 2005). In the resting state only a small fraction of G_qPCR associate with the G_qαβγ protein complex having a GDP bound (Fig. 4.1). The fraction of G_qPCR associated with the G_qα-GDP-βγ complex increases upon receptor activation for yet unknown reasons (Falkenburger *et al.*, 2010b). Activation of these G_qPCR associated with G_qα-GDP-βγ leads to the replacement of the GDP by GTP (Fig. 4.2). This step initiates the dissociation of the receptor-G-protein complex into a G_qα-GTP and a G_qPCR- βγ-complex (Fig. 4.3 and Fig. 5). The G_qα-GTP now propagates signaling to its effectors (Fig. 4.4). The intrinsic GTPase activity of G_qα then terminates signaling by hydrolysis of GTP enabling reorganization of the complex (Fig. 4.5 + 6) (For review see: Gilman, 1987; Mizuno & Itoh, 2009). Both, the Gβγ and the G_qα proteins can propagate G_qPCR signaling (McCudden *et al.*, 2005).

The signaling effect exhibited by Gβγ depends on the exact composition of β and γ subunits. There are 5 genes coding for Gβ and 12 coding for Gγ. Depending on their combination they can initiate different signaling pathways, including activation of inward rectifying potassium channels, various calcium channels and phospholipase C (PLC-β) (Huang *et al.*, 1998; McCudden *et al.*, 2005; Drin & Scarlata, 2007). There is evidence suggesting that the Gβγ composition has a role in specific receptor-effector coupling and thereby in target specific signal propagation (McCudden *et al.*, 2005).

The main function of G_qα is to activate PLC-β, thereby initiating an almost ubiquitous signaling cascade. It additionally activates RhoA via G-protein exchange factors (GEF, Fig. 5) (Mizuno & Itoh, 2009). RhoA itself is well known to play a role in oncogenesis. Additionally RhoA dependent regulation of ion channels has recently been reported (Szaszi *et al.*, 2000; Karpushev *et al.*, 2010).

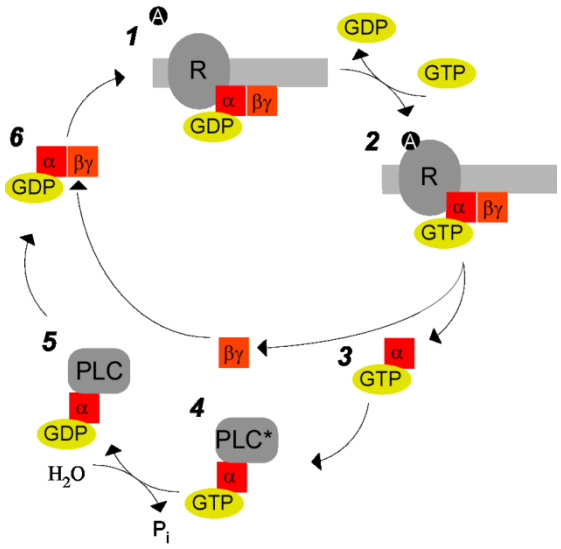

Fig. 4: The G protein cycle. R Receptor, A Agonist, Pi Phosphate, α G-Protein a subunit βγ G-Protein βγ subunits. 1, The G-protein cycle initiates with a G-protein associated with the receptor and a GDP bound. 2, Receptor activation leads to replacement of GDP by GTP. 3, Subsequently the G-protein-Receptor complex dissociates into G_qα-GTP and a receptor-βγ-complex. 4, G_qα-GTP then activates the effector (here PLC-β). 5, Intrinsic GTPase activity hydrolyses GTP to GDP thereby terminating the signaling activity. 6, after GTP hydrolysis G_qα-GDP leaves the effector and re-associates with the βγ subunit.

When activated, PLC-β hydrolyzes phosphatidyl-inositol-4,5-bis-phosphate [PtdIns(4,5)P_2] into inositol-3,4,5-tris-phospate [Ins(1,4,5)P_3], diacyl-glycerol (DAG) and a proton (Huang *et al.*, 2010). Strong PLC-β activation results in a dramatic decrease of PtdIns(4,5)P_2 membrane abundance (Falkenburger *et al.*, 2010b). Finally Ins(1,4,5)P_3 creation leads to an emptying of calcium stores, while DAG activates Protein Kinase C (PKC) (Fig. 5).

Most of the second messengers involved in this signaling cascade have also been shown to regulate ion channels. DAG activates transient receptor potential channels while Ins(1,4,5)P_3 is well known to activate the Ins(1,4,5)P_3 receptor type calcium channel covering the membrane of the endoplasmatic reticulum (Hille, 2001; Dietrich *et al.*, 2005). Direct interaction of G-proteins with ion channels was demonstrated for $K_{ir}3$ channels (Luscher & Slesinger, 2010). PtdIns(4,5)P_2 has received further attention, when it was shown that some K_{ir} and K_v channels are under immediate control of this membrane lipid (Hilgemann & Ball, 1996; Baukrowitz *et al.*, 1998). The hydrolysis of PtdIns(4,5)P_2 by PLC-β is a key process in G_qPCR signaling and will therefore receive further attention in the next chapter.

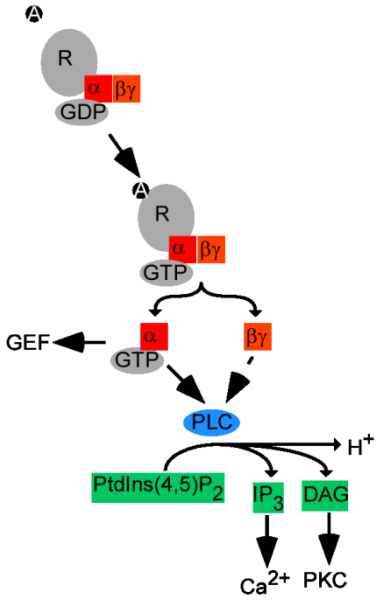

Fig. 5 G_q-Protein Signaling cascade: R Receptor, A Agonist, α G-Protein α subunit, βγ G-Protein βγ subunits. Receptor activation by an agonist leads to replacement of G_qα bound GDP by GTP. Subsequently the G_qαβγ-complex dissociates. G_qα activates PLC-β and GEFs. Also Gβγ can activate PLC-β. Active PLC-β hydrolyses PtdIns(4,5)P_2 to Ins(1,4,5)P_3, DAG and a proton. Ins(1,4,5)P_3 releases calcium from intracellular stores meanwhile DAG activates PKC.

1.4 Phosphoinositides and the role of Phospholipase C

PtdIns(4,5)P_2 is only one representative of the group of phosphoinositides (PtdIns). These lipidic messenger molecules do not only regulate the function of ion channels but they also control a plethora of other cellular processes at the cell membrane. They are a minor component of the eukaryotic plasma membrane and they are maintained at a specific equilibrium by interaction of various lipid kinases and phosphatases (Di Paolo & De Camilli, 2006). Potential interaction, regulation, and distribution mechanisms are still not fully understood. However understanding has dramatically increased within the last years. It has especially become clear that PtdIns(4,5)P_2 may play a permissive role for protein function, i.e. PtdIns(4,5)P_2 dependency does not necessarily mean that a protein is also regulated by PLC-β mediated PtdIns(4,5)P_2 hydrolysis (Gamper & Shapiro, 2007; Hilgemann, 2007; Suh & Hille, 2008; Falkenburger *et al.*, 2010a).

1.4.1 Chemical structures of phosphoinositides and their distribution at the plasma membrane

Phosphatidyl inositol is the precursor molecule of all PtdIns. PtdIns consist of a hydrophilic inositol group connected to a lipophilic lipid backbone. The phospolipidic backbone is assembled by two fatty acids esterified to a glycerol moiety which is phosphorylated in the remaining OH-position. Via this phosphate group the molecule is linked to cyclic myo-inositol, thereby assembling phosphatidyl-inositol. Differential

phosphorylation of one, two or all three of the OH-groups in 3-, 4- or 5-position of the myo-inositol results in seven different molecules termed phosphoinositides (PtdIns, Fig. 6) (Di Paolo & De Camilli, 2006). The lipophilic backbone anchors the PtdIns into the plasma membrane while the inositol group is the main site for protein interaction (Di Paolo & De Camilli, 2006).

Phosphoinositides show an abundance of only 15 % of the phosphatidyl-inositol concentration of the cell membranes, making up approximately 1.5 % of its overall phospholipid content (Di Paolo & De Camilli, 2006; Gamper & Shapiro, 2007; Hilgemann, 2007). PtdIns(4)P and PtdIns(4,5)P_2 are the two most abundant PtdIns, accounting for about 5 % of the total phosphatidyl-inositol concentration each. They thereby exceed the concentration of other PtdIns by a multiple (Di Paolo & De Camilli, 2006; Kwiatkowska, 2010).

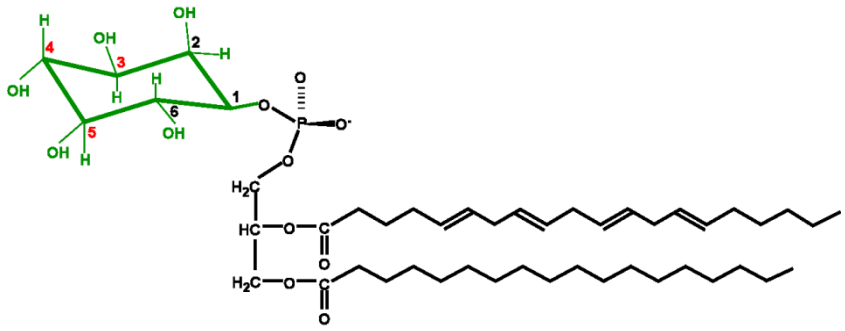

Fig. 6: Chemical structure of Phosphatidyl-inositol. The hydrophilic inositol group is drawn in green, the lipophilic phospholipid backbone in black. By differential phosphorylation in 3 -, 4 - and 5 - positions (red) nine different Phosphoinositide species are obtained. Modified from D. Oliver.

1.4.2 Phospholipase C mediates G_qPCR induced PtdIns signaling

PtdIns(4,5)P_2 was the first PtdIns to receive major attention. It was originally believed to serve only as a precursor molecule for the second messengers Ins(1,4,5)P_3 and DAG in the G_qPCR-PLC-β pathway. It was suggested to be thereby involved into the regulation of ion fluxes and signal propagation (Berridge & Irvine, 1989). More recently it has been demonstrated that PtdIns(4,5)P_2 directly regulates ion channels (Hilgemann & Ball, 1996; Baukrowitz *et al.*, 1998; reviewed in: Suh & Hille, 2008).

PtdIns(4,5)P_2 hydrolysis to Ins(1,4,5)P_3 and DAG is carried out by Phospholipase C enzymes. The diverse group of Phospholipase C consists of thirteen isotypes divided

into six groups (β, γ, δ, ε, η, ξ) (Suh *et al.*, 2008). They all hydrolyze the phosphate bond between the lipidic backbone and the myo-inositol-derived head group of PtdIns(4,5)P_2 (Drin & Scarlata, 2007). However only Phospholipase Cβ (PLC-β) enzymes are activated in consequence to G_qPCR stimulation (Suh *et al.*, 2008). This activation is mainly mediated by GTP-G_qα but can also be achieved by certain Gβγ subunits. It has been shown that Gβγ-mediated activation of PLC-β occurs via membrane recruitment. In contrast the probably more prevalent mechanism of G_qα activation is still not understood (Drin & Scarlata, 2007; Suh *et al.*, 2008).

As a necessary cofactor, all Phospholipase C enzymes need calcium (Lomasney *et al.*, 2012). In case of PLC-β, resting calcium concentrations are sufficient for enzymatic activity: its calcium dependence resembles a bell shaped curve with the maximum at about 100 µM calcium (Ryu *et al.*, 1987). As PLC-β activation liberates calcium from intracellular stores, PLC-β activation might enhance its own activity in a positive feedback manner (Rhee, 2001).

PLC-β activation is a powerful mechanism to reduce PtdIns(4,5)P_2 concentrations to approximately 10 % of their resting values (Falkenburger *et al.*, 2010b). Usually this PtdIns(4,5)P_2 cleavage is counterbalanced by fast subsequent PI5KI 5 -kinase activation (D'Angelo *et al.*, 2008). Thereby PLC-β activation also results in a notable depletion of PtdIns(4)P (Willars *et al.*, 1998; Horowitz *et al.*, 2005). PLC-β also hydrolyzes PtdIns(4)P in vitro (Ryu *et al.*, 1987). If this also happens under physiological conditions has not been demonstrated yet. Regardless if by direct or indirect means strong PLC-β activation results in depletion of PtdIns(4,5)P_2 and PtdIns(4)P. As these two molecules are the two most abundant PtdIns of the plasma membrane, a remarked decrease in overall membrane PtdIns is the consequence (Horowitz *et al.*, 2005).Therefore PLC-β activation can also affect processes that are regulated by PtdIns(4)P.

After termination of PLC-β activity PtdIns(4,5)P_2 and PtdIns(4)P are resynthesized by ATP-dependent phosphorylation steps (Suh & Hille, 2002). Thereby PtdIns(4,5)P_2 and PtdIns(4)P are restored to resting level and the signaling process is terminated (Di Paolo & De Camilli, 2006).

1.4.3 Various ion channels are modulated by Phosphoinositides

PtdIns signaling is involved in many cellular functions. Fast time scale changes in PtdIns levels are especially important for the regulation of ion channels. During the past 15 years a plethora of ion channels has been shown to be regulated by (or to depend on) PtdIns (reviewed in Suh & Hille, 2008). While for many of them a physiological implication is rather speculative, interaction mechanism and physiological function is now well established for others. The K_{ir} and K_v7 ion channel families have been investigated in detail and will serve to exemplify the most common PtdIns interaction schemes.

The family of inward rectifying potassium channels (K_{ir}) consists of eight subfamilies. All family members share the feature of an inward rectification of the potassium flux (Hille, 2001). One member of the K_{ir} family, the $K_{ir}6.2$ or K_{ATP} channel, was the first ion channel for which PtdIns(4,5)P_2 sensitivity was demonstrated (Hilgemann & Ball, 1996). PtdIns modulate K_{ATP} activity by decreasing their affinity to its blocker ATP (Baukrowitz *et al.*, 1998; MacGregor *et al.*, 2002; Suh & Hille, 2008). The interaction of this channel with PtdIns is characterized by low specificity and low affinity. As K_{ATP} channels are low in specifity ion channel activity is changed in consequence to alteration of PtdIns(4,5)P_2, PtdIns(3,4,5)P_3 or PtdIns(3,4)P_2 levels (Rohacs *et al.*, 2003). Due to their low affinity, the decrease in PtdIns concentration achieved by G_qPCR receptor activation is sufficient to alter K_{ATP} activity (Baukrowitz *et al.*, 1998).In contrast to K_{ATP}, $K_{ir}2.1$ channels are highly specific and highly affine towards PtdIns(4,5)P_2. While PtdIns(4,5)P_2 generally activates $K_{ir}2.1$, e.g. by application on excised patches, G_qPCR activation does not modify PtdIns(4,5)P_2 levels enough to alter channel activity (Rohacs *et al.*, 2003; Du *et al.*, 2004; Rohacs, 2009). In this case PtdIns may function as a cofactor which is essential for an ion channel to reach open state, but they will not mediate receptor signaling onto this channel (Suh & Hille, 2008).

The K_v7 family forms part of the superfamily of voltage gated potassium channels and consists of five members ($K_v7.1$-$K_v7.5$, KCNQ1-5). K_v7 channels are present e.g. in cardiomyocytes ($K_v7.1$), neurons ($K_v7.2$/$K_v7.3$) and in cochlear outer hair cells ($K_v7.4$) (for review, see Robbins, 2001). The K_v7 channels are a classical example of potassium channels blocked by G_qPCR activation. Their inhibition in response to application of muscarine was name giving to the “M”-current found in sympathetic neurons back in the 1980 (Brown & Adams, 1980). The M-current has been shown to

be the electrophysiological correlate of the KCNQ 2/3 gene products (Wang *et al.*, 1998). The mechanism underlying its muscarinic inhibition remained unclear for a long time, but could be clearly attributed to be a direct consequence of PtdIns(4,5)P_2 hydrolysis (Suh & Hille, 2002; Zhang *et al.*, 2003; Suh *et al.*, 2006). K_v7 are specifically sensitive to PtdIns(4,5)P_2. For inhibition of K_v7 currents turnover of PtdIns(4,5)P_2 to PtdIns(4)P is sufficient, i.e. the overall PtdIns concentration may remain unchanged (Li *et al.*, 2005; Suh *et al.*, 2006). The mechanism of interaction with phosphoinositides is probably best studied for this group of channels. This makes them a valuable tool to monitor PtdIns(4,5)P_2 changes in the plasma membrane (Suh & Hille, 2002; Zhang *et al.*, 2003; Suh *et al.*, 2004; Li *et al.*, 2005; Winks *et al.*, 2005; Suh *et al.*, 2006; Hernandez *et al.*, 2008; Hernandez *et al.*, 2009; Falkenburger *et al.*, 2010c).

1.4.4 Phosphoinositides do not only regulate ion channels

Beside their direct signaling effect on ion channels PtdIns are also involved in a wide range of other signaling processes. This includes basic functions like cell cycle control, apoptosis, cytoskeleton formation, protein trafficking or exocytosis (Di Paolo & De Camilli, 2006). Accordingly disequilibrium in PtdIns homeostasis has been linked to various pathological conditions (Halstead *et al.*, 2005). In contrast to ion channel regulation these effects are mostly not due to fast changes in PtdIns concentrations mediated by PLC-β activation. They rather result from long term changes in PtdIns concentrations by an altered activity of phosphatases and kinases (Di Paolo & De Camilli, 2006; Suh & Hille, 2008). In the context of this study the effect on these slow processes is of minor importance. To give a general overview, they are summarized in Fig. 7.

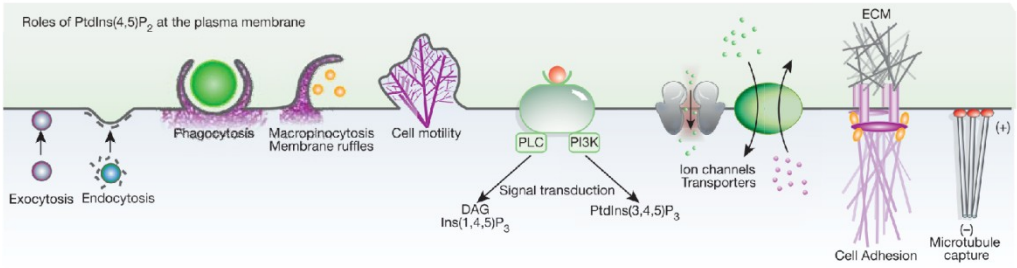

Fig. 7: Common examples of processes regulated by PtdIns(4,5)P_2. These include endo- and exocytosis, cell motility, second messenger creation, regulation of ion channels and transporters, cell adhesion and cytoskeleton formation (Figure from: Di Paolo & De Camilli, 2006).

1.5 Recent insight into the regulation of TASK channels by G_q-protein coupled receptors

The G_qPCR pathway and the physiological relevance of G_qPCR signaling for TASK channel inhibition have been described so far. This thesis investigates how G_qPCR mediated inhibition of TASK is achieved. A number of previous studies have addressed this question before. However, no consensus could be established. To understand the motivation for the present work it is thus necessary to review their experimental findings.

1.5.1 $G_q\alpha$ is essential for receptor inhibition TASK channels

It has been shown that activation of the $G_q\alpha$ subunit is required for TASK channel inhibition. Genetic knock-out and pharmacological blockage of $G_q\alpha$ abolished inhibition of TASK channels by G_qPCR (Chen *et al.*, 2006; Veale *et al.*, 2007). Furthermore constitutive activation of $G_q\alpha$ by a non-hydrolysable GTP analog maintained TASK channels inhibited after G_qPCR activation (Czirjak *et al.*, 2001; Chemin *et al.*, 2003; Chen *et al.*, 2006). It is therefore consensus that activation of $G_q\alpha$ is a necessary step within the cascade leading to TASK inhibition.

1.5.2 Activated $G_q\alpha$ may directly inhibit TASK channels

Results from Chen et al. (2006) provided good evidence for a direct interaction of $G_q\alpha$ with TASK (Fig. 8 A): In cells where $G_q\alpha$ was knocked out, TASK channel inhibition could be reconstituted by transfection of both wild-type $G_q\alpha$ and a mutant of $G_q\alpha$ that was inefficient to activate PLC. The authors could additionally show by co-

immunoprecipitation that activated $G_q\alpha$ associates with TASK channels, also suggesting a direct interaction (Chen *et al.*, 2006).

1.5.3 The role Phospholipase C is unclear

PLC-β is directly activated by $G_q\alpha$. Therefore a requirement of PLC-β in the inhibitory process would exclude a direct inhibition of TASK by $G_q\alpha$. Various studies probed the role of PLC-β for TASK channel inhibition. Some authors find that pharmacological blockage of PLC-β abolishes G_qPCR mediated TASK inhibition (Czirjak *et al.*, 2001; Chemin *et al.*, 2003). However others do not find TASK channel inhibition altered after pretreatment with a PLC-β blocker (Boyd *et al.*, 2000; Chen *et al.*, 2006).

1.5.4 TASK inhibition may result from PtdIns(4,5)P_2 depletion

As some studies found that PLC-β was involved in TASK channel inhibition the role of PtdIns(4,5)P_2 was tested. It was hypothesized that TASK channels may require PtdIns(4,5)P_2 for activity (Chemin *et al.*, 2003; Lopes *et al.*, 2005). As PtdIns(4,5)P_2 is cleaved after PLC-β activation the decrease in PtdIns(4,5)P_2 concentration could be the stimulus for TASK channel closure (Fig. 8 B). Chemin et al. showed that inclusion of PtdIns(4,5)P_2 antibodies into the intracellular solution abolished TASK currents (Chemin *et al.*, 2003). Additionally direct application of PtdIns(4,5)P_2 onto excised patches recovered channels from rundown after patch excision (Chemin *et al.*, 2003; Lopes *et al.*, 2005). Together the results from these studies suggested that the presence of PtdIns(4,5)P_2 is required for the channel to function. However this does not necessarily mean that PtdIns(4,5)P_2 hydrolysis by PLC-β effectively inhibits TASK channels after G_qPCR activation, as the residual PtdIns(4,5)P_2 might still be sufficient to keep the channel fully open (Rohacs, 2009).

It has been shown that wortmannin, a PtdIns(3)- and PtdIns(4)-kinase inhibitor, decelerates the recovery of TASK channels after G_qPCR activation (Czirjak *et al.*, 2001; Chemin *et al.*, 2003). These results suggested that changes in PtdIns(4,5)P_2 concentration as they occur due to G_qPCR activation could be sufficient to inhibit TASK channels. Inconsistently no such findings were observed for staurosporin, a broad spectrum kinase inhibitor also affecting PtdIns(3)- and PtdIns(4)-kinases despite it was used in the same study (Chemin *et al.*, 2003; Karaman *et al.*, 2008).

1.5.5 Downstream messengers have been tested

TASK channel inhibition could be also mediated by downstream messengers like $Ins(1,4,5)P_3$, calcium, DAG or Protein Kinase C (PKC).

The role of $Ins(1,4,5)P_3$ was tested twice, giving contrary results. Addition of $Ins(1,4,5)P_3$ to the intracellular solution induced a rundown of TASK currents (Chemin *et al.*, 2003) while injection of $Ins(1,4,5)P_3$ into oocytes left TASK currents unaffected (Czirjak *et al.*, 2001). Changing intracellular calcium or blocking calcium release from intracellular stores had no effect on TASK currents, suggesting that calcium was not the direct inhibitor of TASK (Czirjak *et al.*, 2001; Veale *et al.*, 2007).

Although a review reported DAG not to have any effect on TASK currents (Mathie, 2007), in fact there is no experimental evidence in literature that the effect of DAG on TASK has really been tested. The role of PKC, as the main downstream effector of DAG, has been extensively probed after the identification of various PKC phosphorylation sites in TASK channels (Duprat *et al.*, 1997; Kim *et al.*, 2000; Lopes *et al.*, 2000; Rajan *et al.*, 2000; Vega-Saenz de Miera *et al.*, 2001; Chemin *et al.*, 2003; Besana *et al.*, 2004; Mathie, 2007; Veale *et al.*, 2007). However it is now clear that PKC does not mediate TASK inhibition (Veale *et al.*, 2007; Schiekel *et al.*, in revision).

In summary, at present there are two competing hypotheses concerning the way G_qPCR transmit their signal to TASK: There could be either a direct interaction between $G_q\alpha$ and the channel (Fig. 8 A) or Phospholipase C mediated hydrolysis of $PtdIns(4,5)P_2$ might provoke TASK inhibition (Fig. 8 B). While an involvement (no matter if by direct or indirect means) of $G_q\alpha$ seems evident, experimental results concerning the role of $PtdIns(4,5)P_2$ are much more controversial.

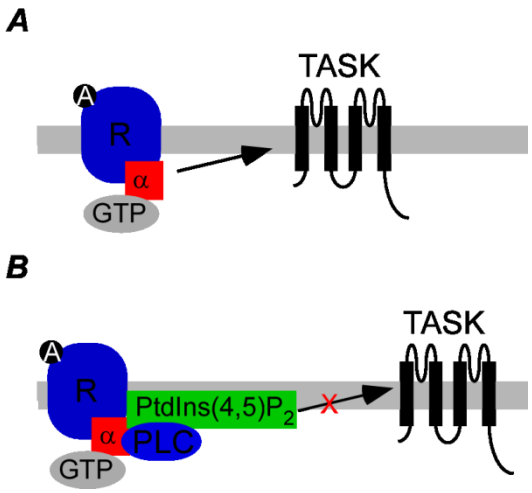

Fig. 8: Competing hypotheses on the mechanism of TASK channel inhibition: A, TASK channels are directly inhibited by $G_q\alpha$ or B, their closure is a direct consequence of PtdIns(4,5)P_2 hydrolysis. Figure adapted from Mathie, 2007.

1.6 Tools for monitoring and manipulating PtdIns levels

To substantially contribute to this highly studied field, monitoring and modulating of the candidate messenger molecules inside the living cell is required. This chapter will present the recent advances for both monitoring and manipulating of PtdIns concentrations and will discuss their limitations.

1.6.1 Live cell imaging of PtdIns dynamics

Studying of PtdIns dynamics in the living cell required the development of specific sensor domains. The discovery that certain proteins specifically interact with one type of PtdIns was an indispensable prerequisite. Study of these proteins revealed the existence of common PtdIns binding motifs. Examples of such binding motifs are the pleckstrin homology (PH) domains (Stauffer *et al.*, 1998). These domains are conserved among distinct proteins were they mediate protein-protein or protein-lipid interaction. Of special interest are the PtdIns binding PH domains which vary in their exact PtdIns specificity. In the context of the present work, two PH domains are especially noteworthy: On the one hand PLC-δ1-PH binds to PtdIns(4,5)P_2 and Ins(1,4,5)P_3, yeast Osh2p-PH on the other hand binds to PtdIns(4)P and PtdIns(4,5)P_2 (Varnai & Balla, 2006; Balla *et al.*, 2008). By coupling such PH domains to fluorescent proteins PtdIns can be "traced": A fluorescently tagged PH domain binds to a membrane where high concentrations of a PtdIns are present. When the concentration of this PtdIns decreases at the membrane the fluorescent tagged PH domain leaves the membrane and moves into the cytosol (Fig. 9). Thus membrane fluorescence

directly correlates to the membrane PtdIns concentration making the optical observation of PtdIns dynamics at the membrane of living cells possible (Stauffer *et al.*, 1998). In this study I made use of two different PH domains: $PH_{PLC\delta1}GFP$ to monitor PtdIns(4,5)P_2 specifically (Stauffer *et al.*, 1998) and $PH_{2xOSH2}GFP$ for combined observation of PtdIns(4)P and PtdIns(4,5)P_2 at the plasma membrane (Balla *et al.*, 2008).

Not only PH domains can function as PtdIns sensors. PtdIns sensors can also arise from proteins structurally unrelated to PH-domains. An example is the C-terminus of the Tubby protein that binds PtdIns(4,5)P_2 highly specific. In contrast to PLC-δ1-PH, it shows no affinity to Ins(1,4,5)P_3 (Santagata *et al.*, 2001; Szentpetery *et al.*, 2009).

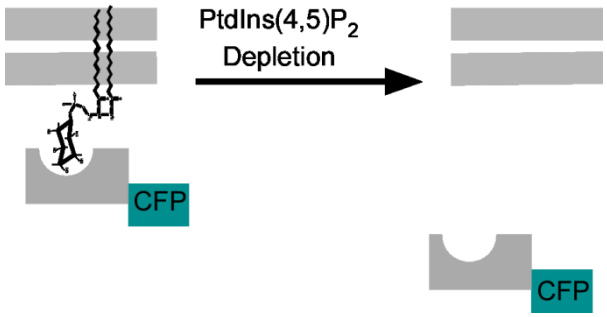

Fig. 9: Scheme of a PtdIns(4,5)P_2 fluorescence sensor. A, Fluorescent protein tagged PtdIns(4,5)P_2 binding domain (like PLC-δ1-PH or Tubby) binds PtdIns(4,5)P_2 and is thereby held at the membrane (left). Upon depletion of PtdIns(4,5)P_2 the sensor dissociates from the plasma membrane (right).

1.6.2 Manipulation of PtdIns(4,5)P_2 levels in intact cells

G_qPCR activation results in alteration of the concentration of various intracellular messengers. To investigate the effect of PtdIns on a protein under observation different approaches have been developed in the past years.

A classical way to probe the affinity of ion channels to different PtdIns is the direct application of water soluble PtdIns analogous (e.g. diC8-PtdIns(4,5)P_2) to an excised patch. Thereby the concentration of PtdIns at the inner membrane surface is increased. The achieved concentrations of PtdIns may strongly exceed physiological concentrations. An opposite effect can be achieved by application of PtdIns specific antibodies onto excised patches, resulting in a massive reduction of PtdIns concentrations (e.g.: Huang *et al.*, 1998). Results from both methods are considered to have limited portability to the situation in intact cell (Balla *et al.*, 2009).

While these both methods usually cannot be used in the intact cell, poly-cationic agents like neomycin or poly-lysine may function as PtdIns scavengers also in the

living cell. They are usually applied by diffusion from the patch pipette into the cell (e.g.: Leitner *et al.*, 2010). But also in this case PtdIns levels achieved can be far outside (i.e. below) the physiological values, and thus observed effects do not necessarily represent physiological PtdIns signals.

A more recent approach to study PtdIns dynamics is the overexpression of PtdIns-kinases. By overexpression of a certain kinase the relative abundance of different PtdIns species and their synthesis kinetics is changed (Winks *et al.*, 2005). Unfortunately such an overexpression may possibly induce long term compensatory effects that will interfere with the effect under observation (Balla *et al.*, 2009).

The latest approaches aim to alter PtdIns concentrations in the intact cell and on a time scale fast enough to be accessible to live-cell observations by electrophysiological and imaging approaches.

In the first of these approaches a chemically inducible dimerisation mechanism is used to recruit PtdIns-converting enzymes to the membrane. This concept is based on the effect of the rapamycin. In nature the membrane permeable rapamycin induces the dimerisation of two protein domains, first the FKBP domain from the FK506 binding protein and second the FRB domain from the “mammalian target of rapamycin”-protein. Both of these protein domains were modified to generate a mechanism for the recruitment different proteins to the membrane (Spencer *et al.*, 1993). On the one hand FRB was fused to the membrane anchoring sequence Lyn11 (Lyn11-FRB). On the other hand FKBP was linked to a cyan fluorescent protein (CFP)-tagged yeast PtdIns(4,5)P_2 5-phosphatase Inp54p (CF-Inp54). Application of rapamycin to cells expressing both constructs lead to a strong membrane translocation of the CF-Inp54 phosphatase and pronounced depletion of PtdIns(4,5)P_2 (Fig. 10 A) (Suh *et al.*, 2004; Varnai *et al.*, 2006).

A distinct approach to deplete membrane PtdIns became available by the characterization of the voltage sensitive phosphatase from Ciona intestinalis (Ci-VSP). Ci-VSP consists of a voltage sensing domain – as known from many voltage-sensitive ion channels – linked to a phosphatase (Murata *et al.*, 2005). The phosphatase domain exhibits 5’phosphatase activity on PtdIns(4,5)P_2 and PtdIns(3,4,5)P_2 (Halaszovich *et al.*, 2009). Membrane depolarization results in a conformational change in Ci-VSP making PtdIns accessible for the phosphatase (Fig. 10 B). By this mechanism Ci-VSP

becomes a tool that quickly, gradually and reversibly alters PtdIns levels upon depolarization (Murata *et al.*, 2005; Halaszovich *et al.*, 2009; Sakata *et al.*, 2011).

Both of these approaches are able to mimic PLC-β induced PtdIns(4,5)P_2 depletion. But in contrast to PLC-β they do not create the downstream messengers Ins(1,4,5)P_3 and DAG (Willars *et al.*, 1998; Horowitz *et al.*, 2005; Suh *et al.*, 2006). Noteworthy the amount of overall membrane PtdIns remains unchanged in both approaches, while it is strongly depleted by PLC-β activation (Willars *et al.*, 1998; Horowitz *et al.*, 2005; Balla *et al.*, 2008).

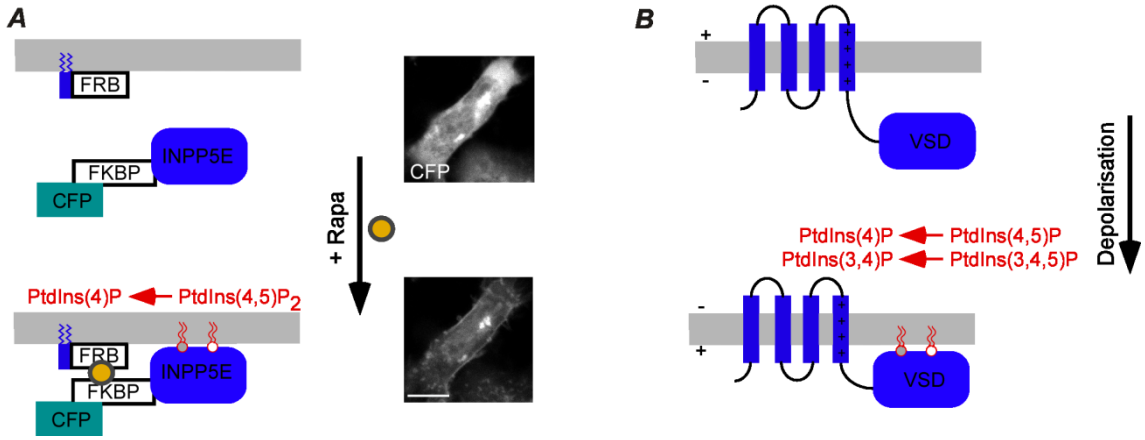

Fig. 10: Recently developed tools to manipulate PtdIns concentrations in the living cell. A, The rapamycin based membrane recruitment strategy consists of a membrane-anchored FRB protein and FKBP protein linked to the 5 -phosphatase Inp54p and a CFP. Application of rapamycin leads to a dimerisation of both constructs and subsequent hydrolysis of PtdIns(4,5)P_2 to PtdIns(4)P. B, The voltage sensitive phosphatase Ci-VSP. Depolarization activates the phosphatase domain resulting in dephosphorylation of PtdIns(4,5)P_2 and PtdIns(3,4,5)P_3 at the 5-position.

1.7 Aim of this study

Despite the crucial physiological relevance of G_qPCR mediated inhibition of TASK channels investigation of the molecular mechanism underlying this inhibition is still unclear (Mathie, 2007). As existing evidence is rather controversial a careful re-evaluation using state-of-the-art methods is required.

Today there are two competing hypothesis how TASK channel inhibition could occur: TASK channels might be either closed by activated $G_q\alpha$, in a PLC-β independent fashion (Chen *et al.*, 2006) or they may be closed by depletion of PtdIns(4,5)P_2 following PLC-β activation (Czirjak *et al.*, 2001; Chemin *et al.*, 2003; Lopes *et al.*,

2005). PLC-β mediated PtdIns(4,5)P_2 hydrolysis has a key function in G_qPCR signaling. Questioning the exact role of PtdIns(4,5)P_2 hydrolysis for TASK channel inhibition can help to evaluate the recently existing hypotheses.

This study therefore aims to clarify the physiological role of PLC-β mediated PtdIns(4,5)P_2 hydrolysis for TASK channel inhibition. I therefore question (1) whether PtdIns(4,5)P_2 represents the direct mediator of TASK channel inhibition, (2) whether functioning of PLC-β is required for successful TASK inhibition and (3) whether PtdIns(4,5)P_2 hydrolysis by PLC-β is a necessary step within the signaling cascade.

2 Materials and methods

2.1 Molecular biology

Generation of expression vectors was performed by Eva Naudascher, Gisela Fischer and Olga Ebers as described elsewhere (Lindner *et al.*, 2011). The constructs used in this study are listed in Tab. 2.

Tab. 2: Constructs used in this study, source or reference and vector informations

Construct	Reference	Vector	See chapter
pEGFP-C1	Clontech, Laboratories, Mountain View, CA, USA	-	-
CF-Inp54	(Suh & Hille, 2008)	pCFP-N1	1.6.2
Ci-VSP-RFP	(Halaszovich *et al.*, 2009)	pRFP-C1	1.6.2
K_v7.4	NM_004700.2	pEGFP-C1	1.4.3
Lyn11-FRB	(Suh & Hille, 2008)	pC_4R_HE	1.6.2
m1-R	NM_000738.2	pSGHV0	1.3
PH_{2xOSH2}GFP	(Balla *et al.*, 2008)	pEGFP-C1	1.6.1
$PH_{PLC\delta1}$GFP	(Halaszovich *et al.*, 2009)	pEGFP-N1	1.6.1
$PH_{PLC\delta1}$YFP	P51178	pcDNA3	1.6.1
RF-PJ	(Lindner *et al.*, 2011)	pEGFP-C1	3.3
RF-PJ-5ptase	(Lindner *et al.*, 2011)	pEGFP-C1	3.3
RF-PJ-dead	(Lindner *et al.*, 2011)	pEGFP-C1	3.3
RF-PJ-Sac	(Lindner *et al.*, 2011)	pEGFP-C1	3.3
TASK-1	(Zuzarte *et al.*, 2009)	pcDNA3.1	1.2
TASK-3	(Rajan *et al.*, 2002)	pcDNA3.1	1.2
$PKC\gamma_{26-89}$YFP	NW_047555	pYFP-N1	3.6
Tubby-RFP	(Santagata *et al.*, 2001)	pRFP-C1	1.6.1
TASK-1_{NQ}	(Zuzarte *et al.*, 2009)	pcDNA3.1	3.5
Et-AR	(Schiekel *et al.*, in revision)	dsRed	3.5

2.2 Cell culture and transfection

Chinese Hamster Ovary (CHO) cells were cultured in MEM alpha Medium (GIBCO, Invitrogen, Carlsbad, CA, USA) with 10% fetal bovine serum (Biochrom AG, Berlin, Germany) and 1% PenStrep (GIBCO, Invitrogen, Carlsbad, CA, USA) added. Cells were seeded on glass cover slips for electrophysiology and confocal microscopy or on glass bottom dishes (WillCo Wells B. V., Amsterdam, The Netherlands) for total internal reflection (TIRF) microscopy experiments. 24 to 48 hours after seeding cells were transiently transfected with JetPEI transfection reagent (PolyPlus Transfection, Illkirch, France), at 70% confluence.

The expression vectors used are summarized in Tab. 2. When multiple constructs were used in the same transfection, the total amount of DNA was kept constant. If no DNA coding for a fluorescent protein was included, the empty pEGFP-C1 vector was

added in a mass ratio of approximately 1:3 to be able to select transfected cells in patch-clamp experiments. All experiments were performed another 24 to 48 hours after transfection. Culturing of the CHO cells was mainly performed by Sigrid Petzold, Olga Ebers, Christian Goecke and intermittently by myself.

For experiments sufficient expression levels of the transfected constructs were verified as follows: When an ion channel was included into the transfection, its presence was documented by electrophysiological recording of the characteristic current. Presence of the fluorescent biosensors $PH_{PLC\delta1}$GFP or PH_{2xOSH2}GFP in TIRF experiments was evidenced by green membrane fluorescence. When Ci-VSP-RFP was included in the transfection cells expressing Ci-VSP-RFP were selected for a clear membrane-bound red fluorescence. For experiments requiring co-expression of the rapamycin system (i.e. membrane anchor and phosphatase) only cells were selected that showed a clear cytosolic CFP or RFP fluorescence respectively. Cells were only included in the analysis when a translocation of the CFP or RFP fluorescence could be observed upon application of rapamycin. Translocation indicates successful expression of both, the membrane anchor and the fluorescence-tagged enzyme.

2.3 Chemicals

A list of chemicals used in this study is given in Tab. 3. XE991 and OxoM were both prepared as 10 mM stock solution in H_2O. Rapamycin was purchased as a solution in Me_2SO and stored in single use aliquots. Analogously, U-73122 and U-73343 were dissolved in Me_2SO to a concentration of 5 mM and stored in single use aliquots. The peptide Et-1 was dissolved in 1 % acetic acid to a stock concentration of 200 mM. All stocks were stored as aliquots at - 20 ° C and diluted to their final concentration in Ex-0 directly before use. Final concentration of Me_2SO did never exceed 0.1 vol% in the application solution. Solutions containing acetic acid were adjusted for pH before use. Application solutions of U-73122 and U-73343 were renewed every 30 to 45 min as the observed effects of U-73122 strongly decreased after this interval of time.

Tab. 3: List of chemicals used with their supplier. Abbreviations are marked as bold.

Substance	Supply
(Et-1): Endothelin-1	Gift from J. Daut (Schiekel *et al.*, in revision)
$CaCl_2$	Cat-No: CN93.1, Carl Roth GmbH + Co. KG, 76231 Karlsruhe, Germany
D-Glucose	Cat-No: X997.1, Carl Roth GmbH + Co. KG
HEPES: 4-(2-Hydroxyethyl)piperazine-1-ethanesulfonic acid	Cat-No: 9105.2, Carl Roth GmbH + Co. KG
K_2EGTA: Ethylenglycol-bis(aminoethylether)-N,N,N′N′-tetraacetic acid	Cat-No: 3054.1, Carl Roth GmbH + Co. KG
K_4BAPTA: 2,2′-(Ethylenedioxy)dianiline-N,N,N′,N′-tetraacetic acid	Cat-No: 19641, MERCK KGAA, 64293 Darmstadt, Germany
KCl	Cat-No: 6781.1, Carl Roth GmbH + Co. KG
KOH	Cat-No: 6751.3, Carl Roth GmbH + Co. KG
Me_2SO: Di-methyl-sulfoxide	Cat-No: D2650, Sigma Aldrich, Sigma-Aldrich Chemie GmbH, Munich, Germany
$MgCl_2$	Cat-No: KK36.1, Carl Roth GmbH + Co. KG
Na_2AMP-PCP: β,γ-Methyleneadenosine-5′-triphosphate	Cat-No: M7510, Sigma Aldrich
Na_2ATP: Adenosine-tri-phosphate	Cat-No: A6559, Sigma Aldrich
Na_3-GTP: Guanosine-tri-phosphate	Cat-No: G8877, Sigma Aldrich
NaCl	Cat-No: 3957.1, Carl Roth GmbH + Co. KG
NaH_2PO_4	Cat-No: 5075.1, Carl Roth GmbH + Co. KG
NMDG: N-Methyl-D-glucamine	Cat-No: M2004, Sigma Aldrich
OxoM: Oxotremorine-Methiodide	Cat-No: 1067, Tocris Bioscience, Bristol, UK
Rapamycin	Rapamycin inSolution, Cat-No: 553211; Merck
U-73122	Cat-No: U6756, Sigma Aldrich
U-73343	Cat-No: M6881, Sigma Aldrich
XE991: (10,10-bis[4-pyridinylmethyl]-9[10H]-anthracenone- dihydrochloride)	Cat-No: 2000, Ellisville, Missouri, USA

2.4 Solutions

Extracellular solution (Ex-0) used to perfuse the cells during measurement contained (mM) 144 NaCl, 5,8 KCl, 1.3 $CaCl_2$, 0.9 $MgCl_2$, 0.7 NaH_2PO_4, 10 HEPES and 5.6 D-glucose. pH was adjusted to 7.4 with NaOH and osmolarity was checked with OSMOMAT 030 (Gonotec GmbH, Berlin, Germany). NaCl was replaced by an equimolar amount of NMDG-Cl when indicated. Osmolarity was 310 +/- 5 mOsm/kg.

Standard intracellular solution (ICS) contained (mM) 135 KCl, 3.5 $MgCl_2$, 0.1 $CaCl_2$ (equals 100nM free Ca^{2+}), 5 K_2EGTA, 5 HEPES, 2.5 Na_2-ATP, 0.1 Na_3-GTP 0 with pH adjusted to 7.3 by adding KOH. Osmolarity was 295 +/- 5 mOsm/kg.

For some experiments Na_2-ATP was replaced by 3 mM Na_2-AMP-PCP. In other experiments the EGTA concentration was either raised to 20 mM or EGTA was replaced by 20 mM BAPTA. As both EGTA and BAPTA are provided as potassium salts the amount of KCl had to be reduced as indicated below. Thereby osmolarity was also held in the desired range. A summary of all ICS used is given in Tab. 4.

Tab. 4: Composition of intracellular solutions used in this study. Values represent the concentrations in mM.

	ICS	ICS-AMP-PCP	ICS-BAPTA	ICS-EGTA
KCl	135	135	105	105
$MgCl_2$	3.5	3.5	3.5	3.5
$CaCl_2$	0.1	0.1	0.1	0.1
K_2EGTA	5	5	0	20
K_4BAPTA	0	0	20	0
HEPES	5	5	5	5
Na_2-ATP	2.5	0	3	3
Na_2-AMP-PCP	0	3	0	0
Na_3-GTP	0.1	0.1	0.1	0.1

2.5 Patch-clamp experiments

When investigating the regulation of any ion channel it is of special importance to observe the current through the channel under observation. Today the patch-clamp technique is a widely established method for the observation of such transmembrane currents (Neher & Sakmann, 1976; Hamill *et al.*, 1981). The following paragraph will not give methodological details but will only describe how patch-clamp experiments were carried out specifically in this study.

Measurements were performed in the whole cell voltage clamp mode either with EPC10 combined patch-clamp amplifier and interface (HEKA Elektronik Dr. Schulze GmbH, Ludwigshafen/Rhein, Germany) or Axopatch 200B (Axon Instruments, Molecular Devices, Sunnyvale, CA, USA) with a separate ITC-16 interface (Instrutech, HEKA Elektronik Dr. Schulze GmbH). Recorded currents were low-pass filtered at 2 kHz and sampled at 5 kHz

Borosilicate glass capillaries (GB100T-8P, Science Products, Hofheim, Germany) or quartz glass capillaries (Q100-70-7.5 Sutter Instrument, Novato, CA, USA) both with an outer diameter of 1 mm were used for patch pipettes. Pipettes were crafted on a P2000 Puller (Sutter) and only used if the open pipette resistance was between 1 and 4 MΩ when filled with ICS.

In all experiments transfected cells were identified by fluorescence as described above using a C-SHG1 mercury lamp (Nikon, Tokyo, Japan) with an Eclipse E600FN Microscope (Nikon, Tokyo, Japan). Patch pipettes and the headstage were fixed to an electrically driven 3-axis mini 25-XL manipulator (Luigs & Neumann Feinmechanik & Elektrotechnik GmbH, Ratingen, Germany) under control of a MCL-3 (Lang GmbH &

Co. KG, Hüttenberg, Germany). Seal formation was achieved by approaching the pipette directly to the cell and subsequently releasing the positive pressure. Pressure (approx. 0.07 bar) was generated by a PR-10 pressure regulator (Scientific Instruments West Palm Beach, Florida). Fast capacitances were compensated after gigaseal formation.

Membrane rupture was performed by short application of negative pressure and a synchronous "Zap" – a 0.1 ms voltage pulse of about -500 mV. By rupture of the membrane the whole-cell mode was achieved. The series resistance (R_s), mainly reflecting the resistance across the ruptured membrane under the pipette tip was subsequently measured. R_s was not compensated, but was carefully observed throughout the measurement for changes. Cells were only accepted if R_s was within the range of 2 to 6 MΩ.

Electrophysiological recordings were controlled by PatchMaster (HEKA Elektronik Dr. Schulze GmbH) on a PC (Dell Inc., Round Rock, TX, USA) or Mac (Apple Inc., Cupertino, CA,USA).

2.6 Microscopy

In this study it was frequently necessary to determine whether a fluorescent probe was localized at the cell membrane or in the cytosol. The resolution of classical wide-field microscopy is usually insufficient for this task. Therefore I made use of Total Internal Reflection Fluorescence Microscopy (TIRF) that allows to specifically observe membrane fluorescence. In some occasions I used confocal microscopy instead of TIRF. Use of confocal microscopy became necessary for the simple practical reason that the confocal microscopy setup used in this laboratory allowed observation of 3 different fluorescent probes at a time, while the TIRF setup did not.

2.6.1 Total internal reflection fluorescence microscopy (TIRF)

TIRF is a highly sensitive method to study changes of fluorescence in regions in nearest proximity to the cell membrane. Briefly in the TIRF technique, the fluorescent probe is not excited directly by the light of a laser source, but rather by an evanescent field. This field is obtained as a "side effect" of total reflection. It occurs as light enters from material of higher into a material of a lower refractive index at an angle that is equal or smaller than a critical angle. The critical angle is a function of the refractive index of the two media. The intensity of this evanescent field exponentially decreases

with the distance from the interface and depends on the wavelength of the laser light, the numerical aperture of the microscope objective, the refractive index and the angle of the exciting light entering the refractive plane. The length constant for the depth of the evanescent field is usually around 80 nm for visible light.

By this decay of the evanescent field only the fluorescent probes in the closest proximity of the refractive plane (i.e. the fluorescent probes in the cell membrane attached to the refractive plane) are excited (Fig. 10 B). A more detailed description TIRF microscopy and its application in bioscience is provided elsewhere (Yuste & Konnerth, 2005).

In this study TIRF imaging was performed with a BX51WI upright microscope (Olympus, Hamburg, Germany) equipped with a TIRF condenser (numerical aperture of 1.45; Olympus) and a 488 nm laser (20 milliwatts; Picarro, Sunnyvale, CA). Fluorescence was observed through a LUMPlanFI/IR 40x/0.8-numerical aperture water immersion objective (Olympus). Image acquisition was carried out with an IMAGO-QE cooled CCD camera (TILL Photonics GmbH, Gräfelfing, Germany). Wide-field fluorescence illumination was achieved with a monochromator (Polychrome IV, TILL Photonics GmbH) coupled to the BX51WI microscope through fiber optics. GFP fluorescence was excited at 488 nm. The laser shutter for TIRF illumination, the monochromatic light source, and image acquisition were controlled by TILLvisION software (TILL Photonics GmbH). For experiments combining electrophysiology and TIRF imaging, data acquisition was synchronized by triggering PatchMaster protocols from the TILL imaging system.

2.6.2 Confocal microscopy

Confocal microscopy is a high resolution fluorescent microscopic method first described in the 1950ies (Minsky, 1957) and subsequently introduced into biosciences (e.g.: Egger & Petran, 1967). For review see (Fine *et al.*, 1988; Fine, 2007).

A confocal microscope (in this case: laser scanning microscope) consists of a laser emitting light of a defined wavelength through an aperture of minimal size onto one spot of a specimen, thereby exciting the fluorescent proteins at that single spot in the focal plane. The size of this spot is described by the point spread function (PSF), determining the maximal resolution of any light microscope. To increase resolution a detector aperture (called pinhole) is introduced in confocal microscopy. This pinhole is

only permeable for light that arises from one single spot. The size of this spot is also determined by the PSF. Ideally the excited spot and detected spot completely overlap. In contrast to wide field microscopy in confocal microscopy the discriminable spot size is determined by the product of the excitation PSF and the detection PSF. Thereby the resolution of confocal microscopy strongly approaches the diffraction limit. By this process not the whole specimen is monitored at a time, but just one single point is detected, the process has to be repeated for each point of the specimen, i.e. it has to be scanned (Fig. 10 A).

In this study I used an upright LSM 710 Axio Examiner.Z1 microscope equipped with a W Plan/Apochromat 20x/1.0 DIC M27 75-mm water immersion objective (Carl Zeiss AG, Jena, Germany). Thereby a lateral resolution of approximately 170 nm can be achieved for an excitation wave length of 458 nm. RFP and CFP were excited at 561 nm using a diode-pumped solid-state laser (Carl Zeiss) and at 458 nm using an Argon laser (Carl Zeiss) respectively. CFP emission was sampled at 454 – 581 nm and RFP emission at 582 – 754 nm. When performing experiments where an additional YFP-tagged sensor was included, this was excited at 514 nm using an Argon laser and sampled at 519 – 583 nm. Additionally the detection bandwidth for CFP was adjusted to 454 – 515 nm.

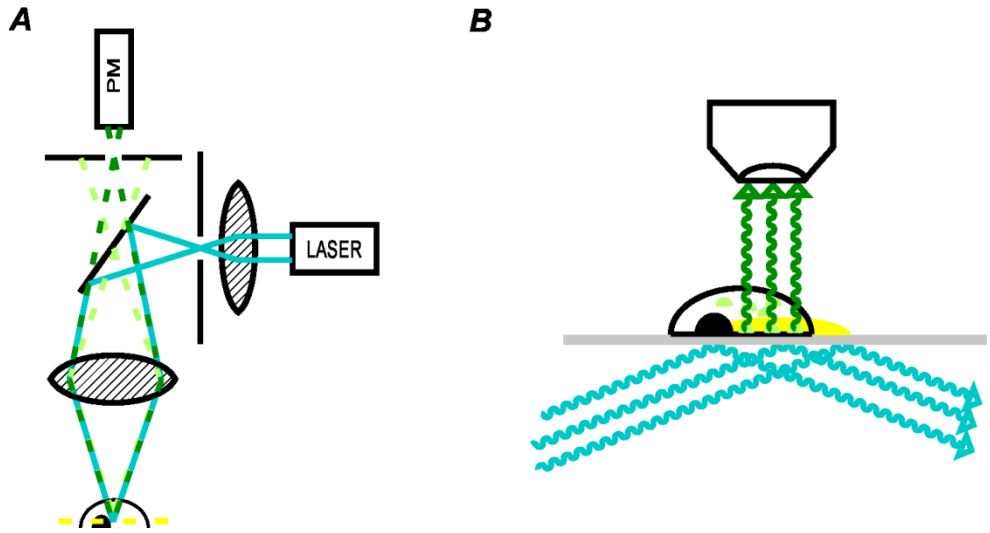

Fig. 10: Schematic drawings illustrating the principles of confocal (A) and TIRF (B) microscopy. A, A single spot of a fluorescent specimen is excited by laser light (cyan). Light emitted from the specimen (dark green) only passes the pinhole if it originates directly from the focal plane (yellow). Light from outside this plane (light green) fails to pass the pinhole. B, Laser light (cyan) is totally reflected at the lower surface of a glass dish (gray), thereby inducing an evanescent field (yellow) that excites fluorescent sensors (light green) in close proximity to the dish's surface.

2.7 Bath chamber and application of chemicals

During both imaging and electrophysiological recordings cells were kept within a bath chamber. This chamber was continuously perfused with Ex-0 to keep the extracellular environment of the cells constant during the experiment. For this work it was of importance to alter the extracellular conditions during the experiments. For instance it was necessary to expose the cell to extracellular solutions which contained the muscarinic agonist OxoM or rapamycin. To quickly exchange extracellular fluids an application barrel (Microfil 28 Gauge, World Precision Instruments Inc., Sarasota, FL, USA) fixed to a custom-built manipulator was placed in front of the cell before the beginning of the recordings. This barrel was connected to various tubes. Each of these tubes could provide a different solution. The flow through these tubes was switchable by a tree way valve. A steady flow of Ex-0 from one of the tubes through the barrel was maintained and switched to an alternative solution when required. The application system was optimized for low dead space, allowing complete exchange of the extracellular solution within a few seconds.

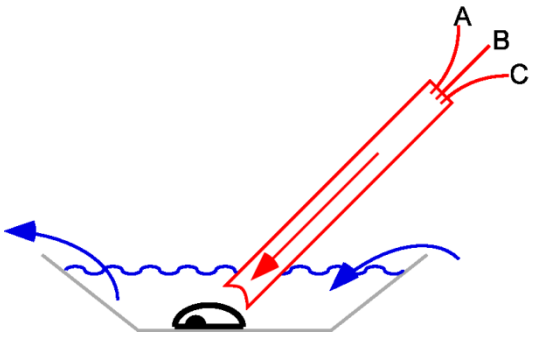

Fig. 11: Schematic view of the bath chamber and the application system. Cell under observation (black) is located in a bath chamber (gray) and continuously perfused with Ex-0 (blue). Alternative solutions (A, B, C) can be applied directly onto the cell via the application system (red).

2.8 Data analysis

Data were analyzed using IgorPro (Wavemetrics, Lake Oswego, Oregon/USA) and TILLvisION software.

Regions of interest (ROI) in TIRF recordings were defined to include the majority of a single cell's footprint. To avoid movement artifacts the margins of the cell were excluded from analysis. F/F_0 -traces were calculated from the TIRF signal intensity F, averaged from the ROI, and the initial fluorescence intensity F_0. Fluorescence intensities were background-corrected. This background correction was achieved by subtracting the signal obtained from a cell-free reference area from the signal obtained from the cell under observation.

All TIRF traces were further corrected for bleaching of the fluorescent proteins. Signal decrease at the beginning of a recording before any other intervention can usually be attributed to bleaching of the fluorescent probes (e.g.: Halaszovich *et al.*, 2009). To correct traces for bleaching the initial signal decay was fit monoexponentially. The obtained fit curve was extrapolated and subtracted from the entire recording.

Time constants were obtained from mono-exponential fits of the single traces. All data are given as mean ± standard error of the mean, with n representing the number of individual cells analyzed. Statistical analysis was performed by ANOVA test followed by a two-tailed Dunett's t-test. Significance was assigned for $p < 0.05$ and marked with asterisks in the corresponding graph.

3 Results

3.1 Reconstitution of G_qPCR induced TASK channel inhibition in an experimentally suitable model system

It is well established that TASK-1 and TASK-3 channels are under control of G_qPCR in both, native tissue and cultured cells (Boyd *et al.*, 2000; Czirjak *et al.*, 2001; Chemin *et al.*, 2003; Lopes *et al.*, 2005; Chen *et al.*, 2006; Mathie, 2007; Veale *et al.*, 2007). To access the question how G_qPCR inhibition of TASK is carried out, an established cell line was used in this study. Chinese hamster ovary (CHO) cells show almost no endogenous electrical currents and are easy to transfect. They are therefore commonly used for electrophysiological studies (e.g.: Leitner *et al.*, 2010). To test if this model system would serve for my purposes I expressed either TASK-1 or TASK-3 alone in CHO cells. Currents were recorded after whole cell formation in response to a voltage ramp from -100 mV to +50 mV (Fig. 13, A). Cells expressing TASK-1 only showed small current amplitudes (100 – 500 pA) compared to those obtained in cells expressing TASK-3 (2 - 6 nA, Fig. 13, a). As expected for cells exhibiting predominantly a potassium conductance the resting potential of these cells was close to the reversal potential of potassium.

TASK currents are inhibited by extracellular acidification (Duprat *et al.*, 1997). To further document that the recorded currents represent TASK, I superperfused the cells with an extracellular solution with pH = 5.9 for 1 min. Under this condition currents in both TASK-1 and TASK-3 transfected cells were almost completely inhibited (Fig. 13, B). With these results I conclude that CHO cells heterologously expressing TASK-1 or TASK-3 provide an experimental environment suitable to study TASK channels.

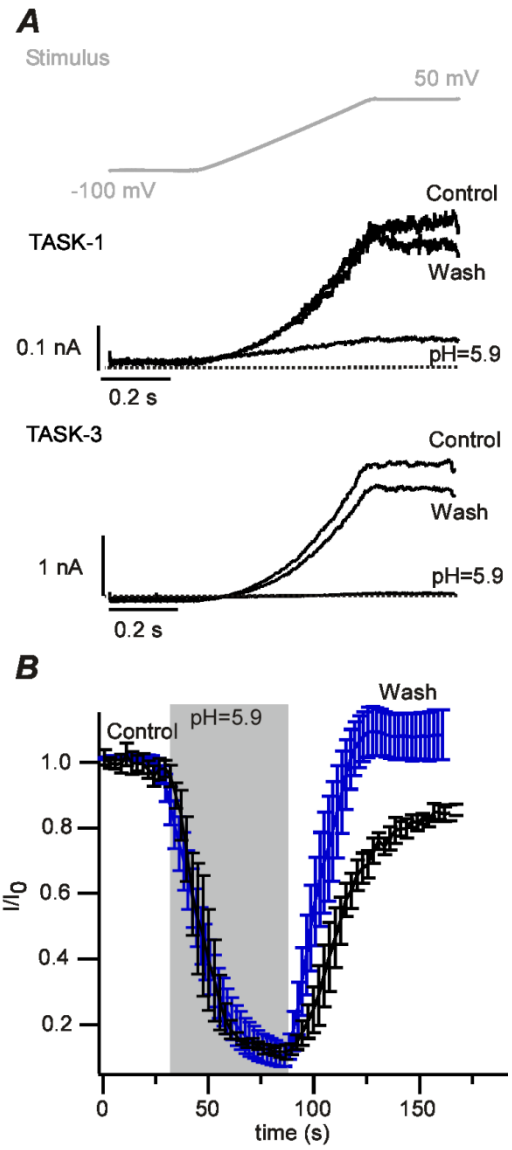

Fig. 13: Whole cell recordings from CHO cells heterologously expressing TASK-1 or TASK-3. A, A stimulus ramp (gray, top) from – 100 to + 50 mV was used to record TASK currents. CHO cells expressing TASK-1 exhibited the characteristic pH sensitive current. The three traces shown were recorded from a representative cell directly before, at the end of, and 1 min after application of an extracellular solution with pH 5.9 (black, middle). Analogous recordings from a CHO cell expressing TASK-3 (black, bottom). B, Average and normalized time courses obtained from CHO cells expressing TASK-1 (black, n=5) or TASK-3 (blue, n=8). The area marked in gray indicates the time interval where cells were exposed to an extracellular solution with pH decreased to 5.9. Upon application of low pH TASK-1 currents drop to 9.9 ± 2.2 % of their original value. Analogously TASK-3 currents were reduced to 9.0 ± 3.6 %.

In a next step it was necessary to reconstitute G_qPCR inhibition of TASK in the model system described above. When TASK-1 or TASK-3 were co-expressed with the G_qα-coupled muscarinic acetylcholine receptor (m1R) 1 minute application of 10 µM of the muscarinic agonist Oxotremorine-M (OxoM) led to a fast and almost complete inhibition of both TASK-1 and TASK-3 currents. Recovery was much slower and only achieved 70% of the initial value, reaching steady state after 4 minutes (Fig. 14 A).

A common and fast downstream mediator of the G_qPCR signaling cascade is PtdIns(4,5)P_2 hydrolysis by PLC-β (e.g.: Horowitz *et al.*, 2005). This lipid has repetitively been shown to mediate G_qPCR induced ion channel inhibition and this role

has also been suggested for TASK-1 and TASK-3 (Czirjak *et al.*, 2001; Chemin *et al.*, 2003; Lopes *et al.*, 2005).

To confirm that G_qPCR activation results in a decrease of PtdIns(4,5)P_2 levels I made advantage of two distinct but well established PtdIns(4,5)P_2 biosensors. The PH-domain of Phospholipase Cδ1 fused to a GFP ($PH_{PLC\delta1}$GFP) as an optical sensor and K_v7.4, a bona-fide PtdIns(4,5)P_2-sensitive voltage gated potassium channel as an electrophysiological sensor were used (Stauffer *et al.*, 1998; Zhang *et al.*, 2003; Delmas & Brown, 2005; Varnai *et al.*, 2006).

In live cell TIRF microscopy changes in $PH_{PLC\delta1}$GFP membrane association were monitored in CHO cells co-expressing m1R and $PH_{PLC\delta1}$GFP. Application of 10 µM OxoM (1 min) lead to a pronounced decrease in membrane fluorescence. Notably decrease of $PH_{PLC\delta1}$GFP signal occurred much slower than inhibition of TASK channels. Recovery kinetic after agonist washout was almost similar to TASK-1 (Fig. 14 B, D). If PtdIns(4,5)P_2 was directly involved in TASK inhibition, inhibition kinetics would suggest that the affinity of $PH_{PLC\delta1}$GFP to PtdIns(4,5)P_2 was higher compared to that of TASK.

Patch-clamp recordings from cells co-expressing m1R and K_v7.4 showed a fast and strong current inhibition when subjected to the same experimental protocol (i.e. 10 µM OxoM for one minute).Total extent of inhibition was comparable to the inhibition observed in TASK, but inhibition kinetics where slower. K_v7.4 current recovery was also incomplete and occurred slightly slower than in TASK (Fig. 14 C, D, Tab. 5). Assuming that PtdIns(4,5)P_2 mediates TASK inhibition these results would suggest that affinity towards PtdIns(4,5)P_2 was higher also in K_v7.4 than in TASK.

In summary activation of m1R resulted in both, inhibition of TASK channels and PtdIns(4,5)P_2 depletion. However, inhibition proceeded consistently faster in TASK than the signal decay of the two bona-fide PtdIns(4,5)P_2 dependent processes monitored.

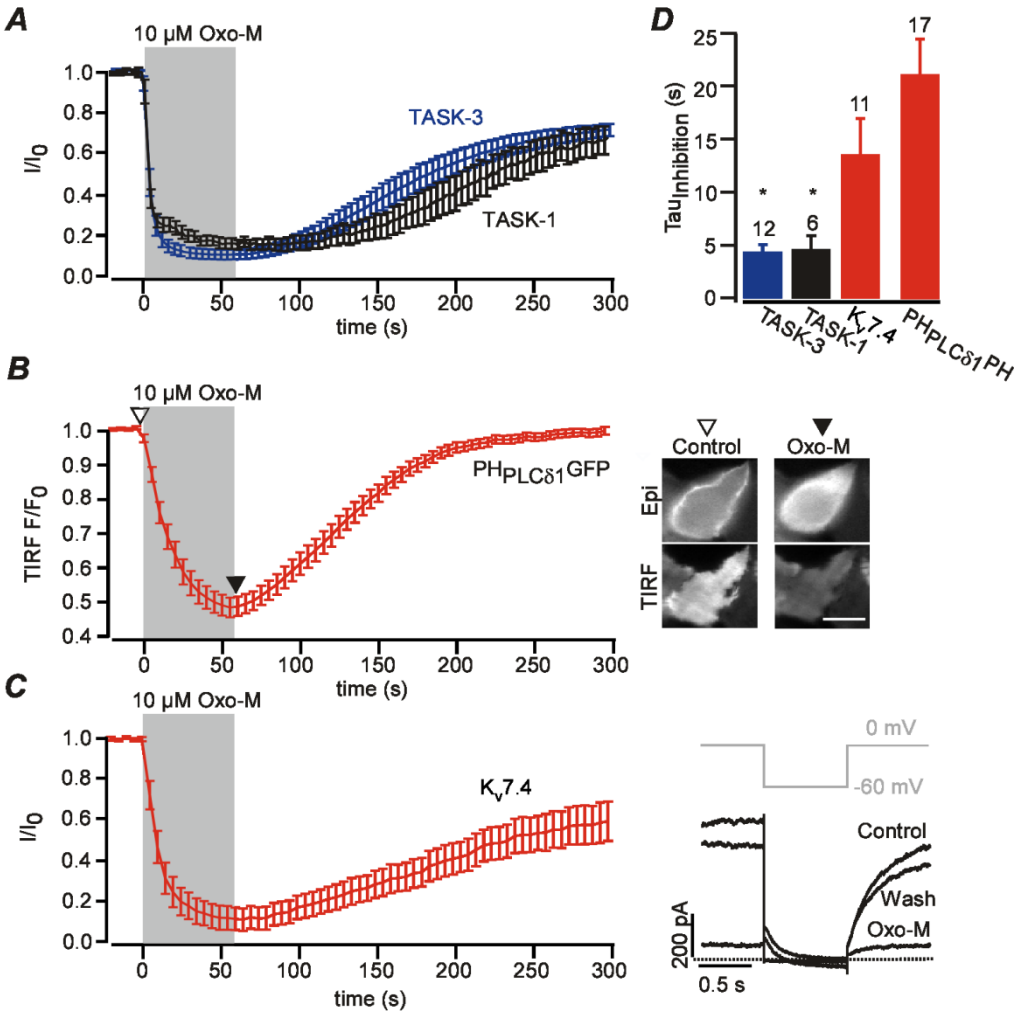

Fig. 14: Receptor-mediated inhibition of TASK channels and concomitant depletion of PtdIns(4,5)P_2**.** A, shows averaged time courses of cells expressing m1R and either TASK-1 or TASK-3. Application of the muscarinic agonist OxoM (10 µM, 60 s) inhibited currents to 17.0 ± 2.4 % for TASK-1 and 9.7 ± 2.4 % for TASK-3. B, TIRF recordings from CHO cells expressing m1R and $PH_{PLC\delta1}$GFP. Application of 10 µM OxoM triggered a strong and reversible decrease in TIRF fluorescence, indicative of translocation of the GFP-fused sensor from the membrane to the cytosol. Insets show epifluorescence (upper) and TIRF image (lower panel) of a representative cell before and after application of OxoM. Scale bar, 10 µm. C left, K_v7.4 recordings analogous to A where OxoM reduced currents to 12 ± 5.5 % of their initial value. C right, voltage protocol (gray) as used for recording of K_v7.4 currents (Brown & Adams, 1980) and current response (black) as obtained from a representative cell. D Average time constants for the onset of current inhibition and $PH_{PLC\delta1}$GFP translocation of the data shown in A-C. Asterisks indicate significantly faster time constants of TASK1 and TASK3 compared to K_v7.4 ($p \leq 0.05$).

Tab. 5: Summary of maximum inhibition and time constants obtained for TASK-1, TASK-3, $K_v7.4$ and $PH_{PLC\delta1}GFP$ on G_qPCR activation.

	I/I_0 or F/F_0	τ(signal decay)	τ(recovery)	N
TASK-1	0.17 (±0.76)	4.82 (±1.18)	104.16 (±25.35)	6
TASK-3	0.097 (±0.73)	4.61 (±0.59)	74.02 (±17.27)	12
$K_v7.4$	0.12(±0.64)	13.8 (±3.28)	166.65 (±72.26)	11
$PH_{PLC\delta1}GFP$	0.49 (±0.03)	21.43 (±3.18)	101.92 (±13.51)	17

3.2 Specific depletion of PtdIns(4,5)P_2 does not inhibit TASK channels

To evaluate the proposed role of PtdIns(4,5)P_2 I used various genetically encoded tools that specifically mimic G_qPCR induced PtdIns(4,5)P_2 depletion without affecting the concentrations of the second messenger molecules, especially DAG, Ins(1,4,5)P_3 or calcium, that might be induced by PLC-β activity.

In a first approach the voltage gated 5 -phosphoinoside-phosphatase Ci-VSP (Murata *et al.*, 2005; Halaszovich *et al.*, 2009) was used. It has been shown that in cells expressing Ci-VSP depolarization results in a rapid dephosporylation of PtdIns(4,5)P_2 to PtdIns(4)P (Halaszovich *et al.*, 2009; Falkenburger *et al.*, 2010c). To verify the efficacy of this approach cells co-expressing Ci-VSP and $K_v7.4$ were patched. In response to a 50 s depolarization step to +80 mV $K_v7.4$ currents were strongly inhibited. Noteworthy the extent of current inhibition achieved was considerably lower than that achieved by m1R activation (Fig. 12 A, Tab. 6).

Subsequently the effect of Ci-VSP induced PtdIns(4,5)P_2 depletion on TASK currents was tested. Ci-VSP was therefore co-expressed with either TASK-1 or TASK-3 and recordings analogously to the experiments with $K_v7.4$ were performed. In contrast to the observations on $K_v7.4$ neither TASK-1 nor TASK-3 currents were altered by depolarization steps to +80 mV (Fig. 12 A, Tab. 6).

To evaluate the extent of PtdIns(4,5)P_2 depletion I compared these results with experiments performed by Michael G. Leitner published elsewhere (Lindner *et al.*, 2011). Here membrane fluorescence was observed by TIRF microscopy in patched cells co-expressing Ci-VSP and $PH_{PLC\delta1}$YFP. Application of a +80 mV depolarization step (50 s) led to a robust decrease of membrane fluorescence, confirming strong PtdIns(4,5)P_2 depletion (Fig. 12 B, Tab. 6).

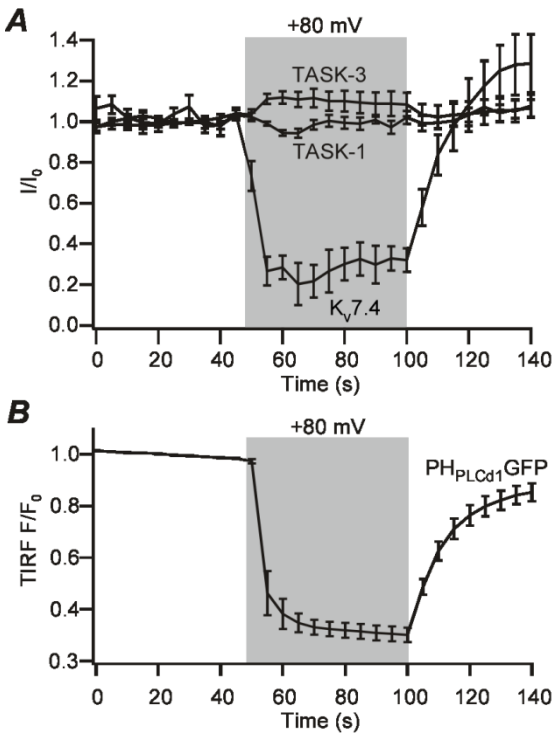

Fig. 12: Insensitivity of TASK currents to Ci-VSP-induced PtdIns(4,5)P_2 depletion. A, Mean time course of currents obtained from cells co-transfected with Ci-VSP and either TASK-1, TASK-3 or K_v7.4. Depolarization to + 80 mV reduced current amplitude to 32.9 (±5.9) % of its original value for K_v7.4 while it remained unchanged for TASK-1 (97.2 (±3.2) %) and TASK-3 108.9 (±6). B, Mean time course of TIRF intensities from voltage clamped cells expressing Ci-VSP and $PH_{PLC\delta1}$GFP decreased to 30.1 (±2.8) % decrease upon depolarization to + 80 mV (Data obtained from: Lindner et al., 2011).

Tab. 6: Effect of Ci-VSP-induced PtdIns(4,5)P2 depletion.

	Residual (%)	Tau (s)	N
TASK-1	97.2 (±3.2)	-	6
TASK-3	108.9 (±6)	-	7
K_v7.4	32.9 (±5.9)	15.43 (±3.24)	10
$PH_{PLC\delta1}$YFP	30.1 (±2.8)	10.65 (±1.41)	7

To verify these results PtdIns(4,5)P_2 was depleted by an additional approach using an established enzyme recruitment strategy (Suh *et al.*, 2006; Varnai *et al.*, 2006). This approach is based on the rapamycin dependent hetero-dimerisation of the FRB-domain from mTOR and the FKBP protein. A Lyn11 membrane anchor is coupled to the FRB-domain (Lyn11-FRB) and a CFP tagged Inp54p-5 -phosphatase to a FKBP protein (CF-Inp54). Rapamycin thus induces the recruitment of the phosphatase to the membrane. This results in PtdIns(4,5)P_2 dephosphorylation and thus decrease of PtdIns(4,5)P_2 abundance at the plasma membrane (See chapter 1.6.2).

First, K_v7.4 and Lyn11-FRB were co-transfected either with or without CF-Inp54. During current recording, 5 µM Rapamycin (1 min) induced a strong inhibition of K_v7.4

currents only in those cells also expressing CF-Inp54. This suggests that the observed PtdIns(4,5)P_2 depletion represents a specific effect of CF-Inp54 recruitment (Fig. 13 B, Tab. 7). After application of Rapamycin subsequently XE991, a selective K_v7 blocker, was applied. XE991 blocked only a small residual current remaining after CF-Inp54 induced PtdIns(4,5)P_2 depletion: This observation indicates that $K_v7.4$ was almost completely blocked by CF-Inp54 activation.

Finally, Lyn11-FRB and CF-Inp54 were co-expressed with either of the TASK channels under observation. For both, TASK-1 and TASK-3, application of 5 µM Rapamycin (1 min) did not induce any current inhibition. To assure that membrane translocation of CF-Inp54 had occurred, translocation of cyan fluorescence was observed simultaneously in wide-field fluorescence microscopy (Fig. 13 C, Tab. 7).

These results can be complemented with results obtained earlier in this group by Christian R. Halaszovich and myself where $PH_{PLC\delta1}$YFP, Lyn11-FRB and CF-Inp54 were co-transfected (Lindner *et al.*, 2011). In TIRF recordings application of 5 µM Rapamycin (1 min) led to a strong $PH_{PLC\delta1}$YFP dissociation from the membrane, also reporting a depletion of membrane PtdIns(4,5)P_2 (Fig. 13 A, Tab. 7).

To summarize, PtdIns(4,5)P_2 was specifically depleted by two different approaches. Despite strong PtdIns(4,5)P_2 depletion by either approach TASK channel activity remained totally unchanged.

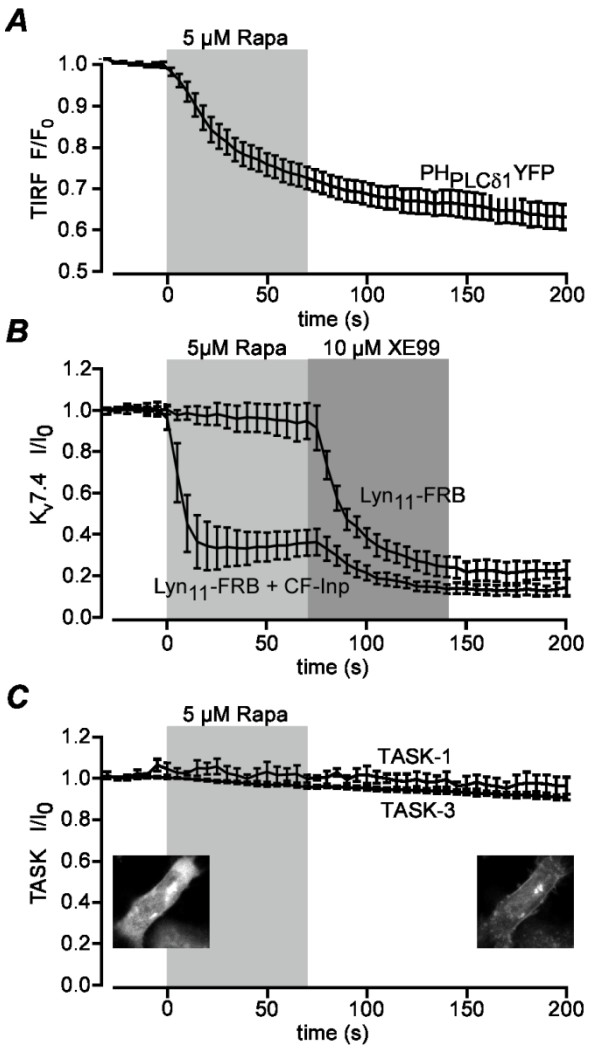

Fig. 13: CF-Inp54-induced PtdIns(4,5)P_2 depletion leaves TASK currents unaltered. A, TIRF recordings from cells co-transfected with $PH_{PLC\delta1}$YFP, CF-Inp54 and Lyn11-FRB. Application of rapamycin decreased TIRF intensity to 73.1 (±2.7) %, indicating dissociation of $PH_{PLC\delta1}$YFP from the membrane (Data obtained from: Lindner *et al.*, 2011). B, K_v7.4-mediated current in cells co-expressing CF-Imp and Lyn11-FRB was robustly suppressed to 36.2 (±6.3) % upon application of rapamycin. When the translocatable phosphatase was omitted (Lyn11-FRB only), currents were not affected by rapamycin. Residual currents were blocked by the K_v7 channel inhibitor XE991. C, normalized current amplitudes measured from cells co-expressing CF-Inp54, Lyn11-FRB and either TASK-1 or TASK-3. Currents were unaffected by application of rapamycin. Current amplitudes 2 min after application of rapamycin were 89.9 ± 4.1% (n = 5) and 89.6 ± 2.5% (n = 6) for TASK-1 and TASK-3, respectively.

Tab. 7: Effects of CF-Inp54 recruitment-induced PtdIns(4,5)P2 depletion.

	Residual (%)	Tau (s)	n
TASK-1	99 (±3.8)	-	5
TASK-3	93,4 (±1.1)	-	5
Kv7.4	36.2 (±6.3)	10.74 (±4.83)	5
PHPLCδ1YFP	73.1 (±2.7)	57.63 (±10.3)	13

3.3 Depletion of overall PtdIns leaves TASK channels unaffected

The effect of the both phosphatases on membrane PtdIns used here strongly differs from the effect of PLC-β. CF-Inp54 and Ci-VSP stoichiometrically convert PtdIns(4,5)P_2 into PtdIns(4)P, leaving the overall PtdIns concentration in the membrane essentially

unchanged. PLC-β in contrast depletes both PtdIns, PtdIns(4,5)P_2 and PtdIns(4)P, resulting in a robust decrease of the overall membrane PtdIns concentration (Willars *et al.*, 1998; Horowitz *et al.*, 2005).

As suggested for other ion channels TASK might be activated unspecifically by PtdIns. In this case simple conversion of PtdIns(4,5)P_2 to PtdIns(4)P would have no effect on TASK currents. To test if TASK channels might be unspecifically regulated by PtdIns a modification of the described heteromerisation approach was used to the effect of PLC-β on PtdIns more closely. This novel construct was generated by Gerry R. Hammond and colleagues as described elsewhere (Lindner *et al.*, 2011). In brief the 5 -phosphatase was replaced by a new protein which was engineered in analog to the native dual-specificity phosphatase synaptojanin (Mani *et al.*, 2007). Inp54p was replaced by a 4 - and a 5 -phosphatase in tandem, namely the yeast phosphatase Sac on the N-terminus and human INPP5E on the C-terminus. In allusion to synaptojanin, this phosphatase was termed pseudojanin (PJ). To allow Rapamycin induced membrane recruitment, an RFP-tagged FKBP was fused to PJ (RF-PJ) (Fig. 14 A, left). Beside this “wild-type” RF-PJ three mutants of RF-PJ were created, to allow an independent depletion of each of the two PtdIns. In the first mutant the 4 -phosphatase activity was inactivated. In accordance to its remaining activity it was termed RF-PJ-5ptase. In the other mutant the 5 -phosphatase was inactivated. It was therefore termed RF-PJ-Sac. Finally a double mutant was created that had no phosphatase activity left (RF-PJ-dead).

This construct had so far not been tested for functionality. Thus Rapamycin-induced membrane translocation of RF-PJ was first confirmed by confocal microscopy. In CHO cells co-transfected with Lyn11-FRB and RF-PJ application of 5 µM rapamycin (1 min) resulted in robust translocation of RF-PJ to the plasma membrane (Fig. 14 A, right).

Before testing its effect on TASK it had to be determined to which extent PtdIns(4)P and PtdIns(4,5)P_2 levels can be changed by activation of this novel phosphatase. Therefore $PH_{PLC\delta1}$GFP or PH_{2xOSH2}GFP were co-transfected together with Lyn11-FRB and RF-PJ or one of its mutants. Changes in membrane association of the fluorescence sensors $PH_{PLC\delta1}$GFP and PH_{2xOSH2}GFP were observed by TIRF imaging. While $PH_{PLC\delta1}$GFP specifically binds PtdIns(4,5)P_2, PH_{2xOSH2}GFP binds both, plasma membrane PtdIns(4)P and PtdIns(4,5)P_2 (Roy & Levine, 2004; Balla *et al.*, 2008). When fully active RF-PJ was transfected, application of 5 µM Rapamycin led to

dissociation of $PH_{PLC\delta1}$GFP from the plasma membrane. The same observation was made for RF-PJ-5ptase. In contrast recruitment of RF-PJ-Sac or RF-PJ-dead to the plasma membrane did not induce translocation of $PH_{PLC\delta1}$GFP (Fig. 14 B, Tab. 8). These results indicate that recruitment of RF-PJ with an intact 5-phosphatase domain results in depletion of PtdIns(4,5)P_2.

When using PH_{2xOSH2}GFP RF-PJ recruitment also lead to a strong decrease in membrane fluorescence, reflecting a robust decrease in concentrations of both PtdIns(4)P and PtdIns(4,5)P_2. Mutation of either (RF-PJ-Sac or RF-PJ-5ptase) or both (RF-PJ-dead) of the phosphatase domains completely abolished this effect. These observations suggest that RF-PJ efficiently depletes PtdIns(4)P and PtdIns(4,5)P_2 and that depletion of both is required for dissociation of PH_{2xOSH2}GFP from the membrane. They additionally show that either of the membrane lipids PtdIns(4)P and PtdIns(4,5)P_2 is sufficient for membrane localization of PH_{2xOSH2}GFP. Additionally these results provide the evidence that RF-PJ efficiently depletes PtdIns(4)P. (Fig. 14 C, Tab. 8).

To finally probe whether TASK channels are activated unspecifically by PtdIns, cells co-transfected with TASK-3, Lyn11-FRB and RF-PJ were studied in patch-clamp experiments. Application of 5 µM Rapamycin (1 min) did not exhibit any effect on TASK-3, despite successful RF-PJ recruitment as verified by RFP translocation to the membrane.

Due to diffusion of pipette solution into the cell patch-clamping may change the composition of intracellular fluid. It seemed possible that this change inactivates RF-PJ. To address this possibility effectiveness of RF-PJ in patched cells expressing K_v7.4 as a PtdIns sensor was tested. Under these conditions application of 5 µM Rapamycin (1 min) led to a robust decrease of K_v7.4 currents. The extent of inhibition was comparable to the observations made for Inp54p recruitment, indicating a similar effectiveness of both phosphatases (Fig. 14 D, Tab. 8).

In conclusion, RF-PJ efficiently depletes both, PtdIns(4)P and PtdIns(4,5)P_2, the most abundant phosphoinositides in the plasma membrane: Yet alteration in the concentration of these lipids does not exhibit any effect on TASK-3 currents.

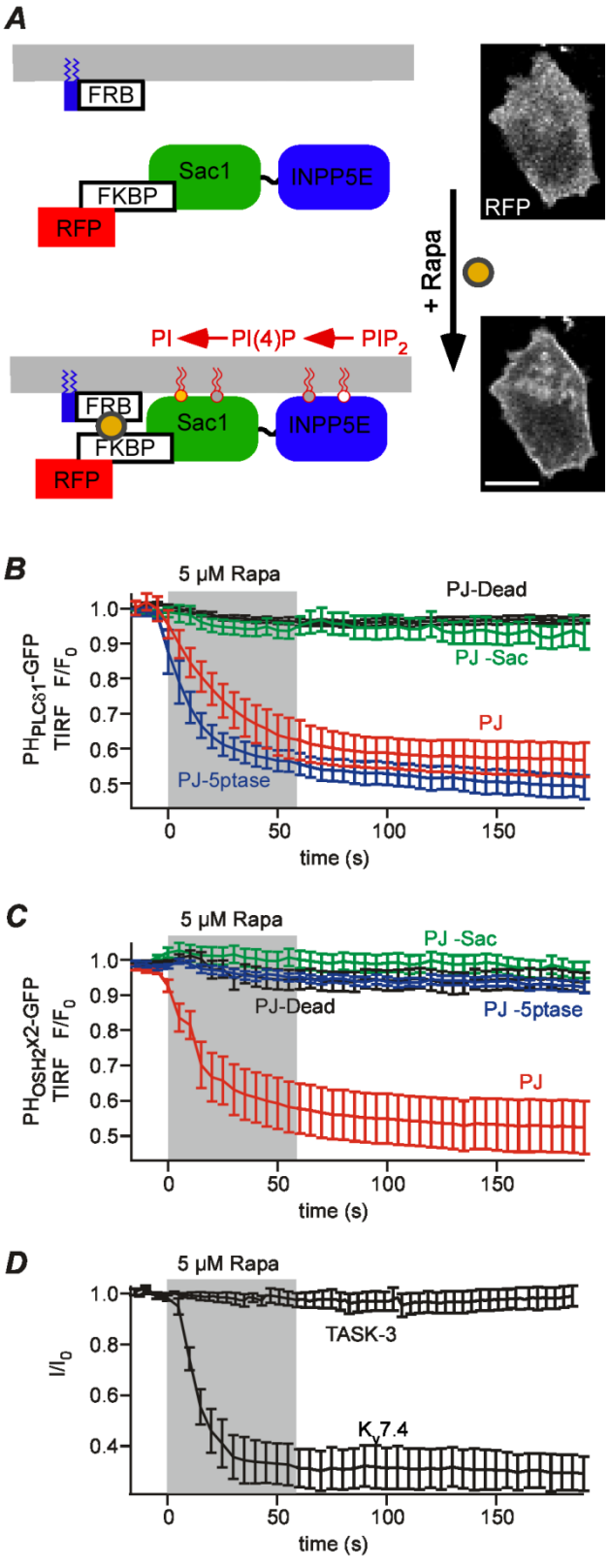

Fig. 14: TASK currents are insensitive to combined depletion of PtdIns(4)P and PtdIns(4,5)P_2 by recruitment of the phosphatase pseudojanin. A, Schematic illustration of the double specificity phosphatase pseudojanin (RF-PJ) and its recruitment to the plasma membrane (left). Confocal images of RF-PJ before and after recruitment to the plasma membrane by 5 µM Rapamycin (right). Scale Bar: 10 µm. B, TIRF recordings, performed on cells co-transfected with $PH_{PLC\delta1}$GFP, Lyn11-FRB, and either of the RF-PJ mutants. Dissociation of $PH_{PLC\delta1}$GFP from the membrane upon application of Rapamycin (shaded) was only observed with intact 5-phosphatase domain. C, Experiments performed analogously to B but with PH_{2xOSH2}GFP. Dissociation of PH_{2xOSH2}GFP from the membrane required both phosphatase domains to be active. D, whole-cell recordings from cells co-transfected with Lyn11-FRB, fully intact PJ and either TASK-3 or K_V7.4. While K_V7.4 currents were robustly inhibited by recruitment of PJ (residual currents, 30.6 ± 7.8%), TASK currents were not affected (residual currents, 97.4 ± 3.9%).

Tab. 8: Mean residual TIRF intensities or current amplitudes in % after membrane recruitment of pseudojanin or its mutants (n>4).

	RF-PJ	RF-PJ-Sac	RF-PJ-5ptase	RF-PJ-dead
$PH_{PLC\delta1}GFP$	63.1 (±5.5)	56.4 (±2.9)	95.3 (±2.4)	96.1 (±9.1)
$PH_{2xOSH2}GFP$	57.7 (±7.1)	95(±1.1)	100 (±2.5)	94.3 (±2.7)
$K_v7.4$	30.6 (±7.8)			
TASK-3	97.4 (±3.9)			

3.4 Recovery of TASK channels from G_qPCR mediated inhibition occurs independently of PtdIns(4,5)P_2 resynthesis.

PtdIns dependency of ion channels can also be demonstrated by observation of their behavior during PtdIns resynthesis after PLC-β-mediated hydrolysis (Suh & Hille, 2002; Halaszovich *et al.*, 2009). In case PtdIns mediated the inhibition of an ion channel its recovery kinetics should change when interfering with PtdIns(4,5)P_2 resynthesis. As PtdIns(4,5)P_2 resynthesis occurs as a cascade of sequential phosphorylation steps that require ATP, omission of intracellular ATP can block PtdIns(4,5)P_2 resynthesis. With such an approach it has been demonstrated that recovery of bona-fide PtdIns(4,5)P_2 dependent K_v7 channels requires ATP (Suh & Hille, 2002). To complement my data it would thus be interesting also to test the effect of interference with PtdIns(4,5)P_2 resynthesis on TASK channels.

The PtdIns(4,5)P_2 dependence of TASK recovery was examined in cells where all intracellular ATP was replaced by the non-hydrolysable analog AMP-PCP. During patch clamp recording the intracellular solution (ICS) filling the patch-pipette diffuses into the cell. The volume of the patch-pipette exceeds that of the patched cell by a manifold. Therefore it leads to a virtually complete replacement of the normal intracellular liquid. It has been previously shown that when the ATP in the ICS is replaced by 3 mM AMP-PCP PtdIns(4,5)P_2 resynthesis can be completely abolished (Suh & Hille, 2002; Halaszovich *et al.*, 2009). Cells co-expressing TASK-3 and m1R were patched and a period of 4 min was waited order to give the AMP-PCP sufficient time to diffuse into the cell. Subsequent application of 10 µM OxoM (1 min) led to a close-to-complete inhibition of TASK-3 currents. Recovery was complete and had similar kinetics as under control conditions where ATP was included (Fig. 15 A & B, Tab. 9). Similar results were obtained for TASK-1.

In contrast, in experiments with $K_v7.4$ recovery from muscarinic inhibition was completely abolished when measuring with intracellular AMP-PCP (Fig. 15 A, Tab. 9) confirming that AMP-PCP efficiently blocked PtdIns(4,5)P_2 resynthesis.

As both TASK-1 and TASK-3 channels recover from m1R induced inhibition in the presence of AMP-PCP it must be concluded that PtdIns(4,5)P_2 depletion does not directly mediate G_qPCR induced inhibition.

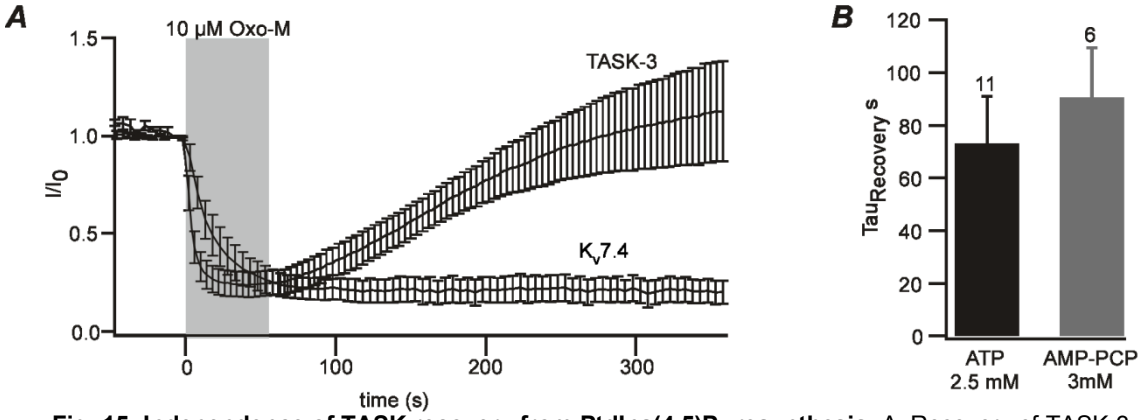

Fig. 15: Independence of TASK recovery from PtdIns(4,5)P_2 resynthesis. A, Recovery of TASK-3 and Kv7.4 when ATP was omitted. CHO cells co-expressing m1R and TASK-3 (n=5) or Kv7.4 (n=6) where patched with 3 mM AMP-PCP in the intracellular solution. Recordings were started 4 minutes after whole-cell formation was achieved. B, Average time constants for recovery of TASK-3 from muscarinic inhibition were similar in presence of 2.5 mM ATP (time courses shown in Fig. 14 A) or 3 mM AMP-PCP (A).

Tab. 9: Averaged recovery time constants (s) in presence of 2.5 mM ATP or 3 mM AMP-PCP

	ATP	**AMP-PCP**
TASK-1	104.16 (±25.35)	100.33 (±8.62)
TASK-3	74.02 (±17.27)	91.34 (±18.53)
$K_v7.4$	117.46 (±30.96)	-

3.5 Inhibition of PLC-β abolishes G_qPCR mediated TASK inhibition

Having excluded the popular hypothesis that hydrolysis of PtdIns(4,5)P_2 would directly inhibit TASK, I went on to evaluate the second proposed mechanism of TASK channel inhibition: i.e. direct interaction with $G_q\alpha$.

Reliable experimental approaches to interfere directly with $G_q\alpha$ activity have not been developed so far. However it is possible to extract informations about the role of $G_q\alpha$ in TASK channel inhibition by accessing the role of PLC-β. In the G_qPCR pathway,

$G_q\alpha$ activation occurs directly upstream to activation of PLC-β. Thus if a direct interaction between $G_q\alpha$ and TASK would mediate the inhibition, any experimental interference with PLC-β activity should not affect TASK channel inhibition. Therefore I tested the effect of PLC-β blockage on G_qPCR-to-TASK signaling by two independent approaches.

3.5.1 Interfering with PLC-β activity by removal of intracellular calcium

It is well established that PLC-β needs calcium as an essential cofactor for enzymatic activity (Rhee, 2001; Bunney & Katan, 2011). Thus PLC-β-dependent signaling on ion channels has been shown to be blocked by removal of intracellular calcium (Horowitz *et al.*, 2005). Therefore it was tested here if G_qPCR activation leads to an inhibition of TASK channels also under calcium-free conditions. To minimize the level of resting free calcium in the cell I used an intracellular solution (ICS) where all calcium was omitted and the concentration of the calcium chelator EGTA was raised to 20 mM. Thereby intracellular calcium should be buffered to virtually zero. Before the beginning of the recordings a period of at least 4 min was waited after whole cell formation to give enough time to the ICS to diffuse into the cell. To check for a successful blockage of PLC-β the effect of m1R stimulation on K_v7.4 was observed in cells expressing these both constructs. As K_v7.4 depend on PtdIns(4,5)P_2, they serve as an indirect monitor of PLC-β activity in these experiments. Upon application of OxoM (10 µM, 1 min) K_v7.4-current inhibition was almost abolished (Fig. 16 A. Tab. 10), indicating a strong blockage of PLC-β, with only minor residual activity.

It was subsequently tested if TASK channels could still be blocked by G_qPCR activation under similar experimental conditions. Therefore TASK-3 currents were observed in cells co-expressing the m1R and TASK-3. In presence of 20 mM EGTA application of OxoM (10 µM, 1 min) only led to a minor inhibition of TASK-3 currents (Fig. 16 A. Tab. 10).

These data are consistent with an involvement of PLC-β, arguing against a direct interaction of $G_q\alpha$ with TASK to mediate TASK inhibition. The remaining inhibition of both K_v7.4 and TASK-3 is probably due to a residual activity of PLC-β. This activity may induce release of calcium from intracellular stores and thereby further facilitate PLC-β activation (see chapter 1.4.2). To more effectively buffer also fast calcium transients experiments were repeated using BAPTA instead of EGTA. BAPTA is another calcium chelator. Although its calcium affinity is equal, it exhibits much faster buffering kinetics

(Fakler & Adelman, 2008). Under these conditions $K_v7.4$ inhibition by m1R activation (10 µM OxoM for 1 min) was completely abolished (Fig. 16 B. Tab. 10), suggesting that PLC-β was essentially blocked.

When performing similar experiments with TASK-3 or TASK-1 transfected, their inhibition was also massively reduced. However a minimal residual inhibition could still be observed (Fig. 16 B. Tab. 10, for TASK-1 data not shown, n=3).

These data strongly suggest an essential involvement of PLC-β in the inhibitory regulation of TASK. Consequently a direct inhibitory effect of $G_q\alpha$ on TASK is very unlikely. Noteworthy abolishment of inhibition by both calcium chelators was less complete for TASK than for $K_v7.4$.

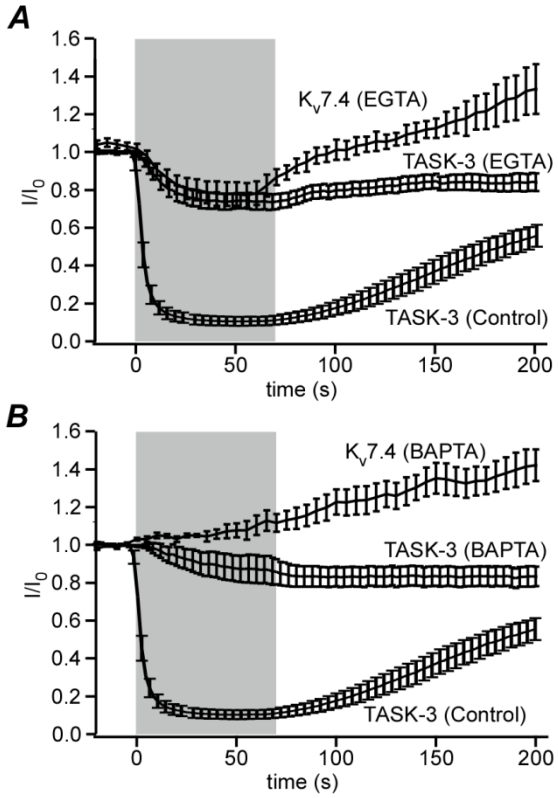

Fig. 16: Removal of intracellular calcium blocks muscarinic inhibition of TASK-3. Cells co-expressing m1R and either TASK-3 or $K_v7.4$. Cells were patch-clamped with a pipette solution containing no calcium and either 20 mM EGTA (A) or 20 mM BAPTA (B). For comparison TASK-3 traces recorded with standard intracellular solution were plotted (also shown in Fig. 14). Recordings were started 4 min after whole-cell was achieved. 10 µM OxoM was applied for 1 min. In presence of EGTA a inhibition was 24.9 (± 3.7) % for TASK-3 and 22.5 (± 6.4) % for $K_v7.4$. When BAPTA was present in the pipette solution Kv7.4 inhibition was completely abolished [-7 (± 5) %] while a minimal inhibition was still present in TASK-3 [15.9 (± 5.9) %]. n > 5 for all traces.

3.5.2 Effect of the PLC-β blocker U-73122 on m1R inhibition of TASK

PLC-β activation is generally considered to be the first calcium-dependent step in the G_qPCR signaling cascade (Horowitz *et al.*, 2005). However there is no evidence demonstrating that $G_q\alpha$ activation is unaffected by the absence of calcium. Therefore

an independent approach was necessary to confirm the involvement of PLC-β in TASK channel inhibition. The PLC-β inhibitor U-73122, an alkylating lipophilic agent, has been repetitively used to study the role of PLC-β in different cell types (Mogami *et al.*, 1997; Horowitz *et al.*, 2005).

This is not the first experiment aiming to investigate the role of PLC-β in TASK channel inhibition by using U-73122. There are rather 5 reports in literature, where the effect of U-73122 on TASK channel inhibition was probed (Boyd *et al.*, 2000; Czirjak *et al.*, 2001; Chemin *et al.*, 2003; Lopes *et al.*, 2005; Chen *et al.*, 2006). As already stated earlier, previously published results were controversial. In those studies who found an effect of U-73122, experiments were not carefully controlled for possible side effects (Czirjak *et al.*, 2001; Chemin *et al.*, 2003; Lopes *et al.*, 2005). Vice versa reports that showed U-73122 to have no effect on TASK channel inhibition at all, did not provide sufficient positive controls for effective PLC-β inhibition (Boyd *et al.*, 2000; Chen *et al.*, 2006).

First the effectiveness of U-73122 was probed in cells co-expressing m1R and $PH_{PLC\delta1}$GFP as a PtdIns(4,5)P_2 sensor. The membrane translocation of $PH_{PLC\delta1}$GFP upon muscarinic stimulation was observed in TIRF recordings. Either U-73122 or its inactive analog U-73343 were applied to the cells in a concentration of 5 µM for 3 minutes previous to application of OxoM (10 µM, 1 min). When pretreated with U-73343, OxoM-induced dissociation of $PH_{PLC\delta1}$GFP was equal to cells which were not pretreated (Fig. 17 B. Tab. 10). In contrast pretreatment with U-73122 led to an almost complete abolishment of $PH_{PLC\delta1}$GFP dissociation, indicating strong blockage of PLC-β.

Several side effects of U-73122 have been reported before (e.g.: Mogami *et al.*, 1997; Horowitz *et al.*, 2005). In my hands application of 5 µM U-73122 (3 min) led to the development of a remarkable unselective conductance that shifted reversal potential towards zero (Fig. 17 A). The cell outward current-density observed at + 50 mV reached values of 67.6 (±14.9) pA / pF after 3 min. Subsequent superperfusion with an extracellular solution where sodium was replaced by the same amount of NMDG (Ex-NMDG) abolished the inward component of this current and repolarized cells to -53 mV (Fig. 17 A). To allow better observation of the current of interest all experiments with U-73122 or U-73343 were performed in Ex-NMDG.

To test whether U-73122 abolished TASK channel inhibition the m1R and TASK-3 were co-transfected. When 5 µM U-73122 was applied to the cells for 3 min channel

inhibition by OxoM (10 µM, 1 min) was fully abolished. In contrast, control experiments where U-73122 was omitted showed fast and robust inhibition (Fig. 17, Tab. 10). To evaluate if U-73122 had the same effect on inhibition of TASK-1 currents I performed analogous experiments with TASK-1_{NQ}. This mutant has a retention-signal removed and thus exhibits 4.5 times bigger currents (Zuzarte *et al.*, 2009). The use of TASK-1_{NQ} instead of TASK-1 became necessary to obtain a better ratio between the TASK current under observation and the outward current induced by U-73122. As already expected from my observations with BAPTA TASK-1_{NQ} channels behave similar to TASK-3, yielding full blockage of inhibition by U-73122 pre-treatment.

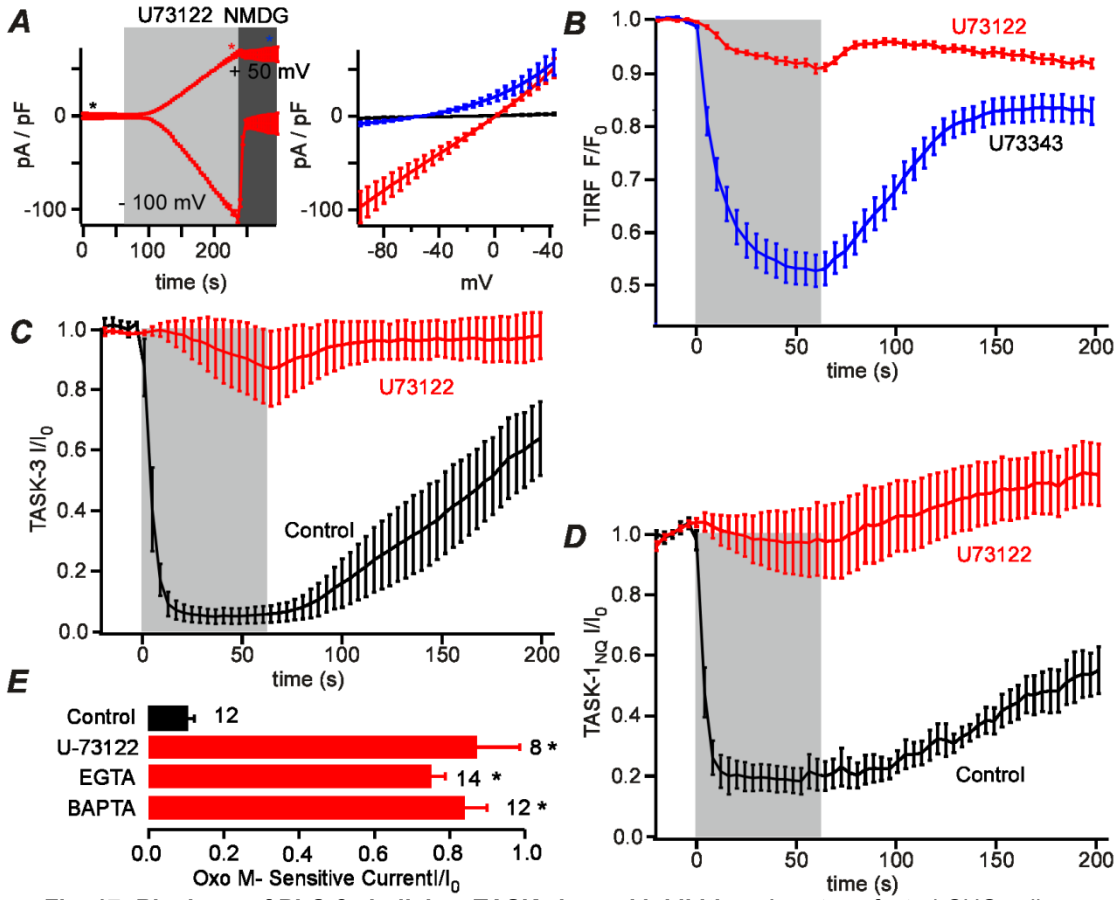

Fig. 17: Blockage of PLC-β abolishes TASK channel inhibition. A, untransfected CHO cells were patch-clamped and exposed to 5 µM U-73122. Left panel shows averaged and cell size adjusted outward current at +50 mV (upper trace) and inward current at -100 mV (lower trace). Within 3 min of application an unselective conductance appeared, whose inward component disappeared when extracellular Sodium was replaced by NMDG (n=5). Right panel shows the cell size adjusted I-V relationships obtained from the same batch of cells before (black) and at the end (red) of U-73122 application and when extracellular sodium was omitted (blue). B, TIRF recordings from cells co-expressing m1R and $PH_{PLC\delta1}$GFP pretreated with either 5 µM U-73122 (red) or 5 µM of its inactive analog U-73343 (black) for 3 min. Subsequent application of 10 µM OxoM for 1 min showed a normal extent of inhibition in presence of U-73343 (47.3 ± 7.5 %, n=22) while it was only residually present when pretreated with U-73122 (8.9 ± 3 %, n=33). Analogous observations were made in patch-clamp recordings of cells co-expressing m1R and TASK-3 (C) or $TASK\text{-}1_{NQ}$ (D). C, for TASK-3 inhibition was 7.3 ± 11 % (n=5) with and 93.4 ± 2.6 % (n=5) without pretreatment with 5 µM U-73122. D, for $TASK\text{-}1_{NQ}$ inhibition was 4.1 ± 10.9 % (n=7) and 83.3 ± 3.8 % (n=8) respectively. E, Summarized OxoM sensitive TASK-3 currents under control conditions (see Fig. 14 A) significantly differ from currents after pretreatment with U-73122 (C) and when intracellular calcium was omitted by EGTA (see Fig. 19 A) or BAPTA (see Fig. 19 B).

Tab. 10: Current inhibition achieved with 10 µM OxoM under different experimental conditions.

	Control	U-73122	EGTA	BAPTA
TASK-1/1NQ	17 (± 2.4) %	4.1 (± 10.9) %	-	1.**3** (± 9.9) **%**
TASK-3	12.5 (± 2.4) %	7.3 (± 11) %	24.9 (± 3.7) %	15.**9** (± 5.9) %
Kv7.4	88 (± 5.5) %	-	22.5 (± 6.4) %	-7 (± 5) %

3.5.3 U-73122 also abolishes endothelin-1 induced TASK channel inhibition

So far it was demonstrated that PLC-β activation is required for inhibition of TASK channels by m1R activation. To test if PLC-β-dependent inhibition represents a general mechanism also present in other G_qPCR TASK channel inhibition by endothelin receptor type A (Et-AR, also from the G_qPCR family) was additionally examined. TASK-1 channels are expressed in rat cardiomyocytes where they are inhibited by endothelin-1 (Et-1) via Et-AR (Schiekel *et al.*, in revision). Et-1 levels are increased in various cardiovascular pathologies like congestive heart failure, atrial fibrillation and hypertension (Damron *et al.*, 1993; Ono *et al.*, 1994; Rubanyi & Polokoff, 1994). Concurrently it leads to a prolongation of action potential in cardiomyocytes (Brunner *et al.*, 2006; Deng *et al.*, 2010; Schiekel *et al.*, in revision). Therefore it was of particular interest to further dissect the underlying signal transduction pathway.

To address this issue CHO cells were first co-transfected with Et-AR and the PtdIns(4,5)P_2 sensor $PH_{PLC\delta1}$GFP. And the effect of the Et-AR agonist Et-1 on PtdIns(4,5)P_2 membrane abundance was observed in TIRF recordings. In consistence with earlier findings (Cho *et al.*, 2005), application of 200 nM Et-1 (1 min) led to strong hydrolysis of PtdIns(4,5)P_2, indicated by $PH_{PLC\delta1}$GFP dissociation to the membrane. Also in consistence with previous findings, fluorescent signals did not recover within the observed interval of time (Fig. 18 A, C) (Chun *et al.*, 1995).

In a next step it was verified that Et-AR induced PtdIns(4,5)P_2 depletion is also due to PLC-β activation. Experiments performed as above were repeated with a 3 min interval of application of 5 µM U-73122 or the same amount of its inactive analog U-73343 directly before the application of 200 nM Et-1 (1 min). PtdIns(4,5)P_2 hydrolysis was totally unchanged after pre-application of U-73343, while 5 µM U-73122 led to a complete abolishment of Et-AR induced PtdIns(4,5)P_2 depletion (Fig. 18 A, C). These findings confirm that Et-AR induced PtdIns(4,5)P_2 depletion represents hydrolysis by PLC-β.

Subsequently it was tested if Et-AR activation could lead to TASK-1_{NQ} channel inhibition, when both were co-transfected in CHO cells. Cells were patched and TASK-1_{NQ} currents were observed in sodium free environment (Ex-NMDG). Application of 200 nM Et-1 (1 min) led to a robust and fast inhibition of TASK currents (Fig. 18 B, D). To test if TASK inhibition by Et-AR is achieved by a similar mechanism as TASK inhibition by m1R I tested whether PLC-β activation is also required. Analogous to the experiments performed with $PH_{PLC\delta1}$GFP 5 µM of either U-73122 or U-73343 (3 min) were preapplied before application of 200 nM Et-1 (1 min). U-73122 totally abolished the inhibitory effect of Et-1 application. In contrast, the inactive U-73343 did not change the effect of Et-1. However U-73343 itself led to a 56.74 ± 11.87 % decrease of TASK-1_{NQ} currents (Fig. 18 B, D), which was completely reversible within 3 min (n=6, data not shown).

U-73122 application makes TASK-1_{NQ} currents insensitive to m1R and Et-AR activation. As hypothesized above, a blockage of PLC-β could underlie this effect. However it is also possible that U-73122 modifies TASK channels in a way that makes them insensitive to G_qPCR induced inhibition or the remaining components of the U-73122 induced unselective current could obscure TASK inhibition. Therefore further experiments were performed to demonstrate that after U-73122 application and subsequent G_qPCR activation the remaining current really represents TASK-1. Cells were co-transfected with the Et-AR and TASK-1_{NQ} and patched in sodium-free Ex-NMDG. To quantify TASK-1_{NQ} current amplitude, Ex-NMDG with pH = 5.9 was applied for 1 min. As expected for TASK channels the recorded current amplitude was massively reduced. In a subsequent interval of 1 min where cells were exposed to Ex-NMDG with the normal pH of 7.4 TASK currents recovered to their original value. Then 5 µM U-73122 was applied for 3 min leaving TASK currents mostly unchanged. U-73122 application was followed by an interval of 200 nM Et-1 application (1 min), which did not result in any current change. Ultimately pH was again reduced to 5.9. This was still effective to robustly block the recorded currents indicating that they still represent TASK (Fig. 18 E). In conclusion U-73122 really blocks G_qPCR signaling on TASK by interfering with the signaling cascade and not directly with the channel.

Similar experiments were performed with native rat cardiomyocytes and confirmed the results obtained in CHO cells (Experiments performed by Julia Schiekel, data not shown) (Schiekel *et al.*, in revision).

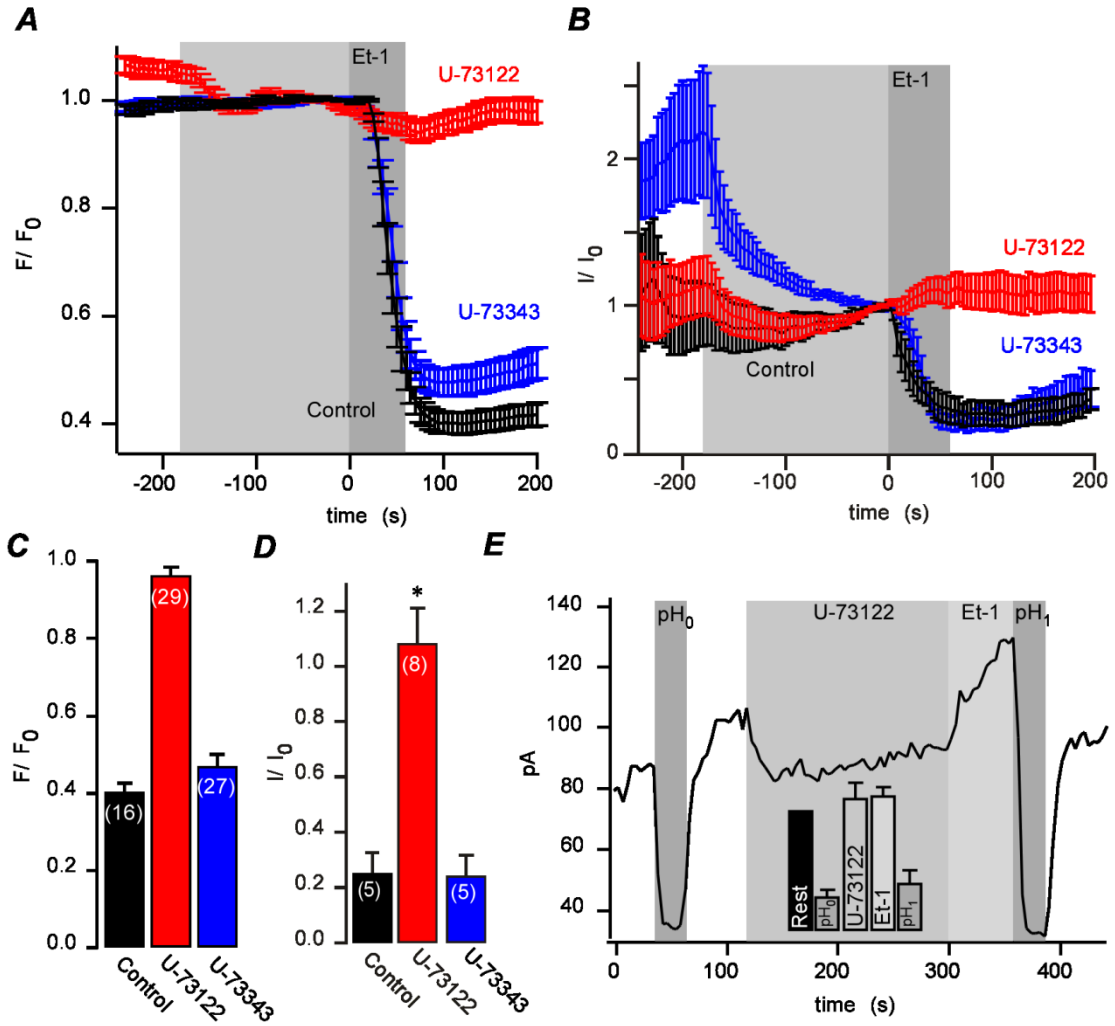

Fig. 18: Et-AR activation inhibits TASK-1$_{NQ}$ by a PLC-β dependent mechanism. A and C, TIRF-recordings from cells co-transfected with Et-AR and PH$_{PLC\delta1}$GFP. A, Shows time courses of cells exposed either to a control solution, 5µM U-73122 or 5µM U-73343 (area highlighted in light gray) before application of 200 nM Et-1 (dark gray). Signal intensities recorded from cells previously exposed to the control solution (black trace) decreased by 59.37 (± 2) % of the resting value (n = 16). In cells pre-exposed to U-73122 (red) Et-1 reduced the signal only by 3.47 (± 1.86) % (n = 29) while it was robustly reduced by 52.75 (± 2.86) % in cells pre-exposed to U-73343 (blue, n = 27). Box-plot illustrating the residual signal intensities after application of Et-1 is given in C. B, Time courses from patch-clamp recordings from cells co-transfected with Et-AR and TASK-1$_{NQ}$ that were subject to a similar protocol as cells in A. D, Corresponding box-plots as in B. Et-1-induced current decrease was 74.8 (± 7.42) % under control conditions (black, n = 5), effectively none (- 8.27 [± 12.82] %, n = 8) in cells previously exposed to U-73122 (red) and 75.86 (± 7.48) % when pre-exposed to U-73343. E, Patch clamp recording from a sample cell demonstrating that currents recorded after application of U-73122 and Et-1 still represent TASK. Areas in the different gray tones represent application of extracellular solution with pH = 5.9 (dark), U-73122 (intermediate) and Et-1 (light) respectively. Inset: Bars represent the mean resting (black) and residual current amplitude from 6 cells subject to a similar treatment as the cell shown. pH sensitive current component was 72.25 (± 6.62) % before U-73122 versus 60.73 (± 12.05) % after Et-1 application. U-73122 and Et-1 left currents unchanged (+ 12.16 [± 13.75] % and + 14.31 [± 7.79] %).

Tab. 11: Relative signal decrease achieved by of 200 nM Et-1 after pretreatment with control solution, 5 µM U-73343 or 5 µM U-73122.

	Control	U-73343	U-73122
TASK-1$_{NQ}$	74.8 (± 7.42) %	75.86 (± 7.48) %	-8.27 (± 12.82) %
PH$_{PLC\delta1}$GFP	59.37 (± 2) %	52.75 (± 2.86) %	3.47 (± 1.86) %

In summary, inhibition of PLC-β by both deprivation of calcium and pharmacological blockage by U-73122 resulted in a close-to-total block of m1R induced signal propagation onto TASK channels. Inhibition of TASK not only by m1R but also by Et-AR activation were blocked by U-73122, suggesting that PLC-β activation is a necessary step for TASK channel inhibition by any G_qPCR. Finally my results could be reproduced in a native system, underlining their physiological relevance. Noteworthy, and in contrast to earlier studies, my approaches to block PLC-β are controlled for effectiveness and specificity by using two independent PtdIns(4,5)P_2 reporters, K_v7.4 and PH$_{PLC\delta1}$GFP.

3.6 G_qPCR mediated TASK inhibition is slower when PtdIns(4,5)P_2 levels are reduced

Up to this point it was shown that signal propagation from G_qPCR to TASK channels requires PLC-β activation. However depletion of PtdIns(4,5)P_2 or other PtdIns does not cause channel closure. This observation suggest that TASK channel inhibition is mediated by a messenger molecule located downstream of PtdIns(4,5)P_2 hydrolysis. However, PLC-β activation might possibly initiate signaling pathways other than the PtdIns(4,5)P_2 pathway. Therefore it remains to be tested if the hydrolysis of PtdIns(4,5)P_2 to Ins(1,4,5)P_3 and DAG is really required for successful signal propagation, i.e. if PtdIns(4,5)P_2 has a permissive role. This can be done by artificially decreasing PtdIns(4,5)P_2 levels (e.g. by CF-Inp54, the switchable phosphatase described above [chapter 3.2]) and observing changes in TASK channel inhibition by subsequent G_qPCR activation.

To test the role of PtdIns(4,5)P_2 as a permissive mediator of G_qPCR induced TASK channel inhibition CHO cells were co-transfected with five different constructs: 1) Lyn11-FRB and 2) CF-Inp54 for Rapamycin induced dimerisation, 3) the m1R, 4) PH$_{PLC\delta1}$GFP as PtdIns(4,5)P_2-sensor and 5) TASK-3. Synchronous TIRF and patch-

clamp recordings were performed to monitor alteration in PtdIns(4,5)P_2 concentration and TASK current at the same time.

The m1R was stimulated with OxoM (10 µM, 1 min) resulting a decrease of $PH_{PLC\delta1}$GFP membrane fluorescence paired with a robust inhibition of TASK-3. After signal recovery recruitment CF-Inp54 by application of Rapamycin (5 µM, 1 min), induced a pronounced dissociation of $PH_{PLC\delta1}$GFP from the membrane. TASK current remained unchanged during this interval of time. By reapplication of OxoM (10 µM, 1 min) no further decrease in $PH_{PLC\delta1}$GFP membrane association was achieved. In contrast TASK currents were strongly inhibited. Interestingly TASK inhibition time constants were slower for the second application of OxoM than for the first (Fig. 19 A & C, Tab. 12).

This experiment did not give the desired “all-or-nothing” result, i.e. TASK inhibition was not fully present or fully abolished, but instead inhibition kinetics were “only” slowed. Do these slower inhibition kinetics reflect the permissive role of PtdIns(4,5)P_2? If so, also the generation of PtdIns(4,5)P_2 hydrolysis products should be only slowed, but not completely abolished. Indeed, it has been shown that DAG is still produced by G_qPCR activation after CF-Inp54 recruitment (Suh *et al.*, 2006). Both, DAG production and TASK channel inhibition after CF-Inp54 recruitment might possibly arise from hydrolysis of residual PtdIns(4,5)P_2 molecules which are accessible to PLC-β, but not to CF-Inp54, e.g. for affinity reasons. In this case G_qPCR activation could still produce an amount of PtdIns(4,5)P_2 downstream messenger molecules, but less than under normal conditions where PtdIns(4,5)P_2 concentrations were high.

To test if DAG production kinetics were changed when PtdIns(4,5)P_2 levels were altered, it became necessary to observe the translocation of CF-Inp54, changes in PtdIns(4,5)P_2 and in DAG simultaneously. Thus 3 different fluorescence proteins had to be observed at a time. This could not be achieved by TIRF microscopy in this laboratory. For this practical reason these experiments were performed using confocal microscopy. In contrast to TIRF that uniquely senses membrane fluorescence, confocal microscopy is more robust to detect cytosolic fluorescence changes. Therefore in these experiments cytosolic fluorescence is monitored and thus an signal increase reflects a translocation of a fluorescent probe away from the membrane (i.e. fluorescence intensities reciprocally correlate with the membrane concentration of the fluorescent sensor).

CHO cells were co-transfected with 1) Lyn11-FRB, 2) CF-Inp54, 3) the m1R, 4) Tubby-RFP to sense PtdIns(4,5)P_2 and 5) PKCγ_{26-89}YFP as DAG sensor. The Tubby domain is another PtdIns(4,5)P_2 sensor, being more specific than PLC-δ1-PH but having some yet not fully understood side effects (Leitner MG, unpublished). Here it was used for the practical reason of having a RFP as fluorescence tag.

The first application of OxoM (10 µM, 1 min) led to a robust and fast decrease of cytosolic PKCγ_{26-89}YFP, indicating DAG synthesis. As usually observed for Tubby-RFP, this G_qPCR receptor stimulation did not result in Tubby-RFP translocation (Leitner MG, unpublished). After recovery of the PKCγ_{26-89}YFP signal a subsequent application of Rapamycin (5 µM, 1 min) left PKCγ_{26-89}YFP constant while both Tubby-RFP translocation into the cytosol and translocation of CF-Inp54 to the membrane could be observed. On second application of OxoM (10 µM, 1 min) PKCγ_{26-89}YFP reassociated with the plasma membrane but only with slower kinetics (Fig. 19 B & C, Tab. 12). Thus PLC-β conducted production of messengers downstream of PtdIns(4,5)P_2 occurs slower after depletion of PtdIns(4,5)P_2 by CF-Inp54.

Both TASK-3 and DAG production are decelerated after decrease of PtdIns(4,5)P_2 levels. The residual DAG production indicates that there is still some PtdIns(4,5)P_2 available for hydrolysis by PLC-β after CF-Inp54 recruitment. As TASK-3 inhibition is still present, but slower, after CF-Inp54 recruitment it is reasonable to conclude that TASK inhibition occurs downstream of PtdIns(4,5)P_2 hydrolysis.

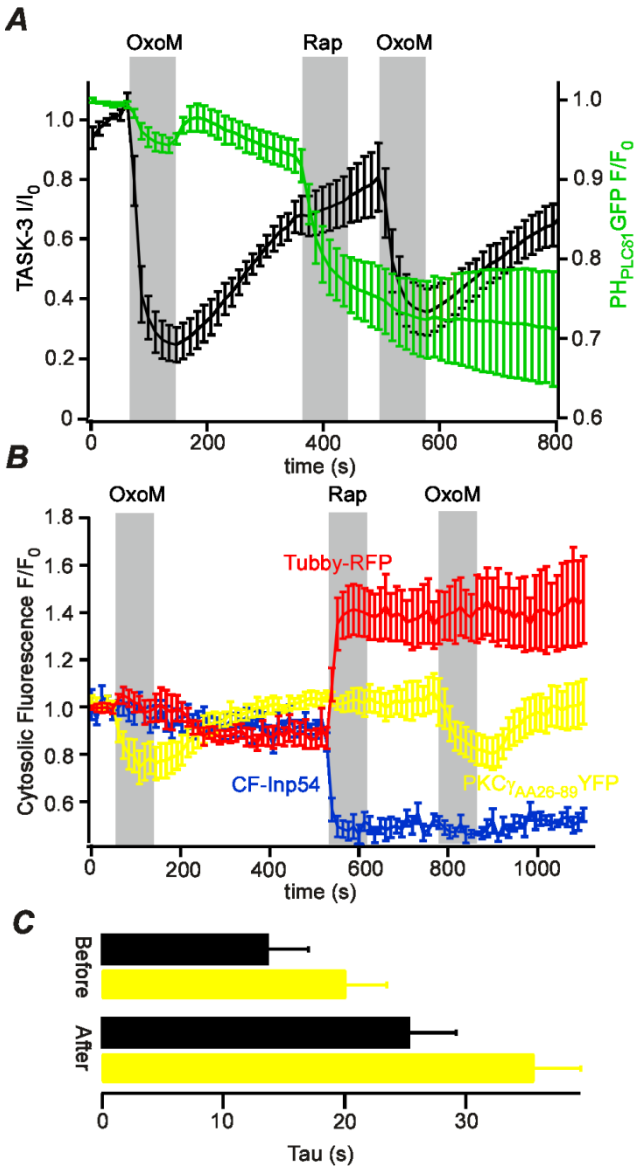

Fig. 19: Chemically induced PtdIns(4,5)P_2 depletion equally decelerates TASK channel inhibition and DAG synthesis. Cells co-transfected with m1R, Lyn11-FRB, CF-Inp54 and either $PH_{PLC\delta1}$GFP and TASK-3 in A or Tubby-RFP and $PKC\gamma_{26-89}$YFP in B. Cells treated subsequently with 10 µM OxoM, 5 µM Rapamycin and again 10 µM OxoM for 1 min each. A, Simultaneous TIRF and Patch-Clamp recordings reveal slower TASK-3 inhibition kinetics after CF-Inp54 recruitment (n = 5). B, Cytosolic fluorescence courses obtained by confocal imaging. Membrane association of $PKC_{\gamma26-89}$YFP indicating DAG production occurs slower after CF-Inp54 recruitment (n = 10). C, Time constants for TASK-3 inhibition (black) and $PKC_{\gamma26-89}$YFP membrane association (yellow) as shown in A and B.

Tab. 12: PtdIns(4,5)P_2 depletion increases time constants for muscarinic TASK-3 inhibition and DAG production.

	$\tau_{Before\ rapamycin}$ (s)	$\tau_{After\ rapamycin}$ (s)	N
$PKC\gamma_{26-89}$YFP	20.09 (±3.37)	35.62 (±3.89)	10
TASK-3	13.6312 (±2.64)	25.3093 (±6.79)	5

3.7 In absence of PtdIns(4,5)P_2 available to PLC-β G_qPCR activation fails to inhibit TASK

TASK channel inhibition and DAG production analogously decelerate after reduction of membrane PtdIns(4,5)P_2 levels, indicating a permissive role of PtdIns(4,5)P_2 for TASK channel inhibition. To fortify the hypothesis of a permissive role of PtdIns(4,5)P_2, it would be interesting to see how TASK channel inhibition was affected when PtdIns(4,5)P_2 virtually unavailable to PLC-β. The previous chapter showed that CF-Inp54 is not able to decrease PtdIns(4,5)P_2 levels far enough. However such a virtual absence might be achieved by activation of PLC-β itself. If the resynthesis of PtdIns(4,5)P_2 after PLC-β activation was blocked, no PtdIns(4,5)P_2 would be available for hydrolysis by a second PLC-β activation.

To create a virtual absence of PtdIns(4,5)P_2 experiments were performed analogously to those in chapter 3.4: Cells were co-transfected with the m1R and TASK-3. Patch pipettes were loaded with an intracellular solution containing no ATP but 3 mM of its non hydrolysable analog AMP-PCP, to block ATP-dependent PtdIns(4,5)P_2 resynthesis. After whole cell formation a period of 4 min was waited to give the AMP-PCP sufficient time to diffuse into the cell. Subsequently 10 µM OxoM (1 min) was applied resulting in a robust inhibition of TASK-3 (70.3 ± 9.7 %). Agonist application was followed by a 4 min wash-out interval. During this period recovery of TASK-3 currents occurred. Upon subsequent application of 10 µM OxoM (1 min) TASK currents remained practically unchanged (currents increased by 1.3 ± 5.5 %, Fig. 1 A and B), suggesting that PtdIns(4,5)P_2 is required to propagate signaling on TASK.

In a similar experimental approach the behavior of DAG was measured instead of TASK-3 (Leitner MG unpublished). Cells were analogously patched and an interval of 4 min was given for AMP-PCP to diffuse into the cell. Afterwards the DAG sensor PKC$\gamma_{26\text{-}89}$YFP was observed by TIRF microscopy. First application of 10 µM OxoM (1 min) resulted in a massive translocation of PKC$\gamma_{26\text{-}89}$YFP to the membrane, representing intensive DAG production. DAG levels recovered to their resting value within 5 min, indicated by a dissociation of PKC$\gamma_{26\text{-}89}$YFP from the membrane. The second application of 10 µM OxoM (1 min) did not result in a novel change in PKC$\gamma_{26\text{-}89}$YFP signal strength. Thus, no DAG was produced when no more PtdIns(4,5)P_2 was available to PLC-β.

These results demonstrated that TASK channel inhibition cannot occur in absence of PtdIns(4,5)P_2. PtdIns(4,5)P_2. therefore forms a permissive mediator in the process of G_qPCR induced TASK channel inhibition.

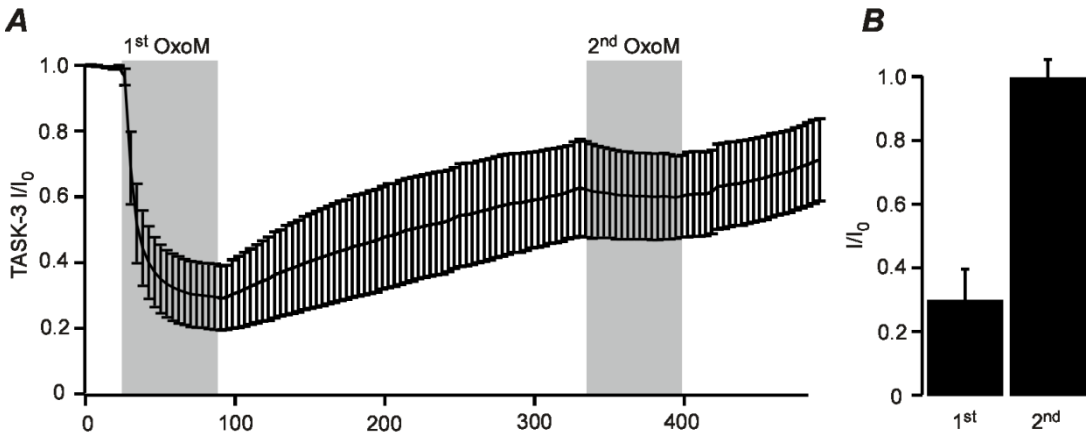

Fig. 20: TASK inhibition only occurs in the presence of PtdIns(4,5)P_2. Cells co-transfected with m1R and TASK-3 were patched with a pipette solution containing 3 mM AMP-PCP instead of ATP. A period of 4 minutes was waited before beginning the experiments. A gives the average time course of 5 cells with gray columns indicating the application intervals of 10 µM OxoM. First application results in an inhibition of TASK currents while the second application leaves TASK currents almost unchanged. B, Mean current inhibition, given as fraction of the pre-application current amplitude.

4 Discussion

In the present work, I investigated the mechanism underlying the G_qPCR-induced inhibition of TASK channels. Up until today there had been two main hypotheses which messenger molecule would directly mediate TASK channel inhibition. It was suggested that inhibition results either from a direct interaction of the channel with activated $G_q\alpha$ or from depletion of PtdIns(4,5)P_2.

To evaluate the these hypotheses distinct approaches to specifically modulate the levels of plasma membrane PtdIns(4,5)P_2 were used here. I consistently found no changes in TASK channel activity suggesting that the depletion of PtdIns(4,5)P_2 itself does not lead to TASK channel inhibition. In a next step it was investigated if the inhibition of TASK could be due to a direct interaction of the channel with $G_q\alpha$ by probing the involvement of PLC-β in channel inhibition. Two differential approaches showed that PLC-β activation is needed for effective signal transduction. As PLC-β is located downstream of $G_q\alpha$ by these results a direct inhibitory effect of $G_q\alpha$ on TASK could also be excluded. Finally the role of PtdIns(4,5)P_2 as one step within the signaling cascade that led to TASK channel inhibition was questioned. By decreasing the level of PtdIns(4,5)P_2 available for hydrolysis by PLC-β the inhibitory effect of G_qPCR activation on TASK was largely abolished. These experimental results demonstrate that the messenger molecule directly inhibiting TASK channels is located downstream of PtdIns(4,5)P_2 hydrolysis.

4.1 Does PtdIns(4,5)P_2 directly influence TASK channel activity?

By a set of switchable phosphatases, namely Ci-VSP, CF-Inp54 and RF-PJ the effect of G_qPCR triggered PLC-β activation on PtdIns(4,5)P_2 was mimicked. Activation of any of these constructs left TASK-1 and TASK-3 currents unchanged. To evaluate the accuracy of these approaches the degree of PtdIns(4,5)P_2 depletion achieved has to be considered. If Ci-VSP, CF-Inp54 and RF-PJ could accurately mimic the effect of PLC-β on PtdIns(4,5)P_2, the degree of PtdIns(4,5)P_2 depletion achieved by G_qPCR and switchable phosphatases should be approximately the same. Two different biosensors were used to monitor changes in PtdIns(4,5)P_2 concentrations: $PH_{PLC\delta1}$GFP as an established and extensively used fluorescent sensor (Stauffer *et al.*, 1998) and K_v7.4 a well characterized PtdIns(4,5)P_2-regulated ion channel (Suh & Hille, 2002; Zhang *et al.*, 2003; Suh *et al.*, 2006). When using $PH_{PLC\delta1}$GFP m1R induced membrane dissociation could be mimicked by recruitment of both CF-Inp54 and RF-PJ. For both constructs

time constants were slower, but the overall degree of $PH_{PLC\delta1}$GFP translocation was the same. Ci-VSP-mediated PtdIns(4,5)P_2 depletion led to a much faster and even more complete $PH_{PLC\delta1}$GFP translocation (Fig. 12 A, Tab. 6). Assuming that $PH_{PLC\delta1}$GFP translocation directly and uniquely reflects PtdIns(4,5)P_2 depletion, these observations suggest that CF-Inp54 and RF-PJ deplete PtdIns(4,5)P_2 to a similar degree as m1R, whereas Ci-VSP depletes PtdIns(4,5)P_2 even stronger. In fact it has to be taken into consideration that $PH_{PLC\delta1}$GFP also binds Ins(1,4,5)P_3 beside PtdIns(4,5)P_2 (reviewed in Varnai & Balla, 2006). Creation of Ins(1,4,5)P_3 on m1R facilitates the translocation of $PH_{PLC\delta1}$GFP to the cytosol. Therefore the degree of PtdIns(4,5)P_2 depletion achieved by m1R activation may be overestimated compared to that achieved by my switchable phosphatases where no Ins(1,4,5)P_3 is created. Thus my findings suggest that the engineered phosphatases deplete PtdIns(4,5)P_2 even more efficient than the m1R.

When using K_v7.4 as a PtdIns(4,5)P_2 sensor inhibition kinetics achieved with the engineered phosphatases were consistently faster than dissociation of $PH_{PLC\delta1}$GFP probably reflecting a lower apparent affinity of the channel for PtdIns(4,5)P_2. This observation is in agreement with recent reports in the literature (Falkenburger *et al.*, 2010c). Inhibition kinetics of K_v7.4 were faster upon PtdIns(4,5)P_2 manipulation by exogenous phosphatases than upon m1R activation, while the total extent of inhibition achieved were equal. These observations are consistent with recent findings from other groups, who described that effects of voltage-sensitive and chemically recruited phosphatases on PtdIns(4,5)P_2 sensitive ion channels were comparable to those of G_qPCR induced PtdIns(4,5)P_2 depletion (Suh *et al.*, 2006; Varnai *et al.*, 2006; Hernandez *et al.*, 2009; Falkenburger *et al.*, 2010c).

Comparing the m1R mediated inhibition of TASK-1 and TASK-3 with that of K_v7.4, inhibition of TASK occurred about threefold faster than inhibition of low PtdIns(4,5)P_2 affinity K_v7.4 (Tab. 5) (Hernandez *et al.*, 2009). If the inhibition of TASK was due to PtdIns(4,5)P_2 depletion, TASK-1 and TASK-3 should have an even lower PtdIns(4,5)P_2 affinity than K_v7.4. Hence, TASK should be more sensitive to activation of Ci-VSP, CF-Inp54 or RF-PJ. In contrast these phosphatases left TASK channels unaffected, while they successfully inhibited K_v7.4. These findings make a direct regulation of TASK channels by PtdIns(4,5)P_2 unlikely.

Earlier findings demonstrate that direct application of PtdIns(4,5)P_2 to excised patches enhanced TASK currents and intracellular application of PtdIns(4,5)P_2 scavengers partially inhibited TASK (Chemin *et al.*, 2003; Lopes *et al.*, 2005). How do those findings fit to the results presented in this study? PtdIns(4,5)P_2 changes achieved by those methods might extremely exceed the changes achieved by the engineered phosphatases used in this study(Rohacs, 2009). As outlined above, they must also exceed the changes achieved by G_qPCR activation. The PtdIns(4,5)P_2 sensitivity observed by Lopes et al. and Chemin et al. therefore does not represent a relevant mechanism for G_qPCR signaling on TASK. However these results may reflect a role of PtdIns(4,5)P_2 as a cofactor necessary for channel function, rather than a regulatory mechanism (see chapter 1.4.3). Such a role of PtdIns(4,5)P_2 as necessary cofactor is suggested as a general mechanism for many other ion channels but still lacks experimental evidence (Hilgemann, 2007). My results do not exclude such a cofactor role of PtdIns(4,5)P_2 and are therefore in accordance with experimental findings from Lopes and Chemin.

4.2 Are other PtdIns involved in TASK channel regulation?

The insensitivity of TASK channels to Ci-VSP and CF-Inp54 activation slows that receptor induced PtdIns(4,5)P_2 depletion is not sufficient for channel inhibition. However it remained possible that not PtdIns(4,5)P_2 depletion as such, but depletion of overall PtdIns or depletion of PtdIns(4)P could mediate current inhibition. It has been shown that ion channels such as K_{ATP} are activated also by PtdIns other than PtdIns(4,5)P_2 (Rohacs *et al.*, 2003). Furthermore it has been demonstrated that PLC-β activation does not only deplete PtdIns(4,5)P_2 but also PtdIns(4)P, which is present in the plasma membrane with comparable abundance (Willars *et al.*, 1998; Horowitz *et al.*, 2005; Di Paolo & De Camilli, 2006). If TASK channels were unspecifically regulated by PtdIns like K_{ATP}, activation of Ci-VSP or CF-Inp54 should fail to inhibit TASK. Therefore a novel switchable dual specificity phosphatase termed RF-PJ was introduced in this study (Lindner *et al.*, 2011). By using an established set of fluorescence sensors I could demonstrate that RF-PJ efficiently depletes both, PtdIns(4)P and PtdIns(4,5)P_2. As PtdIns(4)P and PtdIns(4,5)P_2 are two major PtdIns species at the cell membrane also the overall PtdIns concentration is significantly reduced. However TASK were insensitive to activation of RF-PJ, suggesting that G_qPCR triggered depletion of these membrane lipids does not evoke TASK channel inhibition.

Here it was also tested if TASK channel recovery from receptor induced inhibition could be derailed by blockage of PtdIns(4)P and PtdIns(4,5)P_2 resynthesis. In agreement with my results obtained with RF-PJ, recovery of TASK channels could still occur in the presence of the non-hydrolysable ATP analog AMP-PCP, where PtdIns(4,5)P_2 resynthesis is blocked (Suh & Hille, 2002). Thus these experiments confirm that receptor induced TASK inhibition is carried out neither by single nor combinatorial alteration of PtdIns(4)P or PtdIns(4,5)P_2.

4.3 May specific PtdIns(4,5)P_2 pools be involved in the regulation of TASK channels?

It has been suggested that the plasma membrane harbors functionally distinct pools of PtdIns. Such pools might, e.g. be organized in lipid rafts or caveolae (Cho *et al.*, 2005; Hilgemann, 2007; Johnson *et al.*, 2008; Oldfield *et al.*, 2009; Vasudevan *et al.*, 2009). They have been used to explain receptor-specific PtdIns(4,5)P_2 signaling on potassium channels in cardiomyocytes (Cho *et al.*, 2005). It was additionally demonstrated that G_qPCR induced K_v7 inhibition requires receptor-channel co-localization within the same PtdIns pool even in cultured cells (Oldfield *et al.*, 2009). TASK channel inhibition might be due to G_qPCR induced PtdIns(4,5)P_2 depletion within such a spatially limited PtdIns pool. In this case the m1R must be localized within the same pool as TASK, as it is efficient to inhibit the channel. In contrast the exogenous phosphatases did not have any effect on TASK. If G_qPCR inhibition was due to PtdIns(4,5)P_2 depletion anyhow, the exogenous phosphatases and TASK must exist in distinct pools. As activation of m1R and of the exogenous phosphatases induced a strong signal alteration for all of the bona-fide PtdIns sensors used (K_v7.4, PH_{2xOSH2}GFP and $PH_{PLC\delta1}$GFP) they must be distributed equally over the membrane, i.e. within and outside the exclusively m1R- or TASK-harboring pool. This hypothetical distribution of the TASK, G_qPCR, exogenous phosphatases and the sensor domains is illustrated in Fig. 21. Such a membrane distribution seems very unlikely and could be clearly excluded by other experimental findings presented here: By inhibition of PtdIns resynthesis by AMP-PCP the role of those PtdIns that had been depleted due to m1R activation itself can be specifically accessed. As m1R inhibits TASK it is guaranteed that the correct PtdIns pool was observed. In the experiments with AMP-PCP recovery of TASK channels was not altered. Thus TASK channel inhibition cannot be due to PtdIns depletion within a special pool of membrane lipids.

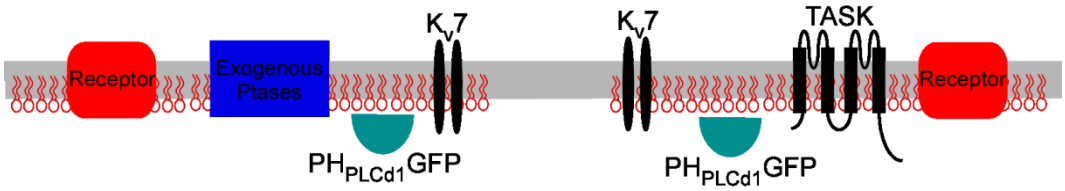

Fig. 21: Hypothetical model of a cell membrane containing PtdIns(4,5)P_2 signaling microdomains. The left domain contains my exogenous phosphatases, the m1R, $PH_{PLC\delta1}GFP$ and the K_v7 channels. In contrast the right domain additionally contains the TASK channel but it is missing the exogenous phosphatases.

4.4 Can a direct inhibitory mechanism by $G_q\alpha$ be excluded?

It is hard to directly and specifically interfere with $G_q\alpha$ signaling, as knowledge on the regulatory mechanism of this protein is still limited. Therefore the role of $G_q\alpha$ was resolved by interfering with the activity of PLC-β, which is directly activated by $G_q\alpha$. If PLC-β was dispensable for TASK channel inhibition this would suggest a direct interaction of $G_q\alpha$ and TASK. PLC-β was blocked by detraction of calcium, which is a necessary cofactor to this enzyme. Strong buffering of intracellular resting calcium with EGTA robustly decreased m1R-induced inhibition of TASK-3, most likely reflecting blockage of PLC-β. Using the fast calcium buffer BAPTA instead of EGTA equally reduced the response of TASK-3 to receptor stimulation. In fact BAPTA was even more effective, probably reflecting a stronger block of PLC-β by buffering also calcium released from intracellular stores. Thus PLC-β is needed for TASK inhibition and a direct inhibitory effect of $G_q\alpha$ on TASK can be excluded.

The necessity of PLC-β for TASK channel inhibition was confirmed by an independent approach using U-73122, an established PLC-β blocking agent (e.g.: Mogami *et al.*, 1997; Stauffer *et al.*, 1998; Suga *et al.*, 2003; Horowitz *et al.*, 2005). In the present work U-73122 was efficient to block the inhibition of TASK-3 and TASK-1_{NQ} channels by two different G_qPCR (namely m1R and Et-AR). Also previous studies have used U-73122 to investigate TASK channel inhibition revealing contradictory results (Boyd *et al.*, 2000; Czirjak *et al.*, 2001; Chemin *et al.*, 2003; Lopes *et al.*, 2005; Chen *et al.*, 2006). However those studies do not provide sufficient controls. This work is the first to provide both positive and negative controls and to report and deal with critical side effects of U-73122 and therefore also helps understand the diverging results obtained before.

PLC-β activation is generally considered the first calcium dependent step in the G_qPCR cascade. It is also considered to be the only step within the cascade blocked by U-73122. But for both, calcium and U-73122, the evidence is missing. To clarify this issue in future it will help to examine the G_qPCR pathway for other calcium dependent or U-73122 sensitive steps e.g. by making use of FRET (fluorescence resonance energy transfer). Thereby e.g. successful dissociation of the G_qPCR-$G_q\alpha\beta\gamma$ complex or conformational changes within the G_qPCR could be monitored.

This work additionally shows that PtdIns(4,5)P_2 hydrolysis by PLC-β is necessary for efficient signal propagation from G_qPCR to TASK. The m1R was activated and TASK currents were monitored either after CF-Inp54 induced PtdIns(4,5)P_2 depletion or after previous PtdIns(4,5)P_2 depletion by m1R activation. TASK channel inhibition was strongly reduced after CF-Inp54 recruitment and completely abandoned after previous m1R activation, most likely as a consequence of reduced PtdIns(4,5)P_2 levels. As this approach interferes with the signaling cascade far downstream of $G_q\alpha$ it provides further evidence arguing against a direct inhibitory mechanism by $G_q\alpha$.

While these experiments convincingly exclude a direct inhibitory effect of $G_q\alpha$ on TASK channels, a different experimental approach by Chen et al. appeared to provide good evidence in favor of a direct inhibitory mechanism by $G_q\alpha$. Thus detailed discussion is required at this point (Chen *et al.*, 2006). In their study Chen et al. used a cell line derived from $G_q\alpha$ knock-out mice. When these cells were transfected only with a G_qPCR and TASK, G_qPCR agonists did not induce TASK channel inhibition. Further co-transfection of $G_q\alpha$ was required to reconstitute the inhibitory effect. However the ability of $G_q\alpha$ to activate PLC-β was seemingly not required: When transfecting a mutant $G_q\alpha$ that was shown to possess a strongly reduced PLC-β affinity in vitro, TASK inhibition was still present (Venkatakrishnan & Exton, 1996; Chen *et al.*, 2006). Noteworthy the study by Chen et al lacks the evidence that activation of PLC-β does really not occur in presence of the mutated $G_q\alpha$. To clarify the discrepancy between my work (Lindner *et al.*, 2011; Schiekel *et al.*, in revision) and the work of Chen et al Bettina Wilke probed if PLC-β activation occurs in presence of the mutated $G_q\alpha$ by performing experiments similar to those by Chen et al but with $PH_{PLC\delta1}$GFP instead of TASK (Wilke *et al.*, Unpublished). Her experiments show that PLC-β activation still occurs in presence of mutated $G_q\alpha$ but not in total absence of $G_q\alpha$. Therefore the results by Chen et al do not help to evaluate the role of $G_q\alpha$ for TASK channel inhibition and the contradiction to the present results is resolved.

4.5 What is the role of PLC-β activity in the inhibition process?

Above experiments, where PLC-β was blocked either pharmacologically or by withdrawal of its calcium were discussed. The discussion so far focused on the conclusions that can be drawn about a direct inhibitory action of $G_q\alpha$ on TASK. These experiments obviously also tell us about the role of PLC-β itself: When PLC-β was bocked by either approach G_qPCR activation did not lead to TASK channel inhibition any more. Thus PLC-β activation is a necessary step for TASK channel inhibition.

PLC-β hydrolyses PtdIns(4,5)P_2 to Ins(1,4,5)P_3, DAG. Frequently ignored it thereby also generates one proton (Huang *et al.*, 2010). It is well established that after blockage of PLC-β neither the concentration of PtdIns(4,5)P_2 will decrease nor will the concentration of Ins(1,4,5)P_3, DAG or protons increase (Horowitz *et al.*, 2005). Having ruled out a direct role of PtdIns(4,5)P_2 my experiments suggest that alteration of any of the other molecules should mediate TASK inhibition. However, also an immediate interaction between activated PLC-β and TASK might explain the results. This possibility could be ruled out by an experiment where Ins(1,4,5)P_3, DAG and protons were not created, while PLC-β activity remained intact. PtdIns(4,5)P_2 was depleted by CF-Inp54 recruitment before the activation of the m1R and the effect of m1R activation on TASK was observed. I found that depletion of PtdIns(4,5)P_2 decreases speed and total extent of TASK inhibition, as it would be expected if this molecule was a permissive mediator in the signaling cascade to inhibit TASK.

Moreover the m1R was used to deplete PtdIns(4,5)P_2 while its resynthesis was blocked by AMP-PCP and afterwards the effect of a novel m1R activation on TASK was observed. Thereby a virtual absence of PtdIns(4,5)P_2 could be achieved. Under this condition m1R activation failed to inhibit TASK despite fully functional PLC-β. These experimental observations show that creation of PtdIns(4,5)P_2 metabolites by PLC-β and not just PLC-β activity as such is essential for TASK channel inhibition.

4.6 The mechanism of G_qPCR mediated TASK inhibition

The present work could clearly attribute TASK channel inhibition to a messenger molecule downstream of PLC-β mediated PtdIns(4,5)P_2 hydrolysis. Remaining candidates therefore include the direct hydrolysis products of PtdIns(4,5)P_2: Ins(1,4,5)P_3, DAG and protons. Also potential downstream messenger molecules have to be considered. Those include calcium, as liberated from the endoplasmatic reticulum

by Ins(1,4,5)P_3, PKC activated by DAG, and DAG metabolites such as phosphatidic acid and monoacyl-glycerol.

4.6.1 PKC

An effect of PKC was clearly excluded before, as G_qPCR mediated inhibition remains present in TASK channels which have all potential phosphorylation sites removed (Czirjak *et al.*, 2001; Chemin *et al.*, 2003; Veale *et al.*, 2007). The present results further show that TASK channel inhibition fully persists when all ATP is removed and thus all phosphorylation processes are blocked. Therefore this work provides additional evidence against an involvement of PKC.

4.6.2 Calcium

The role of calcium is less clear. Literature provides only indirect evidence generally arguing against a role of calcium (Czirjak *et al.*, 2001; Chemin *et al.*, 2003; Veale *et al.*, 2007). In contrast, my results are consistent with calcium as a possible candidate. The fast calcium chelator BAPTA blocks m1R induced inhibition of TASK much more effective than EGTA at equal concentration. Noteworthy BAPTA and EGTA do not differ in buffering capacity but only in buffering speed (Fakler & Adelman, 2008; Enyeart *et al.*, 2011) Therefore BAPTA is considered to be capable to buffer also fast calcium transients as they occur by opening of intracellular Ins(1,4,5)P_3-sensitive stores. The difference in efficiency to block TASK channel inhibition could thus be explained by differences in store-released calcium available to either PLC-β or to TASK. Both of these possible explanations require a minimal residual PLC-β activity in presence of both BAPTA and EGTA that leads to the creation of Ins(1,4,5)P_3 and subsequent release of calcium from intracellular stores.

Previous studies have excluded calcium to have an inhibitory effect on TASK by artificial induction of calcium release from intracellular stores or previous emptying of those (Czirjak *et al.*, 2001; Chemin *et al.*, 2003; Veale *et al.*, 2007). However none of these studies examined the direct influence of calcium on TASK channels. This could be easily done by application of high calcium containing solutions on excised patches or by whole cell patch clamp recordings with an intracellular solution containing high calcium concentrations. Performing such an experiment will be required to safely exclude calcium as a direct inhibitor of TASK.

4.6.3 Ins(1,4,5)P_3 and DAG

The remaining common messenger molecules Ins(1,4,5)P_3 and DAG need further attention. As discussed above (see chapter 4.5), both, TASK channel inhibition and DAG production by G_qPCR activation are only decelerated (but not fully abolished) after previous PtdIns(4,5)P_2 depletion by CF-Inp54. This might suggest that TASK channel inhibition is mediated via the DAG branch.

While earlier research mostly argues against a role of Ins(1,4,5)P_3 (Czirjak *et al.*, 2001; Veale *et al.*, 2007), the role of DAG has never been tested. To clarify this issue the direct effect of these two messenger molecules on TASK channels should be examined. This could be performed e.g. by application of these substances onto an excised patch and subsequent confirmation in the intact cell. In addition a different approach may provide further evidence: Whole-cell patch-clamp experiments could help where the two principal DAG metabolizing enzymes, namely DAG lipase and DAG kinase (Migas *et al.*, 1997; Sakane & Kanoh, 1997; Basavarajappa, 2007; Shulga *et al.*, 2011) are expressed together with a G_qPCR and TASK. If DAG would directly inhibit TASK channels recovery from inhibition should be accelerated by overexpression of DAG lipase or DAG kinase. DAG lipase metabolizes DAG to monoacyl-glycerol and arachidonic acid while DAG kinase phosphorylates DAG to phosphatidic acid (Migas *et al.*, 1997) (Fig. 22). Overexpression of DAG lipase thus results in creation of higher levels of monoacyl-glycerol and arachidonic acid after PLC-β activation. If TASK inhibition was due to one of those molecules, the overexpression of DAG lipase would result in prolonged channel recovery. In contrast overexpression of DAG kinase would sequester the substrate of DAG lipase and therefore result in accelerated recovery. If TASK inhibition was due an increase in phosphatidic acid concentrations, opposite results would be achieved. As specific inhibitors exist for both DAG lipase and DAG kinase these observations could be validated by an independent pharmacological approach.

The hypothesis of a regulation of TASK by DAG or one of its metabolites is especially interesting as a regulatory effect of arachidonic acid is described for TREK and TRAAK channels, both members of the K_{2P} family (Goldstein *et al.*, 2005). A direct effect of DAG on any K_{2P} channel has not been described yet. However regulation of different ion channels by DAG is well established. Well studied examples are channels from the transient receptor potential family, TRPC (Harteneck & Gollasch, 2010).

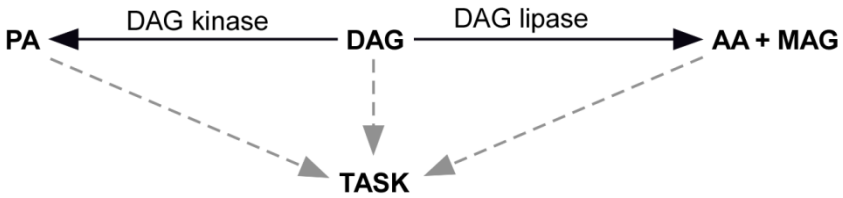

Fig. 22: Metabolism of DAG. DAG or its metabolites might inhibit TASK channels. AA arachidonic acid, MAG monoacyl glycerol, PA phosphatidic acid.

4.6.4 Protons

Hydrolysis of PtdIns(4,5)P_2 also results in the liberation of a proton (Rebecchi & Pentyala, 2000). It has been demonstrated that this proton release results in a slight intracellular acidification in the range of 0.1 pH units (Huang *et al.*, 2010). The response of TASK to intracellular acidification has frequently been tested (Duprat *et al.*, 1997; Rajan *et al.*, 2000; Patel & Honore, 2001). It was consistently shown that decrease of intracellular pH does not affect TASK currents. TASK channel inhibition by protons can therefore be excluded.

4.6.5 Non-canonical inhibitory mechanisms

So far messenger molecules classically known to affect ion channels were discussed. However two very untypical inhibitory mechanisms need to be considered. First, G_qPCR induced TASK channel inhibition may depend on combinatorial alteration of two or even more messenger molecules within the classical G_qPCR cascade. Second, TASK inhibition might be due to activation of the Rho-GEF pathway. This signaling pathway has recently been shown to influence ion channel function (Szaszi *et al.*, 2000; Karpushev *et al.*, 2010) but is classically involved in oncogenesis, cell cycle control, and cytoskeleton formation (Lazer & Katzav, 2010). If the Rho-GEF pathway was involved in the inhibition of TASK channels it would have to contain a calcium dependent and U-73122 sensitive step, as both blocks TASK inhibition. So far no such sensitivity of the Rho-GEF pathway has been reported. Also the permissive role of PtdIns(4,5)P_2 appears to be inconsistent with the Rho-GEF pathway. In conclusion, it is unlikely that the Rho-GEF pathway is important for TASK channel inhibition.

4.7 Concluding remarks

In the present work the mechanism underlying the G_qPCR induced inhibition of TASK channels was investigated. The two popular hypotheses of an inhibitory mechanism where TASK is directly blocked by PtdIns(4,5)P_2 depletion or $G_q\alpha$ activation could be excluded. Additionally it could be shown that beside PtdIns(4,5)P_2, the classical PLC-β substrate, also the depletion of other PtdIns does not result in TASK channel inhibition. Furthermore this work provides clear evidence that hydrolysis of PtdIns(4,5)P_2 to Ins(1,4,5)P_3 and DAG by PLC-β is indispensable for TASK channel inhibition. It therefore demonstrates that the role of PtdIns(4,5)P_2 for TASK channel inhibition is that of a permissive mediator rather than of a direct messenger itself.

Despite of these advances, the final effector of TASK channel inhibition remains to be identified. If no atypical mechanism is involved, the present work only spares a few candidate molecules: Those are Ins(1,4,5)P_3 and calcium, on the one hand and DAG together with its metabolites on the other hand. Finally I have discussed a subsequent experimental approach to identify the molecule that directly mediates TASK channel inhibition.

5 Appendix

5.1 Reference

*Aller MI, Veale EL, Linden AM, Sandu C, Schwaninger M, Evans LJ, Korpi ER, Mathie A, Wisden W & Brickley SG. (2005). Modifying the subunit composition of TASK channels alters the modulation of a leak conductance in cerebellar granule neurons. J Neurosci **25,** 11455-11467.*

*Balla A, Kim YJ, Varnai P, Szentpetery Z, Knight Z, Shokat KM & Balla T. (2008). Maintenance of hormone-sensitive phosphoinositide pools in the plasma membrane requires phosphatidylinositol 4-kinase IIIalpha. Mol Biol Cell **19,** 711-721.*

*Balla T, Szentpetery Z & Kim YJ. (2009). Phosphoinositide signaling: new tools and insights. Physiology (Bethesda) **24,** 231-244.*

*Basavarajappa BS. (2007). Critical enzymes involved in endocannabinoid metabolism. Protein Pept Lett **14,** 237-246.*

*Baukrowitz T, Schulte U, Oliver D, Herlitze S, Krauter T, Tucker SJ, Ruppersberg JP & Fakler B. (1998). PIP2 and PIP as determinants for ATP inhibition of KATP channels. Science **282,** 1141-1144.*

*Bayliss DA & Barrett PQ. (2008). Emerging roles for two-pore-domain potassium channels and their potential therapeutic impact. Trends Pharmacol Sci **29,** 566-575.*

*Berridge MJ & Irvine RF. (1989). Inositol phosphates and cell signalling. Nature **341,** 197-205.*

*Besana A, Barbuti A, Tateyama MA, Symes AJ, Robinson RB & Feinmark SJ. (2004). Activation of protein kinase C epsilon inhibits the two-pore domain K+ channel, TASK-1, inducing repolarization abnormalities in cardiac ventricular myocytes. J Biol Chem **279,** 33154-33160.*

*Boyd DF, Millar JA, Watkins CS & Mathie A. (2000). The role of Ca2+ stores in the muscarinic inhibition of the K+ current IK(SO) in neonatal rat cerebellar granule cells. J Physiol **529 Pt 2,** 321-331.*

Brohawn SJ. (2012). Crystal Structure of the Human K2P TRAAK, a Lipid- and Mechano-Sensitive K+ Ion Channel Science.

*Brown DA & Adams PR. (1980). Muscarinic suppression of a novel voltage-sensitive K+ current in a vertebrate neurone. Nature **283,** 673-676.*

*Brunner F, Bras-Silva C, Cerdeira AS & Leite-Moreira AF. (2006). Cardiovascular endothelins: essential regulators of cardiovascular homeostasis. Pharmacol Ther **111,** 508-531.*

*Bunney TD & Katan M. (2011). PLC regulation: emerging pictures for molecular mechanisms. Trends Biochem Sci **36,** 88-96.*

*Chemin J, Girard C, Duprat F, Lesage F, Romey G & Lazdunski M. (2003). Mechanisms underlying excitatory effects of group I metabotropic glutamate receptors via inhibition of 2P domain K+ channels. EMBO J **22,** 5403-5411.*

*Chen X, Talley EM, Patel N, Gomis A, McIntire WE, Dong B, Viana F, Garrison JC & Bayliss DA. (2006). Inhibition of a background potassium channel by Gq protein alpha-subunits. Proc Natl Acad Sci U S A **103,** 3422-3427.*

*Cho H, Kim YA, Yoon JY, Lee D, Kim JH, Lee SH & Ho WK. (2005). Low mobility of phosphatidylinositol 4,5-bisphosphate underlies receptor specificity of Gq-mediated ion channel regulation in atrial myocytes. Proc Natl Acad Sci U S A **102,** 15241-15246.*

*Chun M, Lin HY, Henis YI & Lodish HF. (1995). Endothelin-induced endocytosis of cell surface ETA receptors. Endothelin remains intact and bound to the ETA receptor. J Biol Chem **270,** 10855-10860.*

*Czirjak G, Fischer T, Spat A, Lesage F & Enyedi P. (2000). TASK (TWIK-related acid-sensitive K+ channel) is expressed in glomerulosa cells of rat adrenal cortex and inhibited by angiotensin II. Mol Endocrinol **14,** 863-874.*

*Czirjak G, Petheo GL, Spat A & Enyedi P. (2001). Inhibition of TASK-1 potassium channel by phospholipase C. Am J Physiol Cell Physiol **281,** C700-708.*

*D'Angelo G, Vicinanza M, Di Campli A & De Matteis MA. (2008). The multiple roles of PtdIns(4)P -- not just the precursor of PtdIns(4,5)P2. J Cell Sci **121,** 1955-1963.*

*Damron DS, Van Wagoner DR, Moravec CS & Bond M. (1993). Arachidonic acid and endothelin potentiate Ca2+ transients in rat cardiac myocytes via inhibition of distinct K+ channels. J Biol Chem **268,** 27335-27344.*

*Davies LA, Hu C, Guagliardo NA, Sen N, Chen X, Talley EM, Carey RM, Bayliss DA & Barrett PQ. (2008). TASK channel deletion in mice causes primary hyperaldosteronism. Proc Natl Acad Sci U S A **105,** 2203-2208.*

*Delmas P & Brown DA. (2005). Pathways modulating neural KCNQ/M (Kv7) potassium channels. Nat Rev Neurosci **6,** 850-862.*

*Deng W, Baki L & Baumgarten CM. (2010). Endothelin signalling regulates volume-sensitive Cl- current via NADPH oxidase and mitochondrial reactive oxygen species. Cardiovasc Res **88,** 93-100.*

*Di Paolo G & De Camilli P. (2006). Phosphoinositides in cell regulation and membrane dynamics. Nature **443,** 651-657.*

*Dietrich A, Mederos y Schnitzler M, Kalwa H, Storch U & Gudermann T. (2005). Functional characterization and physiological relevance of the TRPC3/6/7 subfamily of cation channels. Naunyn Schmiedebergs Arch Pharmacol **371,** 257-265.*

*Donner BC, Schullenberg M, Geduldig N, Huning A, Mersmann J, Zacharowski K, Kovacevic A, Decking U, Aller MI & Schmidt KG. (2010). Functional role of TASK-1 in the heart: studies in TASK-1-deficient mice show prolonged cardiac repolarization and reduced heart rate variability. Basic Res Cardiol **106,** 75-87.*

*Drin G & Scarlata S. (2007). Stimulation of phospholipase Cbeta by membrane interactions, interdomain movement, and G protein binding--how many ways can you activate an enzyme? Cell Signal **19,** 1383-1392.*

*Du X, Zhang H, Lopes C, Mirshahi T, Rohacs T & Logothetis DE. (2004). Characteristic interactions with phosphatidylinositol 4,5-bisphosphate determine regulation of kir channels by diverse modulators. J Biol Chem **279,** 37271-37281.*

*Duprat F, Lauritzen I, Patel A & Honore E. (2007). The TASK background K2P channels: chemo- and nutrient sensors. Trends Neurosci **30,** 573-580.*

*Duprat F, Lesage F, Fink M, Reyes R, Heurteaux C & Lazdunski M. (1997). TASK, a human background K+ channel to sense external pH variations near physiological pH. EMBO J **16,** 5464-5471.*

*Egger MD & Petran M. (1967). New reflected-light microscope for viewing unstained brain and ganglion cells. Science **157,** 305-307.*

Enyeart JJ, Liu H & Enyeart JA. (2011). Calcium-dependent Inhibition of Adrenal TREK-1 Channels by Angiotensin II and Ionomycin. Am J Physiol Cell Physiol.

*Enyedi P & Czirjak G. (2010). Molecular background of leak K+ currents: two-pore domain potassium channels. Physiol Rev **90,** 559-605.*

*Fakler B & Adelman JP. (2008). Control of K(Ca) channels by calcium nano/microdomains. Neuron **59,** 873-881.*

*Falkenburger BH, Jensen JB, Dickson EJ, Suh BC & Hille B. (2010a). Phosphoinositides: lipid regulators of membrane proteins. J Physiol **588,** 3179-3185.*

*Falkenburger BH, Jensen JB & Hille B. (2010b). Kinetics of M1 muscarinic receptor and G protein signaling to phospholipase C in living cells. J Gen Physiol **135,** 81-97.*

*Falkenburger BH, Jensen JB & Hille B. (2010c). Kinetics of PIP2 metabolism and KCNQ2/3 channel regulation studied with a voltage-sensitive phosphatase in living cells. J Gen Physiol **135,** 99-114.*

*Fine A. (2007). Confocal microscopy: principles and practice. CSH Protoc **2007,** pdb top22.*

*Fine A, Amos WB, Durbin RM & McNaughton PA. (1988). Confocal microscopy: applications in neurobiology. Trends Neurosci **11,** 346-351.*

*Fink M, Duprat F, Lesage F, Reyes R, Romey G, Heurteaux C & Lazdunski M. (1996). Cloning, functional expression and brain localization of a novel unconventional outward rectifier K+ channel. EMBO J **15,** 6854-6862.*

*Foord SM, Bonner TI, Neubig RR, Rosser EM, Pin JP, Davenport AP, Spedding M & Harmar AJ. (2005). International Union of Pharmacology. XLVI. G protein-coupled receptor list. Pharmacol Rev **57,** 279-288.*

*Gamper N & Shapiro MS. (2007). Target-specific PIP(2) signalling: how might it work? J Physiol **582,** 967-975.*

*Gilman AG. (1987). G proteins: transducers of receptor-generated signals. Annu Rev Biochem **56,** 615-649.*

*Goldman DE. (1943). Potential, Impedance, and Rectification in Membranes. J Gen Physiol **27,** 37-60.*

*Goldstein SA, Bayliss DA, Kim D, Lesage F, Plant LD & Rajan S. (2005). International Union of Pharmacology. LV. Nomenclature and molecular relationships of two-P potassium channels. Pharmacol Rev **57,** 527-540.*

*Goldstein SA, Bockenhauer D, O'Kelly I & Zilberberg N. (2001). Potassium leak channels and the KCNK family of two-P-domain subunits. Nat Rev Neurosci **2,** 175-184.*

*Gurney A & Manoury B. (2009). Two-pore potassium channels in the cardiovascular system. Eur Biophys J **38,** 305-318.*

*Halaszovich CR, Schreiber DN & Oliver D. (2009). Ci-VSP is a depolarization-activated phosphatidylinositol-4,5-bisphosphate and phosphatidylinositol-3,4,5-trisphosphate 5'-phosphatase. J Biol Chem **284,** 2106-2113.*

*Halstead JR, Jalink K & Divecha N. (2005). An emerging role for PtdIns(4,5)P2-mediated signalling in human disease. Trends Pharmacol Sci **26,** 654-660.*

*Hamill OP, Marty A, Neher E, Sakmann B & Sigworth FJ. (1981). Improved patch-clamp techniques for high-resolution current recording from cells and cell-free membrane patches. Pflugers Arch **391,** 85-100.*

*Harteneck C & Gollasch M. (2010). Pharmacological modulation of diacylglycerol-sensitive TRPC3/6/7 channels. Curr Pharm Biotechnol **12,** 35-41.*

*Heitzmann D, Derand R, Jungbauer S, Bandulik S, Sterner C, Schweda F, El Wakil A, Lalli E, Guy N, Mengual R, Reichold M, Tegtmeier I, Bendahhou S, Gomez-Sanchez CE, Aller MI, Wisden W, Weber A, Lesage F, Warth R & Barhanin J. (2008). Invalidation of TASK1 potassium channels disrupts adrenal gland zonation and mineralocorticoid homeostasis. EMBO J **27,** 179-187.*

*Hernandez CC, Falkenburger B & Shapiro MS. (2009). Affinity for phosphatidylinositol 4,5-bisphosphate determines muscarinic agonist sensitivity of Kv7 K+ channels. J Gen Physiol **134,** 437-448.*

*Hernandez CC, Zaika O & Shapiro MS. (2008). A carboxy-terminal inter-helix linker as the site of phosphatidylinositol 4,5-bisphosphate action on Kv7 (M-type) K+ channels. J Gen Physiol **132,** 361-381.*

*Hilgemann DW. (2007). Local PIP(2) signals: when, where, and how? Pflugers Arch **455,** 55-67.*

*Hilgemann DW & Ball R. (1996). Regulation of cardiac Na+,Ca2+ exchange and KATP potassium channels by PIP2. Science **273,** 956-959.*

Hille B. (2001). Ion channels of excitable membranes. Sinauer Ass., Sunderland, Mass.

*Hodgkin AL & Huxley AF. (1947). Potassium leakage from an active nerve fibre. J Physiol **106,** 341-367.*

*Hodgkin AL & Huxley AF. (1952). A quantitative description of membrane current and its application to conduction and excitation in nerve. J Physiol **117,** 500-544.*

Hodgkin AL & Katz B. (1949). The effect of sodium ions on the electrical activity of giant axon of the squid. J Physiol ***108,*** *37-77.*

Hopwood SE & Trapp S. (2005). TASK-like K+ channels mediate effects of 5-HT and extracellular pH in rat dorsal vagal neurones in vitro. J Physiol ***568,*** *145-154.*

Horowitz LF, Hirdes W, Suh BC, Hilgemann DW, Mackie K & Hille B. (2005). Phospholipase C in living cells: activation, inhibition, Ca2+ requirement, and regulation of M current. J Gen Physiol ***126,*** *243-262.*

Huang CL, Feng S & Hilgemann DW. (1998). Direct activation of inward rectifier potassium channels by PIP2 and its stabilization by Gbetagamma. Nature ***391,*** *803-806.*

Huang J, Liu CH, Hughes SA, Postma M, Schwiening CJ & Hardie RC. (2010). Activation of TRP channels by protons and phosphoinositide depletion in Drosophila photoreceptors. Curr Biol ***20,*** *189-197.*

Johnson CM, Chichili GR & Rodgers W. (2008). Compartmentalization of phosphatidylinositol 4,5-bisphosphate signaling evidenced using targeted phosphatases. J Biol Chem ***283,*** *29920-29928.*

Kang D, Han J, Talley EM, Bayliss DA & Kim D. (2004). Functional expression of TASK-1/TASK-3 heteromers in cerebellar granule cells. J Physiol ***554,*** *64-77.*

Karaman MW, Herrgard S, Treiber DK, Gallant P, Atteridge CE, Campbell BT, Chan KW, Ciceri P, Davis MI, Edeen PT, Faraoni R, Floyd M, Hunt JP, Lockhart DJ, Milanov ZV, Morrison MJ, Pallares G, Patel HK, Pritchard S, Wodicka LM & Zarrinkar PP. (2008). A quantitative analysis of kinase inhibitor selectivity. Nat Biotechnol ***26,*** *127-132.*

Karpushev AV, Ilatovskaya DV, Pavlov TS, Negulyaev YA & Staruschenko A. (2010). Intact cytoskeleton is required for small G protein dependent activation of the epithelial Na+ channel. PLoS One ***5,*** *e8827.*

Kim Y, Bang H & Kim D. (2000). TASK-3, a new member of the tandem pore K(+) channel family. J Biol Chem ***275,*** *9340-9347.*

Kwiatkowska K. (2010). One lipid, multiple functions: how various pools of PI(4,5)P(2) are created in the plasma membrane. Cell Mol Life Sci ***67,*** *3927-3946.*

Lazer G & Katzav S. (2010). Guanine nucleotide exchange factors for RhoGTPases: good therapeutic targets for cancer therapy? Cell Signal ***23,*** *969-979.*

*Leitner MG, Halaszovich CR & Oliver D. (2010). Aminoglycosides inhibit KCNQ4 channels in cochlear outer hair cells via depletion of phosphatidylinositol(4,5)bisphosphate. Mol Pharmacol **79,** 51-60.*

*Lesage F, Guillemare E, Fink M, Duprat F, Lazdunski M, Romey G & Barhanin J. (1996). TWIK-1, a ubiquitous human weakly inward rectifying K+ channel with a novel structure. EMBO J **15,** 1004-1011.*

*Lesage F, Terrenoire C, Romey G & Lazdunski M. (2000). Human TREK2, a 2P domain mechano-sensitive K+ channel with multiple regulations by polyunsaturated fatty acids, lysophospholipids, and Gs, Gi, and Gq protein-coupled receptors. J Biol Chem **275,** 28398-28405.*

*Li Y, Gamper N, Hilgemann DW & Shapiro MS. (2005). Regulation of Kv7 (KCNQ) K+ channel open probability by phosphatidylinositol 4,5-bisphosphate. J Neurosci **25,** 9825-9835.*

*Lindner M, Leitner MG, Halaszovich CR, Hammond GR & Oliver D. (2011). Probing the regulation of TASK potassium channels by PI(4,5)P with switchable phosphoinositide phosphatases. J Physiol **589,** 3149-3162.*

*Liu C, Au JD, Zou HL, Cotten JF & Yost CS. (2004). Potent activation of the human tandem pore domain K channel TRESK with clinical concentrations of volatile anesthetics. Anesth Analg **99,** 1715-1722, table of contents.*

Lomasney JW, Cheng HF, Kobayashi M & King K. (2012). Structural Basis for Calcium and Phosphatidyl Serine Regulation of PLC Delta1. Biochemistry.

*Lopes CM, Gallagher PG, Buck ME, Butler MH & Goldstein SA. (2000). Proton block and voltage gating are potassium-dependent in the cardiac leak channel Kcnk3. J Biol Chem **275,** 16969-16978.*

*Lopes CM, Rohacs T, Czirjak G, Balla T, Enyedi P & Logothetis DE. (2005). PIP2 hydrolysis underlies agonist-induced inhibition and regulates voltage gating of two-pore domain K+ channels. J Physiol **564,** 117-129.*

*Luscher C & Slesinger PA. (2010). Emerging roles for G protein-gated inwardly rectifying potassium (GIRK) channels in health and disease. Nat Rev Neurosci **11,** 301-315.*

*MacGregor GG, Dong K, Vanoye CG, Tang L, Giebisch G & Hebert SC. (2002). Nucleotides and phospholipids compete for binding to the C terminus of KATP channels. Proc Natl Acad Sci U S A **99,** 2726-2731.*

Mani M, Lee SY, Lucast L, Cremona O, Di Paolo G, De Camilli P & Ryan TA. (2007). The dual phosphatase activity of synaptojanin1 is required for

*both efficient synaptic vesicle endocytosis and reavailability at nerve terminals. Neuron **56,** 1004-1018.*

*Mathie A. (2007). Neuronal two-pore-domain potassium channels and their regulation by G protein-coupled receptors. J Physiol **578,** 377-385.*

*McCudden CR, Hains MD, Kimple RJ, Siderovski DP & Willard FS. (2005). G-protein signaling: back to the future. Cell Mol Life Sci **62,** 551-577.*

*Migas I, Chuang M, Sasaki Y & Severson DL. (1997). Diacylglycerol metabolism in SM-3 smooth muscle cells. Can J Physiol Pharmacol **75,** 1249-1256.*

*Millar JA, Barratt L, Southan AP, Page KM, Fyffe RE, Robertson B & Mathie A. (2000). A functional role for the two-pore domain potassium channel TASK-1 in cerebellar granule neurons. Proc Natl Acad Sci U S A **97,** 3614-3618.*

Miller AN. (2012). Crystal Structure of the Human Two–Pore Domain Potassium Channel K2P1 Science.

Minsky M. (1957). US Patent No. 3013467. USA.

*Mizuno N & Itoh H. (2009). Functions and regulatory mechanisms of Gq-signaling pathways. Neurosignals **17,** 42-54.*

*Mogami H, Lloyd Mills C & Gallacher DV. (1997). Phospholipase C inhibitor, U73122, releases intracellular Ca2+, potentiates Ins(1,4,5)P3-mediated Ca2+ release and directly activates ion channels in mouse pancreatic acinar cells. Biochem J **324 (Pt 2),** 645-651.*

*Morton MJ, O'Connell AD, Sivaprasadarao A & Hunter M. (2003). Determinants of pH sensing in the two-pore domain K(+) channels TASK-1 and -2. Pflugers Arch **445,** 577-583.*

*Murata Y, Iwasaki H, Sasaki M, Inaba K & Okamura Y. (2005). Phosphoinositide phosphatase activity coupled to an intrinsic voltage sensor. Nature **435,** 1239-1243.*

*Neher E & Sakmann B. (1976). Single-channel currents recorded from membrane of denervated frog muscle fibres. Nature **260,** 799-802.*

*Oldfield S, Hancock J, Mason A, Hobson SA, Wynick D, Kelly E, Randall AD & Marrion NV. (2009). Receptor-mediated suppression of potassium currents requires colocalization within lipid rafts. Mol Pharmacol **76,** 1279-1289.*

*Ono K, Tsujimoto G, Sakamoto A, Eto K, Masaki T, Ozaki Y & Satake M. (1994). Endothelin-A receptor mediates cardiac inhibition by regulating calcium and potassium currents. Nature **370,** 301-304.*

*Patel AJ & Honore E. (2001). Properties and modulation of mammalian 2P domain K+ channels. Trends Neurosci **24,** 339-346.*

*Patel AJ, Honore E, Lesage F, Fink M, Romey G & Lazdunski M. (1999). Inhalational anesthetics activate two-pore-domain background K+ channels. Nat Neurosci **2,** 422-426.*

*Patel AJ & Lazdunski M. (2004). The 2P-domain K+ channels: role in apoptosis and tumorigenesis. Pflugers Arch **448,** 261-273.*

*Putzke C, Wemhoner K, Sachse FB, Rinne S, Schlichthorl G, Li XT, Jae L, Eckhardt I, Wischmeyer E, Wulf H, Preisig-Muller R, Daut J & Decher N. (2007). The acid-sensitive potassium channel TASK-1 in rat cardiac muscle. Cardiovasc Res **75,** 59-68.*

*Rajan S, Preisig-Muller R, Wischmeyer E, Nehring R, Hanley PJ, Renigunta V, Musset B, Schlichthorl G, Derst C, Karschin A & Daut J. (2002). Interaction with 14-3-3 proteins promotes functional expression of the potassium channels TASK-1 and TASK-3. J Physiol **545,** 13-26.*

*Rajan S, Wischmeyer E, Xin Liu G, Preisig-Muller R, Daut J, Karschin A & Derst C. (2000). TASK-3, a novel tandem pore domain acid-sensitive K+ channel. An extracellular histiding as pH sensor. J Biol Chem **275,** 16650-16657.*

*Rebecchi MJ & Pentyala SN. (2000). Structure, function, and control of phosphoinositide-specific phospholipase C. Physiol Rev **80,** 1291-1335.*

*Reyes R, Duprat F, Lesage F, Fink M, Salinas M, Farman N & Lazdunski M. (1998). Cloning and expression of a novel pH-sensitive two pore domain K+ channel from human kidney. J Biol Chem **273,** 30863-30869.*

*Rhee SG. (2001). Regulation of phosphoinositide-specific phospholipase C. Annu Rev Biochem **70,** 281-312.*

*Robbins J. (2001). KCNQ potassium channels: physiology, pathophysiology, and pharmacology. Pharmacol Ther **90,** 1-19.*

*Rohacs T. (2009). Phosphoinositide regulation of non-canonical transient receptor potential channels. Cell Calcium **45,** 554-565.*

*Rohacs T, Lopes CM, Jin T, Ramdya PP, Molnar Z & Logothetis DE. (2003). Specificity of activation by phosphoinositides determines lipid regulation of Kir channels. Proc Natl Acad Sci U S A **100,** 745-750.*

*Roy A & Levine TP. (2004). Multiple pools of phosphatidylinositol 4-phosphate detected using the pleckstrin homology domain of Osh2p. J Biol Chem **279,** 44683-44689.*

*Rubanyi GM & Polokoff MA. (1994). Endothelins: molecular biology, biochemistry, pharmacology, physiology, and pathophysiology. Pharmacol Rev **46,** 325-415.*

*Ryu SH, Suh PG, Cho KS, Lee KY & Rhee SG. (1987). Bovine brain cytosol contains three immunologically distinct forms of inositolphospholipid-specific phospholipase C. Proc Natl Acad Sci U S A **84,** 6649-6653.*

*Sakane F & Kanoh H. (1997). Molecules in focus: diacylglycerol kinase. Int J Biochem Cell Biol **29,** 1139-1143.*

Sakata S, Hossain MI & Okamura Y. (2011). Coupling of the phosphatase activity of Ci-VSP to its voltage sensor activity over the entire range of voltage sensitivity. J Physiol.

*Santagata S, Boggon TJ, Baird CL, Gomez CA, Zhao J, Shan WS, Myszka DG & Shapiro L. (2001). G-protein signaling through tubby proteins. Science **292,** 2041-2050.*

Schiekel J, Lindner M, Hetzel A, Wemhöner K, Renigunta V, Schlichthörl G, Decher N, Oliver D & Daut J. (in revision). Inhibition of the potassium channel TASK-1 in rat cardiac muscle by endothelin-1 is mediated by phospholipase C. Cardiovasc Res.

*Shulga YV, Topham MK & Epand RM. (2011). Regulation and functions of diacylglycerol kinases. Chem Rev **111,** 6186-6208.*

*Spencer DM, Wandless TJ, Schreiber SL & Crabtree GR. (1993). Controlling signal transduction with synthetic ligands. Science **262,** 1019-1024.*

*Stauffer TP, Ahn S & Meyer T. (1998). Receptor-induced transient reduction in plasma membrane PtdIns(4,5)P2 concentration monitored in living cells. Curr Biol **8,** 343-346.*

*Suga S, Nakano K, Takeo T, Osanai T, Ogawa Y, Yagihashi S, Kanno T & Wakui M. (2003). Masked excitatory action of noradrenaline on rat islet beta-cells via activation of phospholipase C. Pflugers Arch **447,** 337-344.*

*Suh BC & Hille B. (2002). Recovery from muscarinic modulation of M current channels requires phosphatidylinositol 4,5-bisphosphate synthesis. Neuron **35,** 507-520.*

*Suh BC & Hille B. (2008). PIP2 is a necessary cofactor for ion channel function: how and why? Annu Rev Biophys **37,** 175-195.*

*Suh BC, Horowitz LF, Hirdes W, Mackie K & Hille B. (2004). Regulation of KCNQ2/KCNQ3 current by G protein cycling: the kinetics of receptor-mediated signaling by Gq. J Gen Physiol **123,** 663-683.*

*Suh BC, Inoue T, Meyer T & Hille B. (2006). Rapid chemically induced changes of PtdIns(4,5)P2 gate KCNQ ion channels. Science **314,** 1454-1457.*

*Suh PG, Park JI, Manzoli L, Cocco L, Peak JC, Katan M, Fukami K, Kataoka T, Yun S & Ryu SH. (2008). Multiple roles of phosphoinositide-specific phospholipase C isozymes. BMB Rep **41,** 415-434.*

*Szaszi K, Grinstein S, Orlowski J & Kapus A. (2000). Regulation of the epithelial Na(+) /H(+) exchanger isoform by the cytoskeleton. Cell Physiol Biochem **10,** 265-272.*

*Szentpetery Z, Balla A, Kim YJ, Lemmon MA & Balla T. (2009). Live cell imaging with protein domains capable of recognizing phosphatidylinositol 4,5-bisphosphate; a comparative study. BMC Cell Biol **10,** 67.*

*Talley EM & Bayliss DA. (2002). Modulation of TASK-1 (Kcnk3) and TASK-3 (Kcnk9) potassium channels: volatile anesthetics and neurotransmitters share a molecular site of action. J Biol Chem **277,** 17733-17742.*

*Talley EM, Lei Q, Sirois JE & Bayliss DA. (2000). TASK-1, a two-pore domain K+ channel, is modulated by multiple neurotransmitters in motoneurons. Neuron **25,** 399-410.*

*Talley EM, Solorzano G, Lei Q, Kim D & Bayliss DA. (2001). Cns distribution of members of the two-pore-domain (KCNK) potassium channel family. J Neurosci **21,** 7491-7505.*

*Varnai P & Balla T. (2006). Live cell imaging of phosphoinositide dynamics with fluorescent protein domains. Biochim Biophys Acta **1761,** 957-967.*

*Varnai P, Thyagarajan B, Rohacs T & Balla T. (2006). Rapidly inducible changes in phosphatidylinositol 4,5-bisphosphate levels influence multiple regulatory functions of the lipid in intact living cells. J Cell Biol **175,** 377-382.*

*Vasudevan L, Jeromin A, Volpicelli-Daley L, De Camilli P, Holowka D & Baird B. (2009). The beta- and gamma-isoforms of type I PIP5K regulate distinct stages of Ca2+ signaling in mast cells. J Cell Sci **122,** 2567-2574.*

*Veale EL, Kennard LE, Sutton GL, MacKenzie G, Sandu C & Mathie A. (2007). G(alpha)q-mediated regulation of TASK3 two-pore domain potassium channels: the role of protein kinase C. Mol Pharmacol **71,** 1666-1675.*

*Vega-Saenz de Miera E, Lau DH, Zhadina M, Pountney D, Coetzee WA & Rudy B. (2001). KT3.2 and KT3.3, two novel human two-pore K(+) channels closely related to TASK-1. J Neurophysiol **86,** 130-142.*

*Venkatakrishnan G & Exton JH. (1996). Identification of determinants in the alpha-subunit of Gq required for phospholipase C activation. J Biol Chem **271,** 5066-5072.*

*Wang HS, Pan Z, Shi W, Brown BS, Wymore RS, Cohen IS, Dixon JE & McKinnon D. (1998). KCNQ2 and KCNQ3 potassium channel subunits: molecular correlates of the M-channel. Science **282,** 1890-1893.*

*Weber M, Schmitt A, Wischmeyer E & Doring F. (2008). Excitability of pontine startle processing neurones is regulated by the two-pore-domain K+ channel TASK-3 coupled to 5-HT2C receptors. Eur J Neurosci **28,** 931-940.*

*Willars GB, Nahorski SR & Challiss RA. (1998). Differential regulation of muscarinic acetylcholine receptor-sensitive polyphosphoinositide pools and consequences for signaling in human neuroblastoma cells. J Biol Chem **273,** 5037-5046.*

*Winks JS, Hughes S, Filippov AK, Tatulian L, Abogadie FC, Brown DA & Marsh SJ. (2005). Relationship between membrane phosphatidylinositol-4,5-bisphosphate and receptor-mediated inhibition of native neuronal M channels. J Neurosci **25,** 3400-3413.*

Yuste R & Konnerth A. (2005). Imaging in neuroscience and development : a laboratory manual. Cold Spring Harbor Laboratory Press, Cold Spring Harbor, N.Y.

*Zhang H, Craciun LC, Mirshahi T, Rohacs T, Lopes CM, Jin T & Logothetis DE. (2003). PIP(2) activates KCNQ channels, and its hydrolysis underlies receptor-mediated inhibition of M currents. Neuron **37,** 963-975.*

*Zuzarte M, Heusser K, Renigunta V, Schlichthorl G, Rinne S, Wischmeyer E, Daut J, Schwappach B & Preisig-Muller R. (2009). Intracellular traffic of the K+ channels TASK-1 and TASK-3: role of N- and C-terminal sorting signals and interaction with 14-3-3 proteins. J Physiol **587,** 929-952.*

5.2 Academic teachers

The subsequently listed persons have been my academic teachers:

- in Marburg:
  Aumüller, Bals, Bartsch, Daut, Decher, Dietrich, Ebert, Fendrich, Geks, Grundmann, Jonas, Kirchner, Koolman, Lohoff, Maier, Neubauer, Oertel, Oliver, Plant, Preisig-Müller, Richter, Röhm, Rolfes, Rothmund, Ruchholtz, Schlosser, Schultze, Sekundo, Sesterhenn, Teymoortash, Wagner, Werner, Wilhelm
- in Edinburgh
  Murie, Wigemore
- in Bochum
  Eysel, Beyer

5.3 Acknowledgements

First of all I want to express my gratitude to Prof. Dr. D. Oliver for giving me the opportunity to carry out my thesis in his group. His helpful hints and the time he invested in discussion of my results and possible new approaches formed the essential basis to successfully carry out my work.

Special thanks to Michael and Christian H. who practically introduced me into electrophysiology and endured innumerable discussions. Also the conversations with Bettina W. and Florian N. were extremely conductive to my work. My thanks also go to Sigrid and Christian G., for cell culture, to Eva and Gisela, for molecular biology and to Olga E. for both. Additionally I would like to acknowledge Bettina S. and Julia for supremely managing the paperwork.

I owe my deepest gratitude to my parents, who helped me to become who I am and who supported me on all my ways!